Distribution System Planning and Reliability Assessment under High DG Penetration

by

Yasser Moustafa Atwa

A thesis
presented to the University of Waterloo
in fulfillment of the
thesis requirement for the degree of
Doctor of Philosophy
in
Electrical and Computer Engineering

Waterloo, Ontario, Canada, 2010

AUTHOR'S DECLARATION

I hereby declare that I am the sole author of this thesis. This is a true copy of the thesis, including any required final revisions, as accepted by my examiners.

I understand that my thesis may be made electronically available to the public.

Abstract

With power system restructuring, continuous growth of demand, and deregulation, small, scattered generators referred to as Distributed Generation (DG) are predicted to play a key role in the power distribution system. Moreover, among the different types of DG units, it is widely accepted that renewable DG units are the key to a sustainable energy supply infrastructure, since they are both inexhaustible and non-polluting. However the intermittent nature and the uncertainties associated with the renewable resources create special technical and economical challenges that have to be comprehensively investigated in order to facilitate the deployment of these DG units in the distribution system.

The objective of the work proposed in this thesis is to tackle some of the challenges associated with the increased penetration of renewable DG units into existing distribution systems. This includes the study of the impact of different renewable DG units on the supply adequacy of the distribution system, and the development of planning technique that optimally allocate renewable DG units into the distribution system. Furthermore, a methodology is proposed to check the feasibility of implementing energy storage system (ESS) into the distribution system to mitigate the problems associated with the high penetration of renewable DG units. These problems include the maximum reverse power flow limit, the equipment rating limit, and the voltage limit on each bus.

The first step toward the accomplishment of this work is to model the random behaviour of the renewable resources (i.e. wind speed and solar irradiance). Here, different approaches are proposed to model the random behaviour of both wind speed and solar irradiance, either chronologically or probabilistically. Among those approaches are a novel technique of annual wind speed estimation based on a constrained Grey predictor, and a new implementation of the probability density function (pdf) of the clearness index so as to model solar irradiance using Monte Carlo Simulation (MCS).

Supply adequacy of distribution systems is assessed based on well-being criteria during different modes of operation (i.e. grid-connected mode and islanding mode), using analytical and (MCS) techniques. During the grid-connected mode, from the load perspective, the substation transformers act as generating units. Therefore, supply adequacy of distribution systems is assessed by considering that the generating units of the distribution system are the substation transformers and the DG units. During the islanding mode of operation, the island is acting as a small autonomous power system (SAPS) and the most important issue during this mode of operation is to determine the probability of

the island to be successful (the DG power output within the island matches the load) or a failure (there is a deficit in power generation).

The focus of the model developed to optimally allocate the renewable DG units in existing distribution systems is to minimize annual energy losses and at the same time, avoid any violation of the system constraints under any operating condition. The methodology is based on generating a probabilistic generation-load model that combines all possible operating conditions of the renewable DG units with their probabilities, hence accommodating this model in a deterministic planning problem. The objective function of the planning formulation is to minimize annual energy losses; whereas the constraints include the voltage limits, the feeders' capacity, the maximum penetration limit, and the discrete size of the available DG units.

The objective of the methodology proposed for allocating an ESS into distribution systems with high penetration (greater than 20% of the feeder capacity) of renewable energy is to maximize the benefits for both the DG owner and the utility. This is done by sizing the ESS to accommodate the entire surplus of renewable energy, and then allocating it within the system in order to minimize the annual cost of the electricity.

Acknowledgements

First and foremost I would like to thank God whose guidance lead me this far.

My thanks also go to several people whose support helped me to bring forth this work.

I would like first to express my sincere thanks and gratitude to my supervisor Professor Ehab El-Saadany for his guidance, support, and encouragement throughout the course of my program.

I also wish to thank my colleagues whose fruitful discussion inspired me in and out the class.

Thanks are also due to my wife who stood by me and encouraged me. A special thanks to my father and my mother who are though far away constantly encouraged me.

Dedication

This thesis is dedicated to my wife, my sons, and my parents.

Table of Contents

AUTHOR'S DECLARATION ii
Abstract iii
Acknowledgements v
Dedication vi
Table of Contents vii
List of Figures xi
List of Tables xiii
Nomenclature xv
Chapter 1 Introduction and Objectives 1
1.1 Preface 1
1.2 Thesis objective 2
1.3 Thesis outline 3
Chapter 2 Literature Survey 4
2.1 Introduction 4
2.2 Distributed generation definition 4
2.3 Why distributed generation? 5
2.4 Distributed generation technologies 7
2.5 Scenarios of DG operation 8
2.5.1 *Anti-Islanding operation* 9
2.5.2 *Islanded system* 9
2.6 Distribution system planning with DG 9
2.7 Reliability evaluation of distribution system with renewable resources 13
2.8 Integration of energy storage system (ESS) with renewable energy resources 16
2.9 Discussion 17
Chapter 3 Modeling of Renewable Resources 18
3.1 Introduction 18
3.2 Wind Speed Modeling 19
3.2.1 Wind Speed Modeling Using Proper pdf 19
3.2.2 Annual Wind Speed Estimation Utilizing Constrained Grey Predictor (wind model 5) 22
3.2.3 Time Series Method for Wind Speed Modeling (wind model 6) 30
3.3 Wind Turbine Output Power 31

3.4 Solar Irradiance Modeling 33
3.4.1 Bimodal Beta pdf Model (solar model 1) 34
3.4.2 Clearness Index Model (Solar model 2) 35
3.5 PV Output Power 40
3.6 Load Modeling 41
3.6.1 Annual Load Modeling (load model 1) 42
3.6.2 Typical Hour Load modeling (load model 2) 42
3.7 Discussion 44
Chapter 4 Optimal Allocation of Renewable Resources in Distribution Systems 45
4.1 Introduction 45
4.2 Objective Function 46
4.3 Modeling of the Renewable Resources and Load Data 48
4.4 Site matching 49
4.5 Combined Generation Load Model 49
4.6 Planning problem formulation 51
4.7 Case Study 54
4.7.1 System under Study 54
4.7.2 Wind Speed and Wind Turbine Data 55
4.7.3 Solar Irradiance and PV Module Data 56
4.7.4 Biomass DG Unit Data 57
4.7.5 Load Data 58
4.8 Results 58
4.8.1 Wind versus Solar 64
4.8.2 Biomass impact on system loss 64
4.8.3 The impact of the discrete size of the renewable DG units on the annual energy loss 65
4.9 Discussion 67
Chapter 5 Supply Adequacy Assessment of Distribution Systems with Renewable DG 68
5.1 Introduction 68
5.2 Modes of System Operation 68
5.3 Definition of the Reliability Events 70
5.4 Reliability Evaluation Criteria 70
5.4.1 Deterministic Criterion 70

5.4.2 Probabilistic Criterion 70
5.4.3 Well-being Criteria 71
5.5 Methods of Reliability Evaluation 72
5.5.1 Analytical Method for Reliability Evaluation 72
5.5.2 Simulation Method for Reliability Evaluation 75
5.6 Segmentation Concept for Island Reliability Assessment 76
5.6.1 Calculating the Probability of the Island to be created 77
5.6.2 Calculating the Probability of the Island to be a Success 79
5.7 Proposed Approach for Adequacy Assessment 79
5.8 Case Study 82
5.8.1 First Scenario 84
5.8.2 Second Scenario 91
5.9 Extra Reliability Indices Calculation 94
5.10 Discussion 95
Chapter 6 Optimal Allocation of ESS in Distribution Systems 96
6.1 Introduction 96
6.2 Methodology 96
6.3 Procedures 99
6.3.1 Determine the Annual Cost of Spilled Wind Energy 99
6.3.2 Determine the Size of the Proposed ESS 101
6.3.3 Determine the Annual Cost of Integrating the Pre-Sized ESS 101
6.3.4 Determine the Benefits for the Utility 103
6.3.5 Perform a Cost/Benefit Analysis 105
6.4 Case Study 105
6.4.1 Wind Speed and Wind Turbine Data 106
6.4.2 Load Data 106
6.5 Results 106
6.6 Discussion 109
Chapter 7 Conclusions and Contributions 110
7.1 Conclusions 110
7.2 Contributions 111
Appendix A: Distribution System Data 113

Bibliography 115

List of Figures

Figure 1-1 Thesis objective 3
Figure 3-1 Weibull probability density functions with different values of scale and shape indices. ... 20
Figure 3-2 Wind speed profile during the same day in different years 23
Figure 3-3 Correlation coefficient of wind speed at different lag times 23
Figure 3-4 Wind speed clusters of same day at different years 24
Figure 3-5 Wind speed clusters of same month in different years 25
Figure 3-6 Correlation coefficient of wind speed using the proposed technique 25
Figure 3-7 Comparison between the actual data and the estimated data for Jan 29
Figure 3-8 Comparison between the actual data and the estimated data for Apr 29
Figure 3-9 Comparison between the actual data and the estimated data for Aug 30
Figure 3-10 Wind turbine power curve 32
Figure 3-11 Histogram versus Beta distribution 34
Figure 3-12 Photovoltaic characteristics 41
Figure 4-1 Block diagram of the proposed work 46
Figure 4-2 System under study 55
Figure 4-3 CF of the wind turbines available 56
Figure 4-4 CF of the PV modules available 57
Figure 4-5 Power loss in a typical day of each season (scenario 1 vs. scenario 2) 59
Figure 4-6 Power loss in a typical day of each season (scenario 1 vs. scenario 3) 60
Figure 4-7 Power loss in a typical day of each season (scenario 1 vs. scenario 4) 60
Figure 4-8 Power loss in a typical day of each season (scenario 1 vs. scenario 5) 61
Figure 4-9 Power loss in a typical day of each season (scenario 1 vs. scenario 6) 61
Figure 4-10 Power loss in a typical day of each season (scenario 1 vs. scenario 7) 62
Figure 4-11 Power loss in a typical day of each season (scenario 1 vs. scenario 8) 62
Figure 4-12 Hourly percentage power loss reduction (scenario 2 vs. scenario 3) 64
Figure 4-13 Comparison of the maximum penetration and actual penetration for all scenarios 65
Figure 5-1 Schematic diagram of a radial distribution system 69
Figure 5-2 Well-being criteria 72
Figure 5-3 Segmentation concept 77
Figure 5-4 Proposed adequacy assessment technique 81
Figure 5-5 System under study 83

Figure 5-6 Load profile 87
Figure 5-7 MSAM for the total generation 88
Figure 5-8 MSAM for the DG units only 88
Figure 5-9 Comparison between LOLE with and without DG units 90
Figure 5-10 Comparison between LOEE with and without DG units 90
Figure 6-1 Proposed steps for optimal allocation of ESS in distribution systems 99
Figure 6-2 Typical day of each season showing the difference between the wind energy expected to be generated and the wing energy accommodated by the network 107
Figure 6-3 Total profit compared to the annual cost of different ESS technologies 109

List of Tables

Table 3-1 Wind Speed Limits 26
Table 3-2 Annual Average Absolute Error 30
Table 3-3 Different Wind Speed Models 31
Table 3-4 Reflectance Coefficient for Different Ground Covers 37
Table 3-5 Different Solar Irradiance Models 40
Table 3-6 Load Model 1 42
Table 3-7 Weekly Peak Load in Percent of Annual Peak 43
Table 3-8 Daily Peak Load Cycle in Percent of Weekly Peak 43
Table 3-9 Hourly Peak Load in Percentage of Daily Peak 44
Table 4-1 Different Combinations of Load and Wind Power (Matrix *Cg*) 51
Table 4-2 Probability of Different Combinations of Load and Renewable Output Power ($P(Cg)$) 51
Table 4-3 Characteristics of the Wind Turbines Available 56
Table 4-4 Characteristics of the PV Modules Available 57
Table 4-5 Load Profile 58
Table 4-6 Results Using Discrete DG Sizes 63
Table 4-7 Results Using Discrete DG Size 63
Table 4-8 Results with Discrete DG Size Constraint Relaxed 66
Table 4-9 Results with Discrete DG Size Constraint Relaxed 66
Table 5-1 MSAM of the Diesel DG Units 86
Table 5-2 MSAM of the Transformers 86
Table 5-3 Single Wind Turbine MSAM 86
Table 5-4 MSAM for the Two Wind Turbines 87
Table 5-5 Adequacy Indices in Grid-connected Mode (Scenario 1) 89
Table 5-6 Adequacy Indices in Islanding Mode (Scenario 1) 89
Table 5-7 Load Profile 93
Table 5-8 Adequacy Indices in Grid-connected Mode (Scenario 2) 94
Table 5-9 Adequacy Indices in Islanding Mode (Scenario 2) 94
Table 5-10 SAIDI for Different Segments and the Whole System 95
Table 5-11 Improvement in SAIDI 95
Table 6-1Wind Turbine Power Curve 106
Table 6-2 Cost of Spilled Energy 107

Table 6-3 Annual Cost of Different ESS Technologies 107
Table 6-4 Optimum Allocation of ESS in the Distribution System 108
Table 6-5 Utility Profit 108

Nomenclature

ACC	Annualized capital cost.
AGO	Accumulated Generating Operation
ANN	Artificial neural network
ARC	Total Annual storage replacement cost
ARMA	Auto regression moving average
B	Set of candidate buses to connect DG units
BOP	Total cost of the balance of plant
BOPU	Unit cost for the balance of plant
C	Number of charge/discharge cycles in the life of the storage
c	Scale index
cdf	Cumulative density function
C_g	The available reserve
C_g	Number of customers in segment g
C_{LU}	The capacity of the largest unit
$Coff_D$	Off-peak electricity price during day *D* ($/KWh)
Con_D	On-peak electricity price during day *D* ($/KWh)
CRF	Capital recovery factor
C_s	Total number of customers in the system
dn	The day number
DR	Distributed resources
DT_g	Down time of segment g
E	The time equation in minutes
$E_{D,i}^{CH}$	Stored energy in the ESS connected at bus *i* during day *D*
$E_{D,i}^{FINAL}$	Final charge of the ESS connected at bus *i* at the end of day *D*
$E_{D,i}^{DISCH}$	Released energy from the ESS connected at bus *i* during day *D*
EENS	Expected energy not served
E_{ESS}	Actual capacity of the ESS
Ei	Energy capacity of the ESS connected at bus *i*

ESS	Energy storage system
F	Future value of replacement cost ($/KWh)
$f(v)$	Distribution probability of wind speed
$f_b(s)$	Beta distribution function of s
FF	The fill factor which is a measure of the deviation of the real I-V characteristics from the ideal one.
FOR	Forced Outage Rate
GA	Genetic algorithm
GM	Grey Predictor
H	The number of hours in the month under study
$HOWS$	Hourly observed wind speed
$HSWS$	Hourly simulated wind speed
$IAGO$	Inverse accumulated generating operation
IESO	Independent electricity system operator
$I_{g,i,j}$	Current in the feeder connecting busses i and j during state g
i_r	Interest rate
$I_{t,i,j}$	The current in the feeder connecting busses i and j at time t
k	Shape index
kd	The fraction of the hourly radiation on horizontal plane which is diffuse
K_i	Current temperature coefficient A/^{o}C
K_t	Daily clearness index
k_t	Hourly clearness index
k_{tm}	Mean clearness index
k_{tu}	Maximum value of clearness index
K_v	Voltage temperature coefficient V/^{o}C
LAFs	Loss adjustment factors
LDC	Load Duration Curve
LFs	Load factors
LOEE	Loss of energy expectation
LOLE	Loss of load expectation
LOLP	Loss of load probability
m	Number of components in segment $j \in set 1$

MINLP	Mixed integer non linear programming
MSAM	Multi State Availability Model
MTTF	Mean time to fail
MTTR	Mean time to repair
N	Number of charge/discharge cycles per day
n	Total number of buses in the system
N	The total number of discrete states in model R, which is equal to the product of the wind speed states and the solar irradiance states
NLP	Non Linear Programming
N_{OT}	The nominal temperature of the module ^{o}C
NPV	Net present value
OM	Fixed operation and maintenance (O&M) cost ($/KW)
OMC	Total annual fixed operation and maintenance cost
OPA	Ontario power authority
OPF	Optimal power flow
$P\{C_g\}$	A one-column matrix that represents the probability corresponding to matrix C
P_{bus}	Maximum penetration allowable on each bus
PCS	Total cost of power electronics
$PCSU$	Unit cost of power electronics ($/KW)
pdf	Probability Density Function
P_{DGbi}	Rated power of the biomass DG connected at bus i
P_{DGSi}	Rated power of the solar DG connected at bus i
$PDG_{t,i}$	Power output of the wind-based DG connected at bus i at time t
P_{DGWi}	Rated power of the wind-based DG connected at bus i
P_{Di}	Peak active load at bus i
$PD_{t,i}$	Active load at bus i at time t
$P_{D,t,i}^{CH}$	Power input to the ESS connected at bus i during time t of day D
$P_{D,t,i}^{DISCH}$	Power output of the ESS connected at bus i during time t of day D
P_{ESS}	Power rating of the energy storage
P_G	Generated power of the DGs connected to the island
P_{G1}	Substation active power injected

$PG_{t,i}$	Substation active power at time *t*
P_i	Power rating of the ESS connected at bus *i*
P_L	Load power of the same island.
P_{loss}	Power loss in the island
P_{lossg}	Total power loss in the system during state g
$Ploss_{D,t}$	Total power loss at time *t* of day *D*
P_{rated}	Rated wind power
$P_s\{G_y\}$	The probability of the solar irradiance being in state *y*
PV	Photovoltaic
$P_v\{G_w\}$	The probability of wind speed being in state *w*
Q_{Di}	Peak reactive load at bus *i*
$QD_{t,i}$	Reactive load at bus *i* during time *t*
Q_{G1}	Substation reactive power injected
$QG_{t,1}$	Substation reactive power injected at time *t*
R	Complete annual generation-load model
r	Replacement period (year)
R_b	The ratio of beam radiation on the tilted surface to that on a horizontal surface
rt_i	Repair time of component i. in segment j
RTS	Reliability Test System
s	Solar irradiance KW/m^2
SAIDI	System average interruption duration index
SAPS	Small autonomous power system
SC	The solar constant=1367
sfr_i	Sustained failure rate of component i.in segment j
SOP	Standard offer program
S_R	Substation rating
SUC	Total cost of the storage unit
SUCU	Unit cost of the storage unit ($/KWh)
s_{y1} and s_{y2}	The solar irradiance limits of state *y*
t:	The conventional hour expressed in hours
T_a	Ambient temperature ^oC
T_c	Cell temperature ^oC

TCC	Total capital cost
t_S	The solar hour, expressed in hours; this is a function of the longitude of the site and the day of the year
v	Wind speed
V_{ci}	Cut in speed
v_{co}	Cut out wind speed
$V_{g,i}$	Voltage at bus i during state g
v_m	Mean wind speed
V_r	Rated wind speed
v_{w1} and v_{w2}	The wind speed limits of state w
x	Maximum penetration limit as a percentage of the peak load
z	Planning horizon (year)
$\alpha, \beta c$	Parameters of Beta distribution function
η	ESS efficiency
μ_x, μ_y	mean of X and Y
ρ	The reflectance of the ground
$\rho_{x,y}$	Correlation coefficient between X and Y
σ	Standard deviation
ϕ	The latitude, or the angular position of the observation zone at north or south of the equator (positive at north)
β	The inclination angle of the module with respect to horizontal plane
δ	The solar declination
ω	The hourly angle expressed in degrees; this is the angular displacement of the sun at east or at overt of the local meridian due to the rotation of the earth around it's. It's null at the solar midday, positive in the morning and negative in the afternoon
ΔL	The difference in longitude between the meridian used to define the local hour, and the meridian of the locality
β_N	The altitude angle
ϖ	The rotation velocity of the earth around its axis, and is equal to 15°/h

Chapter 1
Introduction and Objectives

1.1 Preface

In the last decade, due to the dramatic growth in demand, the concept of small scale energy sources dispersed over the grid gained increasing interest; these sources are known as Distributed Generation (DG).

Distributed generation, for the moment are loosely defined as small-scale electricity generation, is a fairly new concept in the economics literature about electricity markets, but the idea behind it is not new at all. In the early days of electricity generation, distributed generation was the rule, not the exception. The first power plants only supplied electricity to customers in the close neighbourhood of the generation plant. The first grids were DC-based, and therefore the supply voltage was limited, as was the maximum distance between generator and consumer. Balancing demand and supply was partially done using local storage, i.e. batteries, which could be directly coupled to the DC grid. Along with distributed generation, local storage was also returning to the scene. Later technological evolutions, such as the emergence of AC grids, allowed for electricity to be transported over longer distances, and economies of scale in electricity generation led to an increase in the power output of the generation units. All this resulted in increased convenience with lower per-unit costs, which in turn led to massive electricity systems being constructed, incorporating huge transmission and distribution grids and large generation plants. Balancing demand and supply was done by the averaging effect of the combination of the large number of instantaneously variable loads. Security of supply was increased as the failure of one power plant was compensated for by the other power plants in the interconnected system. In fact, this interconnected high voltage system made an economy of scale in generation possible.

In the last decade, technological innovations and a changing economic and regulatory environment have resulted in a renewed interest in distributed generation. This is confirmed by the International Energy Agency (IEA), which lists five major factors that contribute to this evolution:

- developments in distributed generation technologies;
- constraints on the construction of new transmission lines;
- increased customer demand for highly reliable electricity;
- liberalization of the electricity market;
- concerns about climate change.

Furthermore, as the current electricity infrastructure is moving towards clean and inexhaustible sources of electricity, renewable energy sources, such as wind energy and solar energy, are rapidly becoming an appealing option around the world.

However, distribution systems, whether they are radial-type systems found in rural or suburban areas, or network-type systems found in urban areas, are generally designed to operate without any generation on the distribution system or at customer premises. This is due to the fact that for decades, existing infrastructure and institutions have been focused on the heavily centralized model of generation despite the decentralized model. Therefore, because of this accumulated investment in the existing power system, DG often must adapt to existing systems in order to connect to the grid. This implementation of DG into existing systems can significantly impact the flow of power, protective devices, system reliability, and voltage conditions at customers and utility equipment. All of these impacts, whether positive or negative, change the traditional routine of distribution planning, reliability assessment and operation by increasing the scope and complexity of what must be considered. Hence, many traditional rules of thumb and guidelines may no longer be valid. Moreover, the intermittent nature and uncertainty associated with renewable DG create more challenges that have to be overcome in order to deploy renewable DG rapidly and constructively.

1.2 Thesis objective

The ultimate goal of the work adopted in this thesis, as shown in figure 1-1, is to tackle the problem of distribution system planning and supply adequacy assessment under conditions of high penetration of renewable DG and during different modes of operation (i.e. grid-connected mode and islanding mode). The proposed planning methodology takes into consideration the intermittent nature of the renewable resources, the annual load profile, and the technical constraints of the system. To assess supply adequacy during different modes of operation, analytical and Monte Carlo Simulation (MCS) techniques are proposed to model the random behaviour of the renewable resources and system components. With regards to distribution system planning, the main focus of the proposed methodology is to optimally allocate renewable resources in distribution systems so as to maximize the utility benefits. Moreover, a methodology is proposed to optimally allocate energy storage systems (ESS) in distribution systems to mitigate the problems created by the high penetration of intermittent renewable DG, and at the same time add value to the utility and the DG owners.

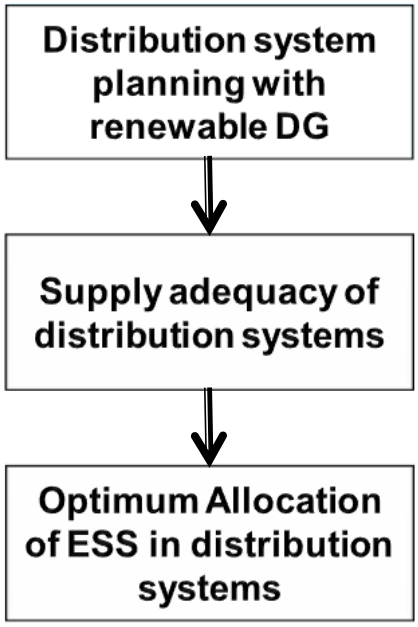

Figure 1-1 Thesis objective

1.3 Thesis outline

This thesis is organized as follows: chapter 2 presents a literature survey on the previous work conducted in the area of planning and reliability assessment of distribution systems with DG. Different models of renewable resources, as well as the advantages, disadvantages, and application of each model are examined in chapter 3. Chapter 4 demonstrates the proposed methodology of distribution system planning with renewable DG. In chapter 5, the proposed technique for distribution system supply adequacy, with renewable DG units during different modes of operation is presented. Chapter 6 addresses the problem associated with the high penetration of renewable DG and how to mitigate this problem using ESS. Finally, the contributions and conclusions are presented in chapter 7.

Chapter 2
Literature Survey

2.1 Introduction

The primary aim of the electricity supply system is to meet customers' demand for energy. Power generation is carried out wherever it can generate the most power for the least cost. The transmission system is used to transfer large amounts of energy from the main generation areas to major load centers. Distribution systems carry the energy further to customers, utilizing the most appropriate voltage level. Traditionally, central power plants constitute the main generation facility in a vertically integrated electricity system. However, with system deregulation other small generating facilities, or what is known as Distributed Generation (DG), are expected to emerge as major contributors to power generation. Although distributed generation can bring numerous advantages to the utility system, such as power loss reduction, VAR control, ancillary services, improved reliability, better efficiency, etc., still there are several technical obstacles that have to be resolved before deploying DG becomes feasible.

Among the main challenges facing the deployment of DG into the distribution system is the development of accurate planning and reliability assessment methodologies which take into account the uncertainty that might arise with the proliferation of renewable DG in distribution systems. In addition, different operational issues that might arise due to DG proliferation in distribution systems have to be addressed. The following subsections will highlight the definition of DG, along with its different technologies, as well as its advantages and its effects on distribution system operation. Further, available literature on various aspects of distribution system planning and reliability assessment with DG related to the presented work is reviewed.

2.2 Distributed generation definition

Over the past 15 years, a number of factors have helped to push DG to the fore of electricity generation: new innovations in DG technologies, the liberalization of electricity markets generally allowing for the participation of more generators, growing concern around climate change, and increasing consumer demand coupled with environmental and social constraints on the construction of new transmission infrastructure, have all combined to make DG - and specifically renewable types - a viable alternative to meet the continuous growth in electricity demand.

Analysis of the relevant literature has shown that there is no generally accepted definition of distributed generation. Some countries define distributed generation on the basis of the voltage level, whereas others start from the principle that distributed generation is connected to circuits from which consumer loads are supplied directly. Other countries define distributed generation as having some basic characteristic (e.g., using renewable sources, co-generation, being non-dispatched). This section reviews the definitions of DG proposed by different institutes, associations, and scholars.

The IEEE defines distributed generation as *the generation of electricity by facilities that are sufficiently smaller than central generating plants as to allow interconnection at nearly any point in a power system*.

The International Council on Large Electricity Systems (CIGRE) defines distributed generation as *all generation units with a maximum capacity of 50 MW to 100 MW, which are usually connected to the distribution network and which are neither centrally planned nor dispatched*.

Chambers [1] also defines distributed generation as *relatively small generation units of 30 MW or less, such units being located at or near customer sites to meet specific customer needs, to support economic operation of the distribution grid, or both*.

Dondi et al. [2] define distributed generation as *a small source of electric power generation or storage (typically ranging from less than a kW to tens of MW) which is not a part of a large central power system and which is located close to the load*. These authors also include storage facilities in the definition of distributed generation, which is not conventional.

Ackermann et al. [3] define distributed generation in terms of connection and location rather than in terms of generation capacity. They define a distributed generation source as *an electric power generation source connected directly to the distribution network or on the customer side of the meter*.

The last definition by Ackermann is the most generic one, because it puts no limit on technology or capacity of the potential distributed generation application.

2.3 Why distributed generation?

For many years, power systems were vertically operated, and large power generation plants produced all of the electrical power. This kind of generation is often related to adequate geographical placement (water sources, technical constraints, etc.). The power is then transmitted towards large consumption centers over long distances using different high-voltage transmission levels. This operating structure was built on the basis of economy, security, and quality of supply. This very centralized structure is operated by hierarchical control centers and allows the system to be monitored and controlled

continuously. The generation is instantly adjusted to match consumption (by monitoring the frequency, and on the basis of very elaborate load forecasting models). The voltage is also controlled to be within specific limits by means of appropriate coordinated devices, generators, online tap changers, reactive compensation devices, etc. This operating mode is changing, due to electric utilities as well as to public organizations. There are several reasons for these changes, including: [4]:

- Saturation of the existing network and reduction of security margins
- Geographical and ecological constraints
- Stability and security problems (need for expensive preventive measures, increase of short-circuit currents)
- Continuous growth of demand, especially in emerging countries
- Need for investments to sustain development in the power demand; this development has led to the breaking up of investments (small generation units, cogeneration)
- Privatization, deregulation, and competitive markets
- Emergence of new rational generation techniques with small ratings, ecological benefits, increased profitability, and which can be combined with heat generation.

For these reasons electric power system planners must consider alternatives, and distributed generation appears to be one of the most viable alternatives. The main reasons for the increasingly widespread use of DG can be summarized as follows [5, 6]:

- DG units are closer to customers so that transmission and distribution costs are avoided or reduced
- The latest technology has made available plants with high efficiency and ranging in capacity from l0kW to 15MW
- It is easier to find sites for small generators than for large ones
- Natural gas, often used as fuel in DG stations, is distributed almost everywhere and stable prices are to be expected
- Usually DG plants require shorter installation times and the investment risk is not as high, compared to traditional plants
- DG plants yield fairly good efficiencies, especially in co-generation and in combined cycles (larger plants)
- The liberalization of the electricity market contributes to creating opportunities for new utilities in the power generation sector

- Transmission and distribution costs have risen while DG costs have dropped
- DG provides a flexible way to choose a wide range of combinations of cost and reliability.

2.4 Distributed generation technologies

Some distributed power components, such as diesel generators and lead-acid batteries, have been around since almost the dawn of the power industry. However, improvements in these technologies and the development of advanced technologies promise to ensure the widespread deployment of distributed generation in distribution network. This overview of specific distributed technologies will discuss conventional DG generating technologies, advanced DG generating technologies using conventional fuels, renewable generation, and technologies that do not generate power from primary energy sources, but support the efficient utilization of this power [7].

- ***Conventional technologies*** **–** The traditional choice for on-site generation and remote power applications is the diesel generator. Although the name "diesel" is always associated with light fuel, these generators can actually be tuned to use a wide variety of liquid and gaseous fuels, including natural gas, propane, and residual fuel oil. Advanced diesel engines using electronic injection control promise to improve system efficiency when used in a load-following mode.
- ***Advanced fossil technologies*** **–** Over the past decade, two new fossil-fuel generation technologies have been developed to the point of commercialization or near commercialization: the micro-turbine and the fuel cell. A micro-turbine is a scaled-down version of the Brayton cycle gas turbine used in large-scale central generation. Although primarily designed to use natural gas, these systems also can be designed to use a variety of gaseous and liquid fuels. As with diesel engines, micro-turbine costs are shared with the transportation industry, through development of the engines for small planes, helicopters, and tanks. Fuel cells rely on electrochemical rather than thermodynamic energy conversion. Although they ultimately require hydrogen, the source of this hydrogen can be virtually any hydrocarbon fuel (natural gas or propane preferred) or even hydrogen electrolyzed from water using renewable energy or off-peak generation. Fuel cells have been developed at a small, sub-kilowatt scale for use in space exploration, but have only recently begun scaling-up for stationary power applications.
- ***Renewable technologies*** **–** Hydroelectric is the only renewable energy resource to be used on a wide-spread basis for central-station power. Small-scale, run-of-river hydro projects have

the potential to provide a type of distributed generation to remote areas with appropriate resources. However, photovoltaic (PV), solar thermal technologies, and wind turbines offer more modular and easily deployable options for renewable distributed generation. The primary limitations on these renewable resources are their lack of dispatchability and the high uncertainty; that is, the power is not available on-demand all the time. This is less of an issue when the technology is used to support an existing large grid, but for use in an expanding village grid, renewable energy resources require energy storage and/or redundant dispatchable capacity, both of which add substantial cost to already capital-intensive capacity.

- ***Efficient technologies*** – Energy storage, co-generation (combined heat and power), and load-control technologies can all improve the utilization of primary generation sources on any grid, especially on a small grid or grid with high-penetration of renewable capacity. Energy storage technologies range from traditional lead-acid and nickel cadmium batteries, to advanced electrochemical systems (rechargeable lithium batteries, and reversible fuel cells), composite flywheels, and superconducting magnets. Batteries (that is, electrochemical systems) can cover a wider range of needs, from several megawatts provided over several hours to a few kilowatts provided with a few seconds notice. Flywheels tend to have less energy capacity, but relatively good response time. Superconducting magnets can provide very high power for a very short period of time, but with extremely fast response time. Co-generation utilizes waste heat from a variety of generation sources (including combustion turbines, diesel generators, and even some fuel cell systems) to provide hot water, space heating, or thermal energy for industrial processes. This increases the overall efficiency of energy use in the cogeneration facility or village. Utilities on well-developed grids have used customer load control devices to reduce peak loads such as air conditioning for the past decade. Such controls could help smaller-scale grid operators adjust the dispatch of deferrable system loads to level the load on a base-load generator or match the output of a renewable resource.

2.5 Scenarios of DG operation

The interconnection of distributed generation with electric power systems is regulated by the IEEE 1547 standard [8]. IEEE 1547 establishes universally-needed criteria and requirements for interconnection of distributed resources (DR) with an aggregate capacity not higher than 10 MVA,

interconnected to the electric power systems at typical primary and/or secondary distribution voltages. The complete protection and control strategy is designed under the assumption that the only source of electric power is the substation transformer. The interconnection requirements are therefore designed to limit the possible negative effects that DG may have on the operation of existing devices. Thus, islanded operation of parts of the feeder is currently not allowed by the utilities. This means that following a fault, the DG has to disconnect and remain disconnected until the fault is cleared. Therefore, with this philosophy of DG implementation, there will be no benefits of DG in improving system reliability. To maximize the DG benefit, most recent work focuses on facilitating the islanding operation of the system. Consequently, in this work two possible scenarios will be examined.

2.5.1 *Anti-Islanding operation*

In this case, the DG has to disconnect during fault, and remain disconnected until the fault is cleared. The sequence of events after the fault occurrence is as follows:

- DG is tripped, and the fault is detected and isolated by one or more protection devices.
- After the fault is cleared, the recloser reconnects the area to the rest of the feeder.
- DG reconnects (synchronized) after normal operating voltage and frequency are established, with the appropriate time delay.

2.5.2 *Islanded system*

In this case, islanded operation is allowed, which means that the DG will remain connected during the fault, if it has enough capacity to feed the loads located on the island. However, proper coordination between DG and feeder protection is required. After clearing the fault, synchronization between the DG and the utility is required in order to restore normal operation. The DG system generally relies on the utility to provide its phase reference, and a phase error between the island and utility voltages can develop while part of the system (equipped with DG) is islanding. The sequence of events is as follows.

- DG remains connected during fault
- After the fault is cleared, reclosers synchronize the DG with the utility.

2.6 Distribution system planning with DG

In the conventional electric power system, the energy is transmitted to the end user through a passive distribution system. However, in the recent years, technological improvements and an urgent need for

environmental friendly electric power have motivated distribution system planners to the utilization of DG. Since DG units are connected to the distribution system or sub-transmission system near the location of customers, distribution systems with DG are no longer passive. This paradigm shift in the distribution system topology may affect the system and the customers both economically and technically. To avoid the degradation of power distribution services, it becomes very important to optimally allocate DG in distribution systems.

From the loss minimization perspective, [9] implemented a Tabu search technique to find how much distribution losses can be reduced if DG units are optimally allocated at the demand side of the distribution system. The work in [10] proposed a fuzzy-GA based technique to resolve the problem of DG allocation in distribution systems. The problem formulation considered the power loss cost as the objective function, whereas the constraints include the size and number of DG units, as well as the deviation of the bus voltage.

In the same context, the work in [11] derived analytical expression to determine the optimal location of DG in radial as well as networked systems for minimizing power losses in the system. They considered uniformly-, centrally- and increasingly-distributed load profiles with time-invariant as well as time-varying load and DG power. The optimization model for minimization of losses through constrained power flows and optimal siting of DGs in a multi-bus distribution network is presented in [12]. The main objective is to minimize the line losses subject to meeting generation revenue, transmission constraints and consumer demand. The main advantage of this work is the development of a novel expression that investigates the behaviour of network losses with the change of bus voltage.

Based on the loss formula, [13] derived an analytical expression to calculate the optimum size of DG at various buses of the primary distribution system and proposed a methodology for reducing total losses in the distribution system. In [14] a method for placement of DG units, so as to minimize the system power loss, is proposed. This algorithm is based on determination of buses that are the most sensitive to voltage collapse using continuous power-flow program. After determination of sensitive bus, one DG unit with certain capacity can be installed on that bus. After installation of the DG unit, the power-flow program is executed and then the objective function is calculated. If the estimation of the objective function is inappropriate, then this algorithm would iterate. In [15] the optimal penetrations of different DG technologies were determined by analyzing the effect that changing the penetration level had on annual energy losses.

Considering total generation cost minimization, the work in [16] proposes a Multi-Attribute Decision Making (MADM) to reach the best DG technique that should be used for different types of loads. MADM technique is applied to three cases: conventional grid, hybrid DG operation and micro-grid. The attributes considered are incremental losses, capital costs and percentage time for which demand is not served for all cases. Moreover, it is assumed that attributes are not related to each other. The results indicate that DGs in micro-grid, as well as hybrid systems, are acceptable strategies for light load conditions since they have very small variance of composite distance. The work in [17] presented a multi-objective formulation based on a genetic algorithm for the siting and sizing of DG resources into existing distribution networks. The methodology adopted permits the planner to decide the best compromise between the cost of upgrading the network, cost of power losses, cost of energy not supplied, and cost of energy required by the served customers. The main comment on this work is that the problem cannot be classified as a multi-objective optimization problem since all the objectives have the same unit.

Another criterion presented in [18] is to minimize the total cost of operation including both fixed and variable costs. The costs of buying energy from the transmission system and from DG units should be considered so as to have a proper assessment of the penetration level of a DG in a distribution system. DG will influence the optimal dispatch of the system.

The work in [19] presents a network capacity expansion algorithm capable of deferring T&D expansion by optimally siting DG units at new or existing substations. It uses a successive elimination algorithm that begins with all expansion options (new lines, upgraded lines, new substations, expanded substations and DG), and then successively eliminates the least cost-effective alternatives until any further elimination violates the system constraints. The main drawback of this work is the use of the successive elimination algorithm which can always hit locally optimal solutions.

On the same track, the work in [20] proposed a deterministic optimization technique to determine the optimum locations and sizes of DG units in order to meet the growth in load. The developed framework objective is total planning cost minimization, taking into consideration both capital investment and O&M, DG costs and including a trade-off between generating power from DG and/or purchasing power from the main grid through an existing substation or intertie. The main advantage of this work is the novelty of formulating the optimization problem using binary decision variables to select among different proposed scenarios of meeting the growth in the load. However, the major drawbacks of this work are considering only the conventional types of DG units with predetermined

sizes, and disregarding the impact of the DG units on system reliability while formulating the optimization problem.

A heuristic approach to DG-capacity investment planning with respect to competitive electricity market auctions was proposed in [21]. The optimal allocations of DG units were obtained through a cost-benefit analysis from the perspective of a distribution company.

Under the constraint of maximizing the total power injected from DG units, the work in [22] and [23] proposed a three-step procedure, based on Genetic Algorithms (GAS) and Decision Theory to optimally allocate renewable DG in distribution systems. The procedure provides the best DG location and sizing, taking into account uncertainties introduced by distributed power production as well as technical constraints, such as feeder capacity limits, feeder voltage profile and three-phase short circuit currents in the network nodes.

In [24] the authors developed a methodology to optimally allocate DG capacity on the distribution network. The objective of this methodology is to maximize DG penetration in the distribution system, while the constraints considered were voltage rise, thermal limit, short circuit capacity, short circuit level, energy resource and customer initiatives. The methodology ensured that network sterilization was avoided and the network capacity maximized. However, no account was taken for losses.

The studies in [25] and [26] utilized an iterative methodology for the allocation of DG units in the distribution system to maximize the quantity of DG connected to the system. They used an analysis of power flow equations for both voltage sensitivity and loss sensitivity to identify the best sites for placing DG units in the distribution system. In [27] a new approach has been proposed for the allocation of DG on distribution networks. The ultimate goal of this approach is to maximize DG penetration, thus the impact of DG in radial distribution networks on losses has been modeled. It has been shown that neither the maximization of capacity alone nor the minimization of losses alone is the optimal way to maximize the benefit of DG to society, but rather an objective function which takes account of both losses and capacity. In [28] optimization of distribution networks in the presence of DG units is achieved by means of a GA-based network reconfiguration methodology. This methodology allows the maximization of DG penetration in distribution networks without violating network constraints. The aim of the work in [29] is to present a new method for the allocation of new generation capacity, which takes into account fault level constraints imposed by protection equipment such as switchgear. It simulates new generation capacities and connections to other networks using generators with quadratic cost functions. The relation between capacity and sub-transient reactance of generators is used during the estimation of fault currents, and an iterative

process allocates new capacity using optimal power flow mechanisms, and readjusts capacity to bring fault currents within the specifications of switchgear.

A new optimal power flow (OPF) based technique to facilitate capacity DG growth at predetermined locations is presented in [30]. The (OPF) is used to maximize capacity at specified locations, and because such an objective function is not available with proprietary OPF packages, an alternative approach was necessary. This involves modeling DG units as negative loads and maximizing capacity through load addition, which is considered to be the main drawback of this work.

The work in [31] proposed a multi-period steady-state analysis for maximizing the connection of intermittent distributed generation through an optimal power flow-based technique. The proposed technique considered the different loading levels of the system under study, as well as the intermittent nature of wind outputs.

For determining the optimal fuel mix of different DG technologies, [32] and [33] formulated a mixed integer linear program to optimally utilize the available energy resources for a section of a distribution network. The objective function incorporates loss adjustment factors (LAFs) along with individual generation load factors (LFs), thus facilitating the determination of the optimal DG plant mix for a network section.

This review of the literature shows that considerable work has been done with respect to the allocation of DG units in the distribution system; however, most of the work presented assumes that the output of the DG is dispatchable and controllable. Most of the available methods are unable to model the intermittent nature of the output power. To the authors' knowledge, only a few studies have considered the uncertainties in power output from renewable DG units [11], [15], [22], and [23] or the optimal fuel mix problem [32] and [33]. Hence, the problem of the optimal allocation and fuel mix of renewable DG units still requires attention.

2.7 Reliability evaluation of distribution system with renewable resources

The ability of a generation system to provide an adequate and qualitative supply of electrical energy is measured by the generation system reliability. Reliability analysis quantifies system adequacy and security. Adequacy indicates the ability of the generation system to meet the demand for electricity, while security indicates the ability of the system to respond to unexpected contingencies such as the sudden loss of a major generating plant. Adequacy assessment handled the steady state conditions, whereas the transient and dynamic disturbances happening in the system are considered in the security evaluation.

In this thesis, reliability assessment of the distribution system is limited to the area of adequacy assessment; hence, the terms ‘reliability’ and ‘adequacy’ are used interchangeably.

Distribution system reliability is one of the most important challenges that system planners encounter, especially when renewable DG units are deployed in the system. The reliability aspects of utilizing renewable energy have largely been ignored in the past, due to the relatively insignificant contribution of these sources in major power systems, and also due to the lack of appropriate techniques.

Currently, the global trend toward increasing the sustainable power penetration into the existing power system dictates a very serious need to consider their effect on system adequacy.

The work in [34] proposed two probabilistic techniques to model the wind generation system. The first one is in the form of a capacity outage probability table based on the Weibull probability density function (pdf) of the wind speed, while the second is a Markov model based on detailed hourly mean speed data. In [35], a probabilistic approach to capture the uncertainty associated with the renewable sources is used. The methodology used long-term historical data in isolation to calculate the probability density function (pdf) parameters for each hour of a typical day of any season. Analytical approaches are proposed in [36-40]. In [36] an analytical approach to model wind turbine generators as a multi-state unit is used. In this model, the effects of various wind turbine/interface system component forced outage rates on the expected annual energy output of the farm are considered. In [37, 38] an analytical approach to model renewable energy sources, taking into account the correlation between the load and the renewable sources, is proposed. The system was divided into subsystems to model the conventional and unconventional units separately. The developed models for unconventional sources were modified hourly to account for the fluctuating power from such resources. Hence, these models are combined with the conventional models to determine loss of load expectation (LOLE) for the hour under consideration. In [39, 40] an approach to estimating the Loss of Power Supply Probability (LPSP) of stand-alone solar generation system is developed. The pdf of the difference between daily array output and load is approximated with two events and the daily storage charge/discharge process is represented as a one-step Markov process. In this model, the daily load is assumed to be constant.

Deterministic chronological simulation is proposed in [41, 42] to estimate (LPSP). In [41] the proposed method was able to determine the minimum and economical size of the solar cell array and storage system so as to assure a reliable power supply to the load. While in [42], a general method to determine the LOLP of a stand-alone photovoltaic system as a function of normalized PV array output and energy availability at battery is proposed.

Monte-Carlo Simulation (MCS) is extensively used in [43-45] to evaluate the system reliability by modeling the random output of the renewable sources, load variation and the forced outage rate (*FOR*) of the system component over a sufficiently long study period. In [43], they applied a Monte Carlo simulation (MCS) method to assess the performance of a grid-connected wind farm. The hourly random variation in wind output and load are obtained by random simulation over a sufficiently long period of time. Hence, the cost-effectiveness of wind energy and the economic limitations of penetration into electrical power systems are determined. A MCS technique for wind power modeling and reliability assessment is proposed in [44, 45]. The hourly wind speed data is predicted by time series methods, considering auto-correlation between wind speeds, and the forced outage of various generating units are modeled by proper pdf. Both energy credit and capacity contribution of a wind energy conversion system are assessed using this approach.

The work in [46] proposed a general probabilistic approach to model a wind generation system composed of several wind turbines, of same or different characteristics, connected to a load and battery storage. The model is based on estimating the joint probability distribution of the total available wind power and hardware availability of the wind turbines. This model is also able to determine the size of the battery storage required for a certain number of wind turbines to satisfy a load with predetermined expected energy not served (EENS). This work is extended in [47] to include photovoltaic (PV) systems in the probabilistic model. Utilizing the developed wind farm model [46], the work presented in [48] developed a probabilistic production costing model for diesel-wind system. The model allows the simulation of a Diesel system with a wind farm of different wind turbine types considering system stability, and outages due to hardware failure and primary energy fluctuations. The production costs of diesel units are deduced from the EENS using a unit de-convolution technique in reverse economic order.

During the beginning of the 21st century, Billinton *et al*. [49-52] made pioneering efforts to apply system well-being criteria to the Small Autonomous Power System (SAPS) including renewable energy sources. They use a sequential (MCS) approach for adequacy assessment of the SAPS with renewable energy sources. Later [53-55] applied a sequential (MCS) approach to calculate the Loss of Load Expectation (LOLE) and the Loss of Energy Expectation (LOEE) of the renewable energy sources based SAPS with battery storage.

From the above discussion, it is obvious that sufficient work has been done to assess the adequacy of SAPS with renewable DG units. The system well-being approach is a relatively new concept which combines the deterministic and probabilistic methods to evaluate the system adequacy. However,

only the MCS method has been used extensively for the well-being assessment of a system with renewable DG units, and analytical methods have yet to receive full attention. Moreover, most of the work in this area is focusing on SAPS, while the adequacy of the distribution system with renewable DG units during islanding mode of operation has not been yet assessed. Therefore, the problem regarding the distribution system supply adequacy with renewable DG units during different modes of operation still requires more attention.

2.8 Integration of energy storage system (ESS) with renewable energy resources

Recently, the integration of energy storage systems (ESSs) with renewable energy resources has become one of the most viable solutions for facilitating increased penetration of renewable DG resources. These dispatchable storage technologies will provide added benefits for utilities, DG owners, and customers through greater reliability, improved power quality, and overall reduced energy costs [56-58].

The energy storage sizing problem has been frequently addressed in the literature [59-62], especially for remote areas [63-68], using a variety of optimization techniques.

In [59] and [60], dynamic programming algorithms were utilized to maximize fuel-cost savings and benefits due to energy-pricing differences between peak-load and light-load periods. The methods involved optimizing battery size and ESS charge scheduling, respectively. The work in [61] used a non-dominated sorting genetic algorithm optimization technique with a multi-objective function in order to evaluate the impact of the specific costs of energy storage on the net present value (NPV) of energy storage installations in distribution substations. In [62], the authors presented both deterministic and stochastic formulations for the problem of scheduling different power system reserves. In [63], on the other hand, a two-stage stochastic optimization problem was proposed to address the problem of ESS sizing for isolated wind-diesel power systems, with the objective of minimizing the cost of the energy supplied. In [64-66], both operational costs and fixed costs were incorporated into the formulation of the optimization problem. Reliability design criteria were imposed through the use of adequacy constraints, which can be met through the inclusion of storage or additional diesel capacity. The work in [67] incorporated dynamic security criteria in a linear programming optimization problem that was able to determine both the power capacity and the best reservoir capacity for a potential pumped storage station in an island system. Fuzzy clustering techniques were used to deal with the stochastic nature of the load and of renewable production in order to generate different scenarios for the optimization problem. Research [68] presented an

integrated electricity production cost analysis for autonomous electrical networks based on renewable energy sources and energy storage configurations. The proposed analysis took into consideration the initial cost of the energy storage equipment, the costs of the input electricity and fuel, and the fixed and variable O&M costs for the entire installation.

From another perspective, [69] presented an interesting technique for a simple economic feasibility evaluation of small energy storage facilities. The technique calculated the cost added to each kilowatt hour of energy that is stored and later returned to the grid.

2.9 Discussion

In this chapter, it can be seen that distribution system reliability assessment and planning are becoming important issues especially with the proliferation of renewable DG units in the distribution system. Throughout this chapter, the benefits and challenges facing the implementation of DG are discussed. Different planning methodology for optimally allocating DG units in distribution systems, based on different criteria (e.g., loss minimization, total generation cost minimization, and maximization of the injected power of DG units), are reviewed. From the reliability perspective, this chapter reviewed the different techniques and criteria utilized to assess distribution system reliability with DG. Finally, the work done in the area of sizing and scheduling ESS when integrated with distribution systems and SAPS has been reviewed.

Chapter 3
Modeling of Renewable Resources

3.1 Introduction

Keen interest in the development and utilization of renewable distributed generation (wind-based/solar DG units) has been recently observed worldwide for several reasons. Among these are: controlling the emission of environmentally harmful substances; limiting the growth in energy costs associated with the use of conventional energy sources; and encouraging the independent power producers for participation in the electricity market system.

Both wind and solar energy rely greatly on meteorological conditions such as wind speed, solar irradiance, ambient temperature and so forth. Consequently, analyzing the characteristics of wind speed and solar irradiance at the installation location, so as to provide proper models that adequately represent these characteristics, is the very first step to facilitate the deployment of the renewable DG units into the distribution system.

On another aspect, there is no unique model for these renewable resources, but different approaches can be used to model them. For example, wind speed and solar irradiance can be modeled chronologically using time-series methods, or probabilistically using a proper probability density function during a certain time segment. The selection of the appropriate approaches to model these renewable resources is reliant heavily on the application (e.g., long term planning, unit commitment, reliability assessment), as well as the technique utilized to carry out this application (e.g., analytical technique or Mont Carlo Simulation technique).

Therefore, this chapter presents different approaches used to model the random behaviour of the wind speed and the solar irradiance, accompanied with the application of each approach. This includes the use of proper probability density functions (pdfs) to model wind speed and solar irradiance probabilistically, and the use of time series and MCS techniques to model them chronologically. Furthermore, a more accurate model is proposed to model solar irradiance, probabilistically and chronologically, through modeling of the clearness factor. And a novel technique for estimating the annual wind speed, based on a constrained Grey predictor, is demonstrated here. The characteristics of the wind turbines and the PV modules are also included in this chapter. Finally, different models used in this work to describe the load profile are presented.

3.2 Wind Speed Modeling

Wind power is currently one of the most technologically advanced and commercially competitive of the new renewable energy technologies. It offers many countries the opportunity to reduce their dependence on fossil fuels, while satisfying the requirements of both energy and the environment. However, the resource is dispersed and intermittent, and providing a proper modeling of wind speed is an important issue, the solution to which will help to appropriately integrate wind-based DG units in distribution systems.

In the next subsections different models of wind speed are presented.

3.2.1 Wind Speed Modeling Using Proper pdf

The wind speed distribution primarily determines the performance and the feasibility of wind power systems. Once the wind speed distribution is known, the potential energy - and thus the economic viability - can be easily determined. Modeling wind speed using a proper pdf provides a few key parameters which can illuminate the characteristics of a wide range of wind speed data; this is why it is most desirable to use this modeling in the long term planning problems.

Weibull distribution function (3.1) is one of the most common pdfs used to describe the random behaviour of wind speed [70]. Its success derives from the two adjustable parameters, which can provide a great flexibility in fitting the distribution function to the measured values with different behaviours as shown in figure 3-1. This figure shows that the higher the value of *k*, the more the curve looks like an inverted bell, while as the value of *c* increases, the curve spreads out even more.

$$f(v) = \frac{k}{c}\left(\frac{v}{c}\right)^{k-1} \exp\left[-\left(\frac{v}{c}\right)^{k}\right] \tag{3.1}$$

Different methods can be used to calculate the Weibull parameters [71, 72]. Here, the parameters *k* and *c* are calculated, approximately, using the mean wind speed and the standard deviation as follows:

$$k = \left(\frac{\sigma}{v_m}\right)^{-1.086} \tag{3.2}$$

$$c = \frac{v_m}{\Gamma(1+1/k)} \tag{3.3}$$

$$v_m = \frac{1}{n}\left(\sum_{i=1}^{n} v_i\right) \tag{3.4}$$

$$\sigma = \left[\frac{1}{n-1}\sum_{i=1}^{n}(v_i - v_m)^2\right]^{0.5} \tag{3.5}$$

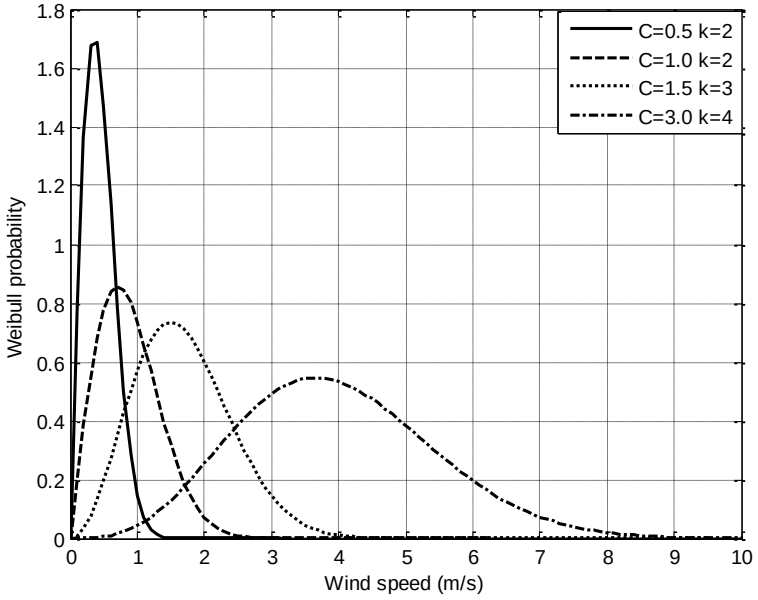

Figure 3-1 Weibull probability density functions with different values of scale and shape indices.

When the shape index *k* equals to 2, the pdf is called Rayleigh probability density function as given in (3.6) which pdf mimics most wind speed profiles. If the mean value of the wind speed for a site is known, then the scale index *c* can be calculated as in (3.7) and (3.8).

$$f(v) = \left(\frac{2v}{c^2}\right)\exp\left[-\left(\frac{v}{c}\right)^2\right] \tag{3.6}$$

$$v_m = \int_0^{\infty} v.f(v)dv = \int_0^{\infty}\left(\frac{2v^2}{c^2}\right)\exp\left[-\left(\frac{v}{c}\right)^2\right]dv = \frac{\sqrt{\pi}}{2}c \tag{3.7}$$

$$c \approx 1.128 v_m \tag{3.8}$$

Weibull and Rayleigh functions are usually used to describe the random behaviour of the wind speed in a given location over certain period of time, typically annually. Moreover, these two functions can describe wind speed distribution for a typical hour of the year. In the present study, two models are

developed to describe the annual wind speed distribution and the wind speed distribution during a typical hour of the year.

3.2.1.1 Annual Wind Speed Modeling

In this model Weibull or Rayleigh pdf are utilized to describe the annual wind speed distribution in the site under study. From the available historical data, the annual mean and standard deviation of wind speed are calculated; hence, the scale and shape indices of a Weibull pdf (*wind model 1*) are calculated, or the scale index of a Rayleigh pdf is calculated (*wind model 2*).

This model is characterized by its simplicity and is extensively used for long term planning applications. The main drawback of this model is that the correlation of wind speed with other random variables in the system, such as load profile, does not exist. Moreover, this model is not applicable when accompanied with solar irradiance modeling because there is no probabilistic annual solar irradiance model.

3.2.1.2 Typical Hour Wind Speed Modeling

In this model a selected study period of one year is divided into four seasons, and a typical day is generated for each season in order to represent the random behaviour of the wind speed during each period. For the site under study, the hourly wind speed data is modeled by a Weibull pdf (*wind model 3*) or a Rayleigh pdf (*wind model 4*). The pdf that is required for modeling the hourly wind speed is based on *y* years of historical data that have been collected from the site under study. Each year is divided into 4 seasons, with each season being represented by any day within that season. The data are then utilized to generate for each season a typical day's frequency distribution of the wind speed measurements. The day representing each season is further subdivided into 24-hour segments (time segments), each referring to a particular hourly interval for the entire season. Thus, there are 96 time segments for the year (24 for each season). Considering a month to be 30 days, each time segment then has (90*y*) wind speed level data points (*y* years x 30 days per month x 3 months per season). From this data, the mean and standard deviation for each time segment are calculated, and from them, the Weibull or Rayleigh pdf is generated for each hour.

This model does provide the correlation between wind speed and load profile, and can be used for long term planning applications. Furthermore, this model can be accompanied with solar irradiance modeling. However, this model is more complicated and generates more wind states when compared to the annual wind speed model.

3.2.2 Annual Wind Speed Estimation Utilizing Constrained Grey Predictor (wind model 5)

The methodology proposed to estimate the annual wind speed profile is based on two steps utilizing three years of historical data. The first step is to divide the data into clusters, whereas in the second step, a constrained Grey predictor is utilized to estimate the wind speed profile.

3.2.2.1 Data Clustering

In this step the data is divided into clusters based on the seasonality of the wind. This will provide a good correlation among the data in the same cluster which will positively be reflected upon the estimated wind profile. In order to reach a reasonable clustering outcome, three years of historical data for the site under study (2004, 2005 and 2006) are utilized (better clustering might be achieved if more data were available). The correlation coefficient between any two variables X and Y can be given by (3.9) as:

$$\rho_{x,y} = \frac{\sum (x-\mu_x)(y-\mu_y)}{\sqrt{\sum (x-\mu_x)^2 \sum (y-\mu_y)^2}} \tag{3.9}$$

By analyzing the available data, and calculating the correlation coefficient among the wind speeds of the same period of time for different years, the following features were observed:

- The wind speed profile varies randomly during the same period of time for different years with very weak correlation as shown in figure 3-2 and figure 3-3, respectively. This indicates that even artificial intelligence techniques, such as ANN will not be able to effectively estimate the annual wind speed profile.

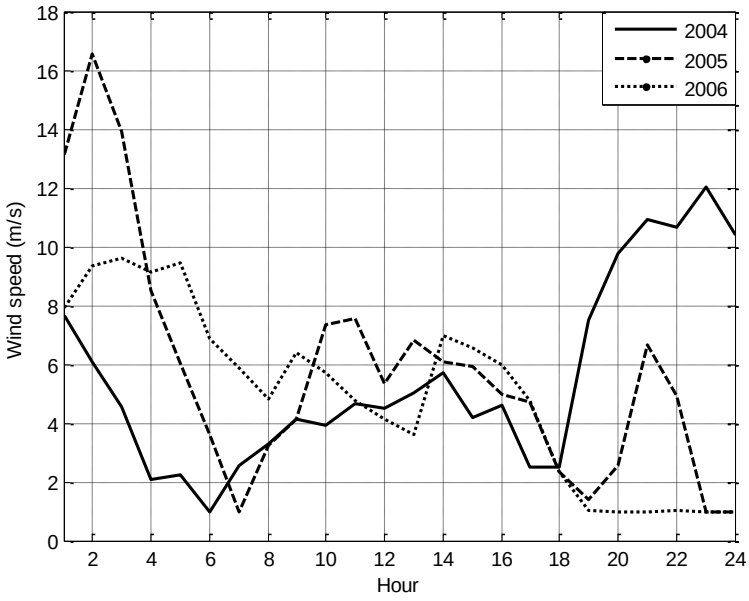

Figure 3-2 Wind speed profile during the same day in different years

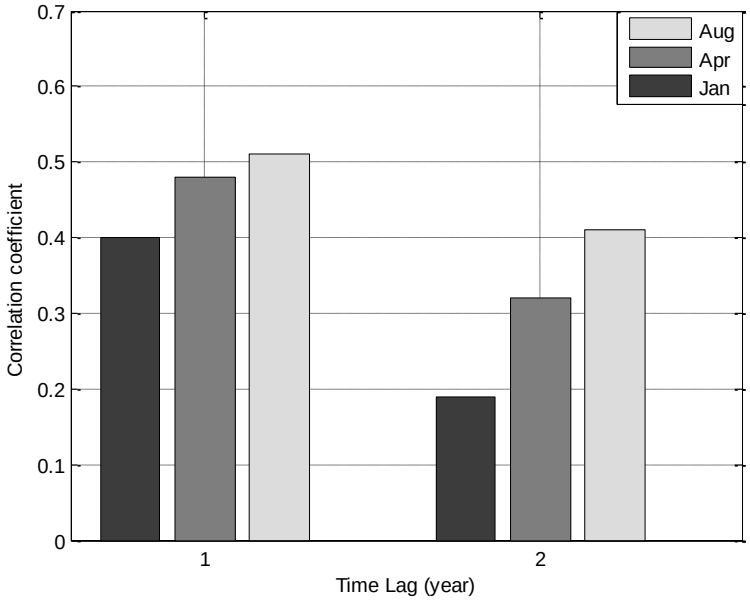

Figure 3-3 Correlation coefficient of wind speed at different lag times

- The annual wind speed data is divided into clusters, where each cluster includes the hourly data of one month in the year. Further, each monthly cluster is divided into sub-clusters based on the wind speed. Each sub-cluster includes the number of hours in which the wind is within certain limits as shown in Table 3-1, where 4 m/s, 14 m/s and 25 m/s are the common cut-in speed, rated speed and cutoff speed of most commercial wind turbines, and j is the sub-cluster index. This means that at the end of the clustering process there will be, for each year, twelve monthly clusters each contains 12 elements (sub-clusters). This can be represented in vector form as S_c (j) where c is the month index (c=1, 2…12), (e.g., S_3 (4) means the number of hours in which the wind speed is between 6 and 7 m/s in March). To evaluate the effect of clustering on the reduction of randomness, the clustering technique is applied to the wind speed data of figure 3-2 as shown in figure 3.4. By comparing figure 3-2 to figure 3-4, it can be found that the amount of randomness is decreased among the daily clustered data of different years. Moreover, a greater reduction in the amount of randomness is achieved when the period is extended from one day to one month (the proposed clustering period) as in figure 3-5. In addition, the correlation coefficient among the annual historical data is improved as shown in figure 3-6.

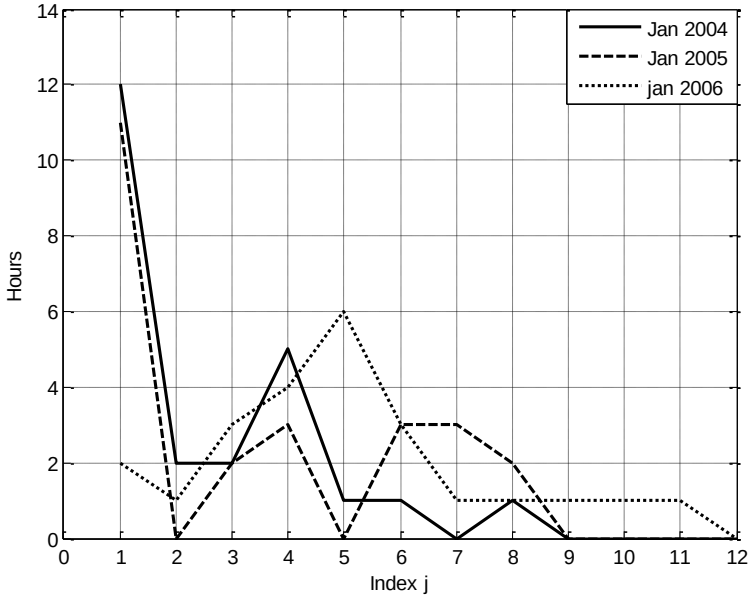

Figure 3-4 Wind speed clusters of same day at different years

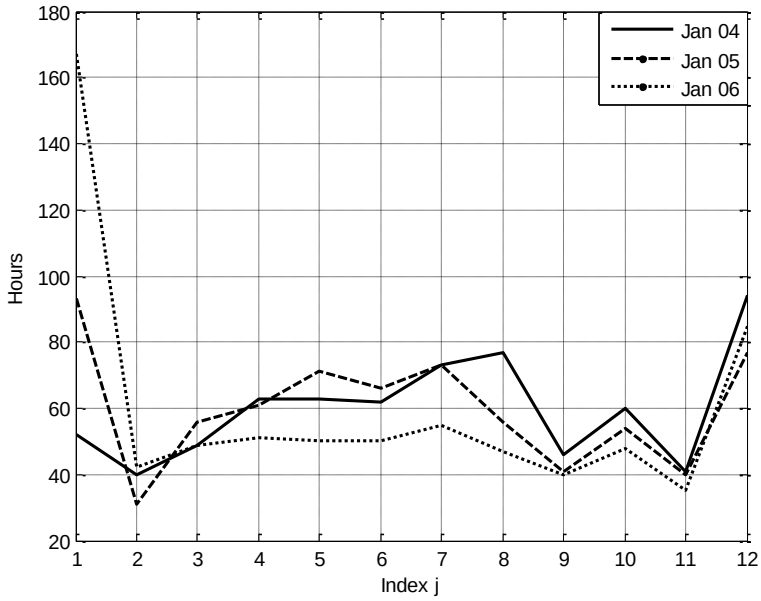

Figure 3-5 Wind speed clusters of same month in different years

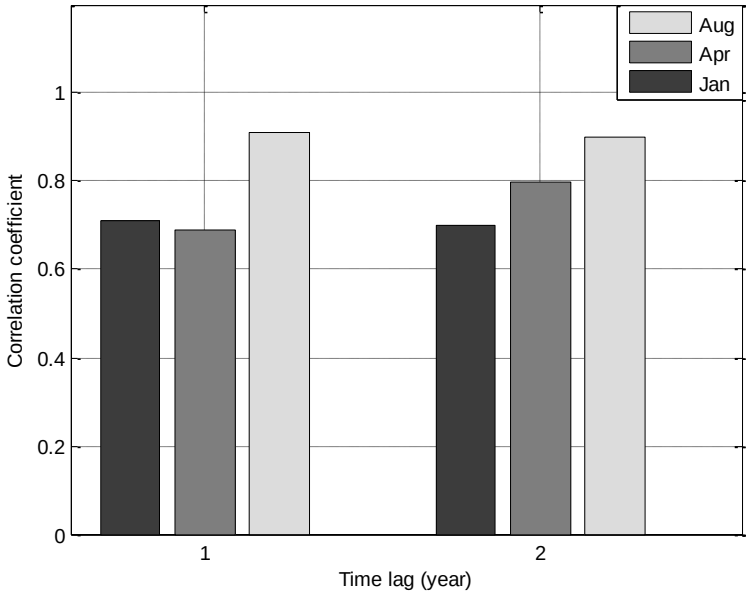

Figure 3-6 Correlation coefficient of wind speed using the proposed technique

Table 3-1 Wind Speed Limits

Index (j)	Wind speed limits	Index (j)	Wind speed limits
1	0 to 4	7	9 to 10
2	4 to 5	8	10 to 11
3	5 to 6	9	11 to 12
4	6 to 7	10	12 to 13
5	7 to 8	11	13 to 14
6	8 to 9	12	14 to 25

3.2.2.2 Wind Speed Estimation

Based on the results in the previous step, it can be concluded that utilizing a clustering technique is better than using a time-based technique to estimate the wind speed profile. However, in the clustering technique some randomness still exists. In order to minimize this amount of randomness, a Grey predictor GM(1,1) is utilized to estimate the annual wind speed profile of the site under study. The main advantages of the Grey predictor technique are:

- Utilizing an accumulated generating operation (AGO) technique to convert the original set of data into a new set of data (AGO) series; this new set of data is characerized by reduced noise and randomness and smoother pattern;
- Small amount of data is required in the estimation process; just three points are utilized to estimate the fourth one.

However, the main disadvantage of the traditional GM(1,1) model is the occurrence of overshoots in the predicted data which reduce prediction accuracy [73]. These overshoots are mitigated in this work by the proposed constraints controlling the prediction process.

The different steps to estimate the wind speed profile using Grey predictor GM(1,1) are:

Accumulated Generating Operation (AGO)

The aim of this operation is to convert the original set of data $X^{(0)}$ into a new set $X^{(1)}$ using (3.10).

$$X^{(1)}(K) = \sum_{i=1}^{k} X^{(0)}(i), \qquad \forall K = 1,.....n \tag{3.10}$$

1. ***Grey differential equation***

The general differential equation of GM(1,1) model is:

$$\frac{dX^{(1)}}{dt} + aX^{(1)} = b \tag{3.11}$$

The coefficients *a* and *b* are determined using least-squares.

2. ***Prediction equation for the GM(1,1)***

Estimated values of the AGO series ($X'^{(1)}$) are calculated as:

$$X'^{(1)}(i+1) = (X^{(0)}(1) - \frac{b}{a})e^{-ai} + \frac{b}{a} \tag{3.12}$$

3. ***Inverse Accumulated Generating Operation (IAGO)***

The original set of predicted data ($X'^{(0)}$) is calculated as:

$$X'^{(0)}(1) = X'^{(1)}(1) \tag{3.13}$$

$$X'^{(0)}(i+1) = X'^{(1)}(i+1) - X'^{(1)}(i) \tag{3.14}$$

The application of the proposed technique requires 12 Grey predictors for each month with 12 different *a* and *b* constants. To estimate a given element, in the year under study, the Grey predictor, assigned for this element will utilize the same element of the last *three* years (i.e. K=1, 2, 3). Since, the total number of estimated hours in any cluster S must be equal to the number of hours in the month presented by this cluster, this condition might not be fulfilled because the 12 Grey predictors of each cluster estimate the elements independently. To overcome this problem a constrained Grey predictor was developed. The key idea of this predictor is to calculate the constants *a* and *b* of the Grey predictors for all elements of any cluster S by formulating a non-linear optimization problem (NLP), with the objective being to minimize the summation of square errors of all the Grey predictors of each cluster while one of the constraints is that the total number of estimated hours in each cluster S must equal to the number of hours of the month presented by this cluster. The formulation of the NLP for each month is as follows:

Objective: The objective is to minimize the total square errors

$$Minimize \qquad C = \sum_{j=1}^{12} e_j \tag{3.15}$$

Constraints:

1. ***AGO***

$$X_j^{(1)}(K) = \sum_{i=1}^{k} X_j^{(0)}(i), \qquad \forall K, j \tag{3.16}$$

2. ***Prediction equation for the GM(1,1)***

$$X'^{(1)}_j(i+1) = (X_j^{(0)}(1) - \frac{b_j}{a_j})e^{-a_j i} + \frac{b_j}{a_j} \qquad \forall i, j \tag{3.17}$$

3. ***Summation of square errors for each predictor***

$$e_j = \sum_{i=1}^{3} (X'_j{}^{(1)}(i) - X_j{}^{(1)}(i))^2 \qquad \forall j \tag{3.18}$$

4. ***Inverse Accumulated Generating Operation (IAGO)***

$$X'_j{}^{(0)}(4) = X'_j{}^{(1)}(4) - X'_j{}^{(1)}(3) \qquad \forall j \tag{3.19}$$

5. ***Monthly hours constraints***

$$\sum_{j=1}^{12} X'_j{}^{(0)}(4) = H \tag{3.20}$$

This NLP was developed in GAMS, while MINOS is the solver.

3.2.2.3 Technique Validation

In order to check the validation of the proposed technique, three years of hourly historical data (2004, 2005 and 2006) of the site under study was collected, while the proposed technique was used to estimate the wind speed profile in 2007. Figure 3-7, figure 3-8 and figure 3-9 present a comparison between the actual data and the estimated data using this technique for different months.

Moreover, a comparison was conducted between the proposed technique and the common method of estimating the wind speed profile using a Weibull pdf. Table 3-2 shows that the proposed technique outperforms the Weibull pdf method, as should be apparent from comparison of the annual average absolute error calculation with respect to the actual data.

The most significant advantage of this model is that it does not need many years of historical data; just three years of historical data are sufficient to estimate the annual wind speed profile for the next year; hence, the profile can be updated annually. Therefore, this model is suitable for short term applications (up to one year). The main drawback of this model is its inability to fit with long term applications.

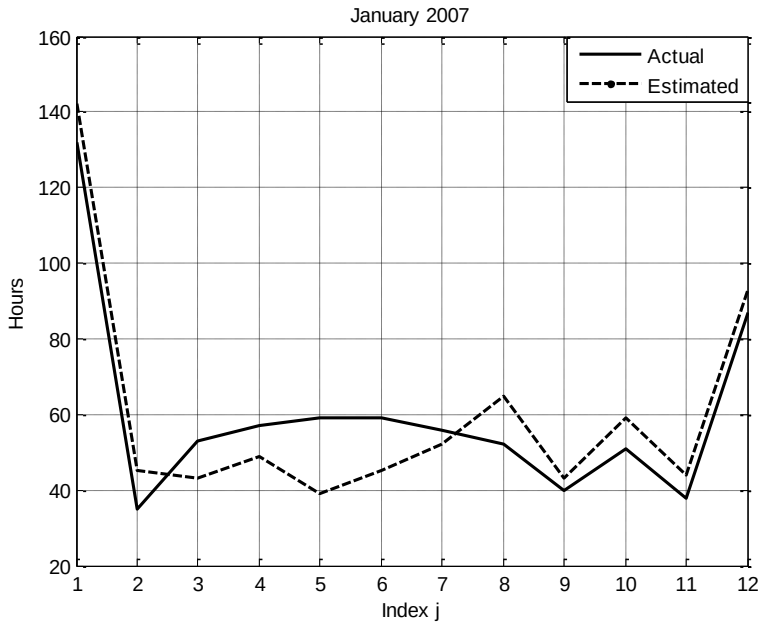

Figure 3-7 Comparison between the actual data and the estimated data for Jan

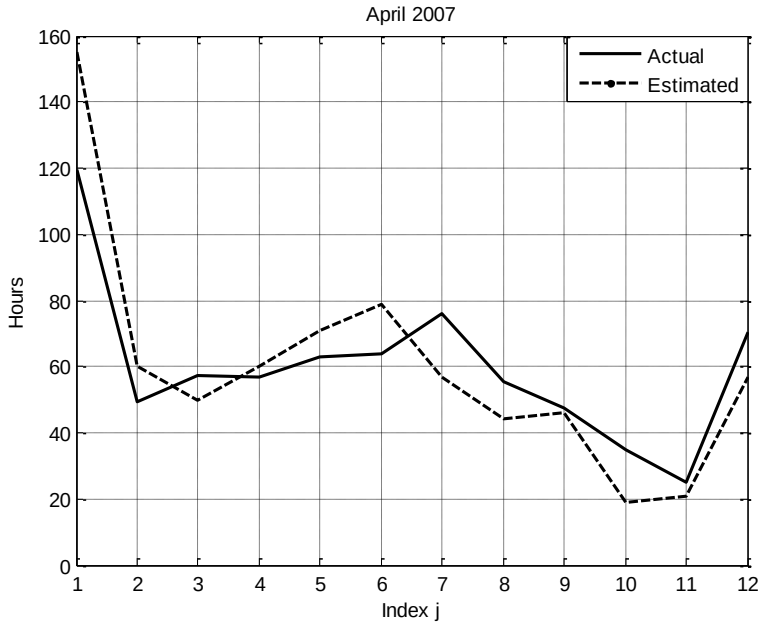

Figure 3-8 Comparison between the actual data and the estimated data for Apr

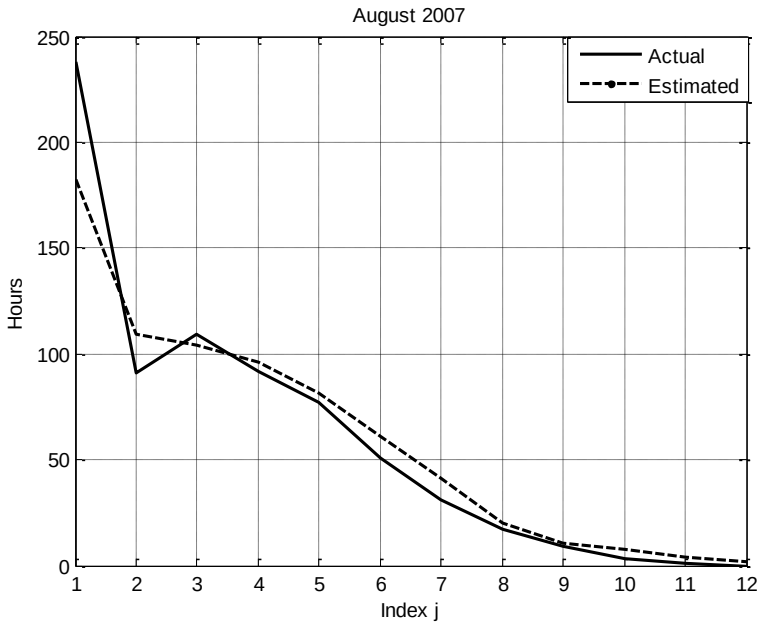

Figure 3-9 Comparison between the actual data and the estimated data for Aug

Table 3-2 Annual Average Absolute Error

Technique	Annual average absolute error
Proposed technique	13.4%
Weibull pdf	19.8%

3.2.3 Time Series Method for Wind Speed Modeling (wind model 6)

A time series is a sequence of data points, measured typically at successive times, spaced at time intervals. Wind speed modeling using a time series technique is based on the fact that observations close together in time will be more closely related than observations further apart. Moreover, time series techniques will often exploit the natural one-way ordering of time so that values in a series for a given time will be expressed as functions from past values, rather than from future values.

In this work, the auto regression moving average (ARMA) technique is used to model wind speed [74]. The ARMA(p, q) model is composed of two subcomponents: the autoregressive (AR) model, which involves lagged terms in the time series itself (wind speeds from previous hours), and the moving average (MA) model, which involves lagged terms in the noise or residuals, which are random (normally distributed). The annual site-specific hourly data for the mean wind speed (μ_t) and

standard deviation (σ_t) are utilized in order to calculate the ARMA parameters; hence, generating hourly wind speed data for the entire year as follows:

First, the hourly observed wind speed is utilized to calculate y_t; hence, y_t can be used to create the wind speed model as in (3.22). Finally the hourly simulated wind speed can be obtained from (3.23).

$$y_t = (HOWS_t - \mu_t)/\sigma_t \tag{3.21}$$

$$y_t = \sum_{i=1}^{p} \alpha_i y_{t-i} + e_t - \sum_{i=1}^{q} \theta_i e_{t-i} \tag{3.22}$$

$$HSWS_t = \mu_t + \sigma_t y_t \tag{3.23}$$

This model is very suitable for applications that required time series representation of wind speed such as unit commitment and storage scheduling. However, the main drawback is that a large amount of information is required to calculate the model parameters.

Table 3-3 summarizes the different models of wind speed accompanied by the advantages, the disadvantages and the applications of each model.

Table 3-3 Different Wind Speed Models

Model	**Application**
Wind model 1 and 2	Simple but the correlation between wind speed and load profile does not exist. It is suitable for long-term application
Wind model 3 and 4	More complicated, but provide the correlation between wind speed and load profile. It is suitable for long-term application
Wind model 5	It does not need many years of historical data, but it needs annual updates. It is suitable for short-term applications (up to one year).
Wind model 6	Very suitable for applications that require time series representation of wind speed as unit commitment and storage scheduling

3.3 Wind Turbine Output Power

Wind turbine is a machine that converts wind kinetic energy into mechanical energy in the shaft and finally into electrical energy in the generator. Currently, two types of wind turbines are commonly used today: vertical axis wind turbines and horizontal axis wind turbines. The rated power of a wind turbine is the maximum power allowed for the installed generator and the control system, and it must be ensured that this power is not exceeded in high winds. The number of blades is usually two or

three. Two-bladed wind turbines are cheaper since they have one blade fewer, but they rotate faster and appear more flickering to the eyes, whereas three-bladed wind turbines seem calmer and therefore less disturbing in a landscape. The rotational speed of a wind turbine rotor is approximately 20 to 50 rpm and the rotational speed of most generator shafts is approximately 1000 to 3000 rpm. Therefore a gearbox must be placed between the low-speed rotor shaft and the high-speed generator shaft.

There are three main factors that determine the power output of a wind turbine:

- power output curve (determined by aerodynamic power efficiency, mechanical transmission efficiency and converting electricity efficiency) of the chosen wind turbine;
- wind speed distribution of the selected site;
- tower height.

The data provided by the manufacturer regarding wind turbines are: the rated power, cut in speed, rated speed, and cut out speed. From these data the power output curve can be extracted; hence, the output power at any wind speed can be calculated. In this work, the power curve of the wind turbine is assumed to be linear [75, 76] as shown in figure 3-10 and equation (3.24).

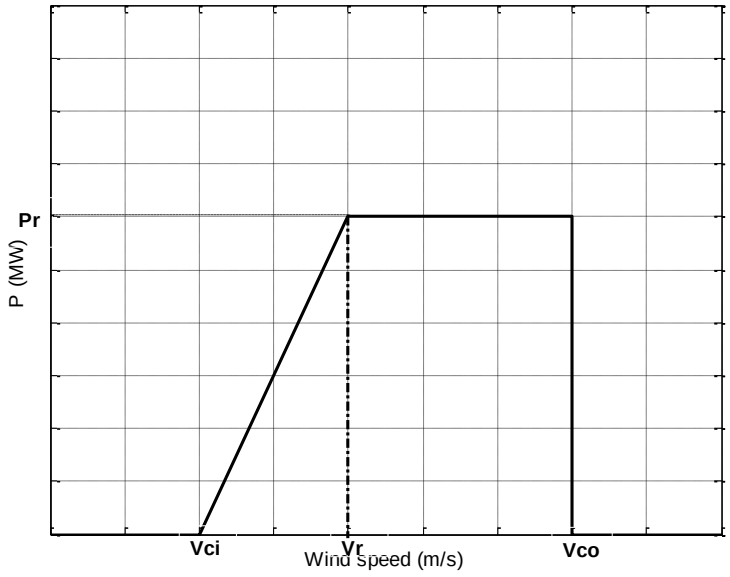

Figure 3-10 Wind turbine power curve

$$P(v) = \begin{cases} 0 & 0 \le v \le v_{ci} \\ P_{rated} * \dfrac{(v - v_{ci})}{(v_r - v_{ci})} & v_{ci} \le v \le v_r \\ P_{rated} & v_r \le v \le v_{co} \\ 0 & v_{co} \le v \end{cases} \tag{3.24}$$

3.4 Solar Irradiance Modeling

Solar energy can be used in two ways: 1) directly for heating of air or water without using an intermediate electric circuitry; 2) convert it into electricity by using photovoltaic (PV) modules. The second one is the most promising way of utilizing solar energy. The advantages of using photovoltaic effect to generate electricity are largely due to absence of pollutants during operation, silent operation, low maintenance requirements, and long service life. Moreover, solar energy is abundant, free, clean and inexhaustible.

Unlike wind speed, there is no way to utilize a pdf to describe the random behaviour of annual solar irradiance (as wind model 1). The rationale behind that is that in order to use a pdf to model a random variable, the variable must be totally random. However, this is not the case when dealing with solar irradiance as at night time, the value of solar irradiance is certain to be zero.

Therefore, to describe the random phenomenon of solar irradiance, a selected study period of one year is divided into four seasons, and a typical day is generated for each season in order to represent the random behaviour of the solar irradiance during each period. In other words, each year is divided into 4 seasons, with each season being represented by any day within that season. Furthermore, the day representing each season is subdivided into 24-hour segments (time segments), each referring to a particular hourly interval for the entire season. Thus, there are 96 time segments for the year (24 for each season). Considering a month to be 30 days and *y* years of historical data, each time segment then has 90*y* solar irradiance level data points (*y* years x 30 days per month x 3 months per season). From this data, the mean and standard deviation for each time segment are calculated, and thus, the proper pdf is generated for each hour. Here two different techniques are utilized to model the solar irradiance. The elaboration of these two techniques is introduced in the following subsections.

3.4.1 Bimodal Beta pdf Model (solar model 1)

This is a simple model to describe the random behaviour of solar irradiance, considering that all the solar irradiance enters the atmosphere and incidence in a given area is collected by the surface of the PV module.

For the same hour of the typical day in each season, irradiance data usually have a bimodal distribution function. In order to model this random phenomenon, the data are divided into two groups; each group has a unimodal distribution function. Hence, Beta pdf is utilized for each unimodal [77, 78], as set out in (3.25). The histogram and the probability density functions for solar irradiance for a typical day in April at 12:00 pm are shown in figure 3-11.

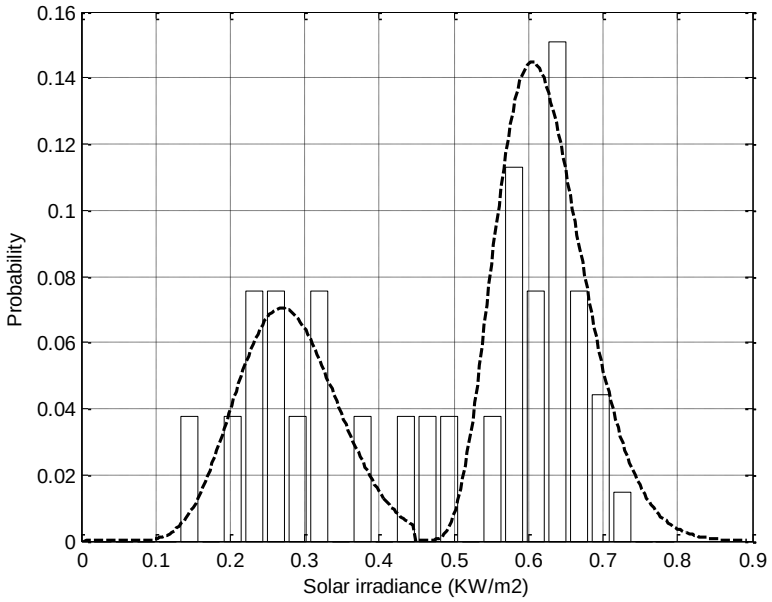

Figure 3-11 Histogram versus Beta distribution

$$f_b(s) = \begin{cases} \dfrac{\Gamma(\alpha+\beta c)}{\Gamma(\alpha)\Gamma(\beta c)} * s^{(\alpha-1)} * (1-s)^{(\beta c-1)} & for\ 0 \le s \le 1, \alpha \ge 0, \beta c \ge 0 \\ 0 & otherwise \end{cases} \quad (3.25)$$

To calculate the parameters of the Beta distribution function, the mean (μ) and standard deviation (σ) of the random variable s are utilized as follows:

$$\beta c = (1-\mu) * (\frac{\mu * (1+\mu)}{\sigma^2} - 1) \quad (3.26)$$

$$\alpha = \frac{\mu * \beta c}{1 - \mu} \tag{3.27}$$

This is a simple model that is viable for use with long term applications; however its accuracy is questionable, therefore it is a poor fit for short term applications, which require more accurate representation of the random variables.

3.4.2 Clearness Index Model (Solar model 2)

The amount of solar radiation that reaches the ground, besides the daily and yearly apparent motion of the sun, depends on both geographical location (latitude and altitude) and on the climatic conditions (e.g., cloud cover). Many studies have proved that cloudiness is the main factor affecting the difference between the values of solar radiation measured outside the atmosphere and at Earth's surface. Two clearness indices can be used to account for the difference between these two values:

- Daily clearness index (K_t): the ratio of a particular day's total solar radiation H_t (J/ m^2) to the extraterrestrial total solar radiation for that day H_o (J/ m^2), both referred to a horizontal surface
- Hourly clearness index (k_t): the ratio of the irradiance on a horizontal plane I_t (kW/ m^2), to the extraterrestrial total solar irradiance I_o (kW/ m^2).

Once the hourly clearness index is determined, the solar irradiance on a surface with inclination β can be calculated.

In this method, the hourly clearness index is modeled using a proper pdf; hence, different levels of solar irradiance with their probabilities, on the surface of a PV module with inclination β, are determined. From these levels and PV module characteristic, the output power can be calculated. Furthermore, the cumulative density function (cdf) of the clearness index pdf is calculated, and then inverted using a Lambert *W* function [79]. This invertible cdf is then utilized to model the clearness index chronologically using a MCS technique.

3.4.2.1 Modeling of Clearness Index

Here, the pdf proposed in [80-82] is utilized to model the random behaviour of the clearness index as in (3.28).

$$P(k_t) = C \frac{(k_{tu} - k_t)}{k_{tu}} \exp(\lambda k_t) \tag{3.28}$$

where C and λ are functions of the maximum value of clearness index (k_{tu}) and the mean clearness index (k_{tm}) as follows:

$$C = \frac{\lambda^2 k_{tu}}{(e^{\lambda k_{tu}} - 1 - \lambda k_{tu})} \tag{3.29}$$

$$\lambda = \frac{(2\gamma - 17.519\exp(-1.3118\gamma) - 1062\exp(-5.0426\gamma)}{k_{tu}} \tag{3.30}$$

$$\gamma = \frac{k_{tu}}{k_{tu} - k_{tm}} \tag{3.31}$$

Therefore, once λ is determined from (3.30) for a specific value of k_{tm}, the corresponding value of C can be determined from (3.29).

From the hourly clearness index, the hourly solar irradiance on a surface with inclination β to the horizontal plane (I_β) can be calculated as in (3.32):

$$I_\beta = \left[R_b + \left(\frac{1+\cos\beta}{2} - R_b \right) kd + \rho \frac{1-\cos\beta}{2} \right] . I_t \tag{3.32}$$

where

R_b: the ratio of beam radiation on the tilted surface to that on a horizontal surface;

kd: The fraction of the hourly radiation on horizontal plane which is diffuse;

ρ: The reflectance of the ground.

Further, I_t can be expressed as a function of k_t and I_o as follows:

$$I_t = I_o . k_t \tag{3.33}$$

In order to calculate the value of R_b, firstly, the following terms have to be calculated:

$$\beta = 90 - \beta_N \tag{3.34}$$

$$\beta_N = 90 - L + \delta \tag{3.35}$$

$$\delta = 23.45\sin\left[360\left(\frac{284+dn}{365} \right) \right] \tag{3.36}$$

$$\omega = \varpi(12 - t_s) \tag{3.37}$$

$$t_S = t + \frac{E}{60} + \frac{\Delta L}{15} \tag{3.38}$$

$$E = 9.87\sin(2B) - 7.53\cos(B) - 1.5\sin(B) \tag{3.39}$$

$$B = \frac{360(n-81)}{364} \tag{3.40}$$

For the site under study ΔL can be calculated as follows:

$$\Delta L = 90 - 83.8444 \tag{3.41}$$

Finally, R_b is calculated as follows:

$$R_b = \frac{\cos(\phi - \beta)\cdot\cos\delta\cdot\cos\omega + \sin(\phi-\beta)\cdot\sin\delta}{\cos\phi\cdot\cos\delta\cdot\cos\omega + \sin\phi\cdot\sin\delta} \tag{3.42}$$

Regarding the diffuse fraction (k), the correlation between it and the clearness index can be approximated with a piecewise linear function as follows [83]:

$$kd = p - qk_t \tag{3.43}$$

The constants p and q are calculated based on the range of k_t as follows:

$$kd = \begin{cases} 1 - 0.249k_t & k_t \le 0.35 \\ 1.557 - 1.84k_t & 0.35 \le k_t \le 0.75 \\ 0.177 & k_t \ge 0.75 \end{cases} \tag{3.44}$$

Whereas, the reflectance of the ground (ρ) is calculated based on the nature of the ground itself [84] as shown in Table 3-3.

Table 3-4 Reflectance Coefficient for Different Ground Covers

Ground cover	**Reflectivity (ρ)**
Water	0.07
Coniferous forest	0.07
Bituminous and gravel roof	0.13
Dry bare ground	0.2
Weathered concrete	0.22
Green grass	0.26
Dry grassland	0.2-0.3
Desert sand	0.4
Light building surfaces	0.6

Further, I_t can be expressed as a function of k_t and I_o as follows:

$$I_t = I_o.k_t \tag{3.45}$$

$$I_o = SC\left[1+0.33\cos(\frac{360n}{365})\right](\cos\phi\cos\delta\cos\omega+\sin\delta\sin\phi) \tag{3.46}$$

Hence, the final formula of I_β as function of clearness index is as given in (3.47).

$$I_\beta = \left[\left(R_b+\rho.\frac{1-\cos\beta}{2}\right)+\left(\frac{1+\cos\beta}{2}-R_b\right).p\right]I_o.k_t - \left(\frac{1+\cos\beta}{2}-R_b\right).q.I_o.k_t^2 \tag{3.47}$$

From this formula, it can be figured out that once the clearness factor is modeled, the solar irradiance and the output power of the PV module can be determined.

3.4.2.2 Development of Clearness Index Model for MCS Applications

In order to chronologically model the clearness index using MCS technique, the clearness index pdf is integrated, and then inverted to get the inverse transform of the clearness index cumulative density function (cdf). Once the invertible cdf is created, MCS can be utilized to model the clearness index. The process of generating the invertible cdf is elaborated herein.

The pdf of the clearness index can be written as in (3.48); hence, by integrating the pdf, using integration by parts, the cdf of the clearness factor is found to be as in (3.50).

$$P(k_t) = \left[e^{\lambda.k_t} - \frac{1}{k_{tu}}.k_t.e^{\lambda.k_t}\right] \tag{3.48}$$

$$cdf(k_t) = \int P(k_t).dk_t + c \tag{3.49}$$

$$cdf(k_t) = \frac{C}{\lambda}\left[\left(\frac{\lambda.k_{tu}+1-\lambda.k_t}{\lambda.k_{tu}}\right).e^{\lambda k_t}\right] + c \tag{3.50}$$

The integration constant c is found from the final value condition mentioned in (3.51).Based on this condition, the integration constant was found to be as shown in (3.52).

$$cdf(k_{tu}) = 1 \tag{3.51}$$

$$c = -\frac{C}{\lambda}(1+\frac{1}{\lambda.k_{tu}}). \tag{3.52}$$

In order to get the inverse of the cdf, the original cdf is rearranged using mathematical manipulation as in (3.53-3.55). Then a Lambert *W* function is used to get the inverse of the cdf.

$$cdf\,(k_t) = \frac{C}{\lambda}\left[\left(\frac{\lambda.k_{tu}+1}{\lambda.k_{tu}} + \frac{-1}{k_{tu}}.k_t\right).e^{\lambda k_t}\right] + c \tag{3.53}$$

$$cdf\,(k_t) = \frac{C}{\lambda}\left[(a + b.k_t).e^{\lambda k_t}\right] + c \tag{3.54}$$

$$cdf\,(k_t) = \frac{C}{\lambda}\left[(a + b.k_t).e^{\lambda k_t}\right] + c \tag{3.55}$$

where

$$a = \frac{\lambda.k_{tu}+1}{\lambda.k_{tu}} \tag{3.56}$$

$$b = \frac{-1}{k_{tu}} \tag{3.57}$$

Then, by doing the substitutions shown in (3.58) and (3.59), the cdf is changed to the form shown in (3.60)

$$y = a + b.k_t \tag{3.58}$$

$$z = \frac{\lambda.y}{b} \tag{3.59}$$

$$cdf = \frac{C}{\lambda}(y.e^{\lambda(\frac{y-a}{b})}) + c = \frac{C}{\lambda}(y.e^{(\frac{\lambda.y}{b})}.e^{(\frac{-\lambda.a}{b})}) + c = \frac{C}{\lambda}.e^{(\frac{-\lambda.a}{b})}(y.e^{(\frac{\lambda.y}{b})}) + c \tag{3.60}$$

$$cdf = const.z.e^{z} + c \tag{3.61}$$

$$const = \frac{C.b}{\lambda^2}e^{(-\frac{\lambda a}{b})} \tag{3.62}$$

Last, a Lambert *W* function is used to find the inverse of the cdf as follows:

$$z.e^{z} = (cdf - c)/const \tag{3.63}$$

$$z = W((cdf - c)/const). \tag{3.64}$$

Table 3-5 summarizes the different models of solar irradiance accompanied by the advantages, the disadvantages and the applications of each model.

Table 3-5 Different Solar Irradiance Models

Model	**Application**
Solar model 1	This is a simple model that is viable for use with long term applications; however its accuracy is questionable
Solar model 2	More accurate, but more complicated It is suitable for long-term and short-term applications

3.5 PV Output Power

The basic element of a solar energy conversion system is the PV module/cell, which absorbs photons of light from the incident solar radiation, and releases electrons to provide a DC current to a closed electrical circuit. The rating of a PV module is expressed in peak-watt and is equal to the maximum power produced by a module under standard test conditions (STC)[1]. However, a single PV module has limited potential to provide power at high voltage or high current levels. It is thus mandatory to connect PV modules in series and parallel, in a form of array, in order to scale-up the voltage and current to reach a given level of electrical power.

The manufacturers of PVs usually provide the characteristic of their PV module under STC by specifying I_{sc} (short circuit current in A), V_{oc} (open-circuit voltage in V), I_{MPP} (current at maximum power point in A), V_{MPP} (voltage at maximum power point in V), and N_{OT} (nominal operating temperature of cell in ^{o}C).

A typical graphical presentation of the current-voltage and power-voltage characteristics of a PV module is shown in figure 3-12. This current-voltage characteristic is valid for a particular radiation level and ambient temperature. The short circuit current is directly proportional to the solar radiation, whereas the voltage is inversely proportional to the temperature. Moreover, most of the PV modules are equipped with a maximum power point tracker which helps the PV system to operate near the knee of the I-V curve all day long to generate maximum power from the PV in different weather conditions.

[1] STC corresponds to a radiation level of 1 kW/m^2 and a cell temperature of 25°C.

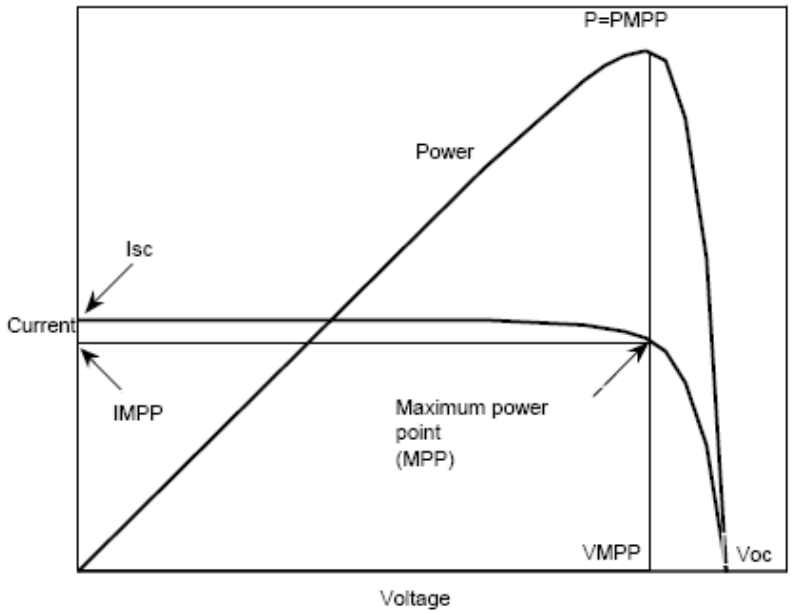

Figure 3-12 Photovoltaic characteristics

The current-voltage characteristics of a PV cell can be determined for different radiation levels and temperatures by using equations (3.65) to (3.69) [85].

$$Tc = T_A + I_\beta(\frac{N_{OT} - 20}{0.8}) \tag{3.65}$$

$$I = I_\beta[I_{sc} + K_i(Tc - 25)] \tag{3.66}$$

$$V = V_{oc} - K_v * Tc \tag{3.67}$$

$$P = N * FF * V * I \tag{3.68}$$

$$FF = \frac{V_{MPP} * I_{MPP}}{V_{oc} * I_{sc}} \tag{3.69}$$

3.6 Load Modeling

In this work, two different models are used to describe the annual system load profile. In these two models, it is assumed that the peak load follows the load shape of the IEEE-RTS system. A detailed elaboration of these two models is as follows:

3.6.1 Annual Load Modeling (load model 1)

In this model it is assumed that the load is divided into ten levels [86] using the clustering technique, based on the central centroid sorting process developed in [87, 88], which verifies that choosing ten equivalent load levels provides a reasonable trade-off between accuracy and fast numerical evaluation. Table 3-6 shows the ten load levels accompanied by their probabilities.

Table 3-6 Load Model 1

% Peak	Probability (%)
100	01
85.3	5.6
77.4	11.97
71.3	17.54
65	17.54
58.5	17.3
51	16.55
45.1	10.11
40.6	5.71
35.1	4.54

3.6.2 Typical Hour Load modeling (load model 2)

In this model, the load profile is assumed to follow the IEEE-RTS system presented in [89]. This system provides weekly peak load as a percentage of the annual peak load, daily peak load cycle as a percentage of the weekly peak, and hourly peak load as a percentage of the daily peak load as shown in Table 3-7 to Table 3-9.

Table 3-7 Weekly Peak Load in Percent of Annual Peak

Week	Peak load	Week	Peak load
1	86.2	27	75.5
2	90	28	81.6
3	87.8	29	80.1
4	83.4	30	88
5	88	31	72.2
6	84.1	32	77.6
7	83.2	33	80
8	80.6	34	72.9
9	74	35	72.6
10	73.7	36	70.5
11	71.5	37	78
12	72.7	38	69.5
13	70.4	39	72.4
14	75	40	72.4
15	72.1	41	74.3
16	80	42	74.4
17	75.4	43	80
18	83.7	44	88.1
19	87	45	88.5
20	88	46	90.9
21	85.6	47	94
22	81.1	48	89
23	90	49	94.2
24	88.7	50	97
25	89.6	51	100
26	86.1	52	95.2

Table 3-8 Daily Peak Load Cycle in Percent of Weekly Peak

Day	Peak load
Monday	93
Tuesday	100
Wednesday	98
Thursday	96
Friday	94
Saturday	77
Sunday	75

Table 3-9 Hourly Peak Load in Percentage of Daily Peak

Hour	Winter	Spring	Summer	Fall
12-1 am	67	63	64	63
1--2	63	62	60	62
2--3	60	60	58	60
3--4	59	58	56	58
4--5	59	59	56	59
5--6	60	65	58	65
6--7	74	72	64	72
7--8	86	85	76	85
8--9	95	95	87	95
9--10	96	99	95	99
10--11	96	100	99	100
11--12pm	95	99	100	99
12--1	95	93	99	93
1--2	95	92	100	92
2--3	93	90	100	90
3--4	94	88	97	88
4--5	99	90	96	90
5--6	100	92	96	92
6--7	100	96	93	96
7--8	96	98	92	98
8--9	91	96	92	96
9--10	83	90	93	90
10--11	73	80	87	80
11--12am	63	70	72	70

3.7 Discussion

In this chapter different approaches to model the random behaviour of wind speed and solar irradiance are presented. With regards to wind speed, Weibull and Rayleigh pdfs are used to model annual and typical day wind speed profiles probabilistically, while ARMA is used to model it chronologically. Furthermore, a novel constrained Grey predictor technique was utilized to estimate the wind speed profile. The validity of the proposed technique was checked by comparing the estimated wind speed profile of this technique with estimated wind speed profile using the common Weibull pdf.

As to solar irradiance, Bimodal Beta pdf and the pdf of the clearness index are used to model a typical day solar irradiance profile. The latter one has been developed to adopt with the applications that require MCS. Finally, different load models used in this work are presented.

Chapter 4

Optimal Allocation of Renewable Resources in Distribution Systems

4.1 Introduction

It is widely accepted that renewable energy sources are the key to a sustainable energy supply infrastructure since they are both inexhaustible and non-polluting. A number of renewable energy technologies are now commercially available, the most notable being wind power, photovoltaic, solar thermal systems, biomass, and various forms of hydroelectric power.

However, due to the intermittent nature of most of renewable resources such as wind speed and solar irradiance, any improper allocation of these DG units in the distribution system may negatively impact the system performance in terms of the acceptable voltage limit, the capacity of the distribution feeder, and the acceptable amount of reverse power flow. Therefore, proper allocation of DG units into an existing distribution system is one of the most important aspects of DG planning.

This chapter presents the methodology that is proposed, as shown in figure 4-1, for optimally allocating different types of renewable distributed generation (DG) units in distribution systems so as to minimize annual energy loss. The methodology is based on generating a probabilistic generation-load model that combines all possible operating conditions of the renewable DG units with their probabilities, hence accommodating this model in a deterministic planning problem. The planning problem is formulated as mixed integer non-linear programming (MINLP), with an objective function to minimize the system's annual energy losses. The constraints include the voltage limits, the feeders' capacity, the maximum penetration limit, and the discrete size of the available DG units. This proposed methodology is applied to a typical rural distribution system with different scenarios, including all possible combinations of the renewable DG units.

This chapter is organized as follows: the next four sections explain the objective function, the renewable resource modeling, the load modeling and the combined generation-load modeling. Then Section 4.6 presents the mathematical formulation of the proposed planning technique, and Section 4.7 introduces the case study of a distribution system. The results are shown in section 4.8, and then contributions of the proposed methodology and discussion are presented in the last two sections.

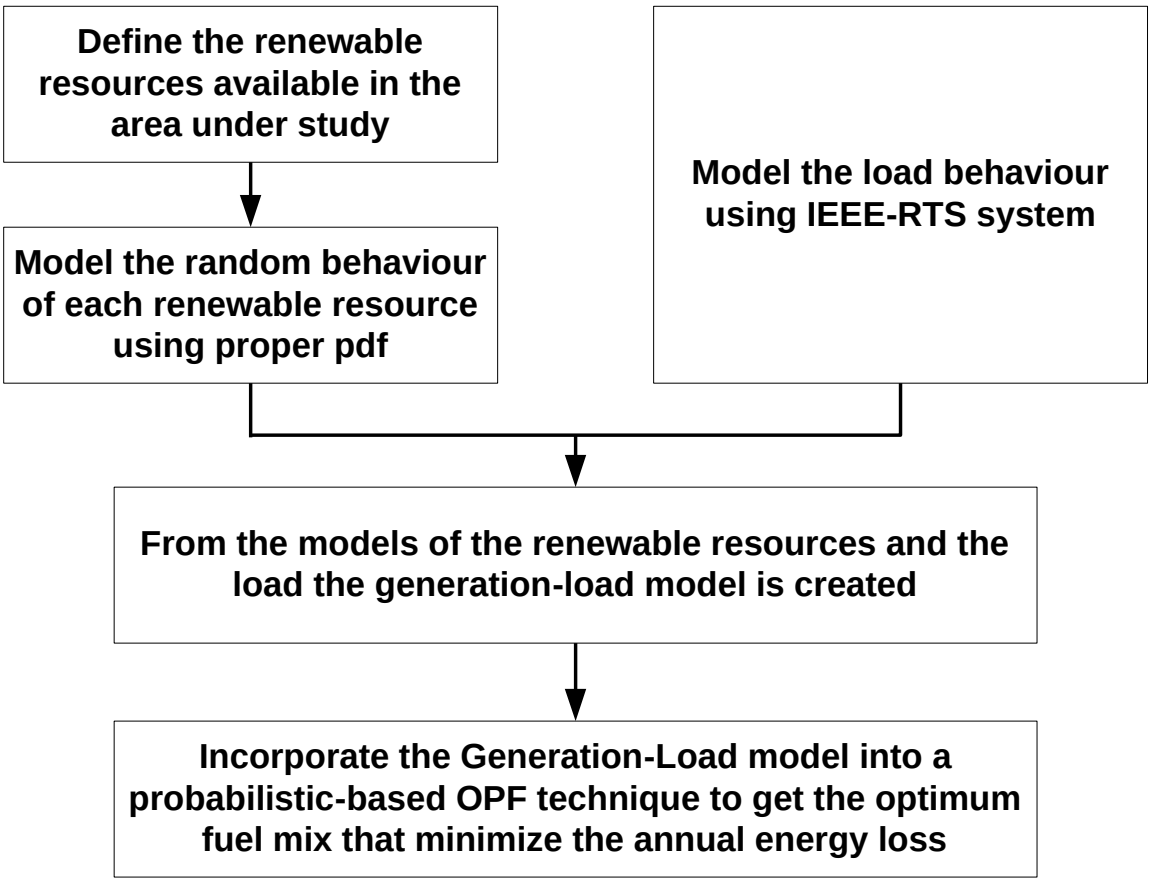

Figure 4-1 Block diagram of the proposed work

4.2 Objective Function

Due to the environmental concerns and fuel cost uncertainties associated with the use of conventional energy sources, attention has been directed toward implementing renewable DG units in distribution systems. Therefore, in Canada, based on Ontario's Standard Offer program (SOP) [90], local distribution companies (LDCs) are required to accept a given percentage of *customer-owned* wind-based DG units in their system. Consequently, LDCs can use the proposed method to select the allocations that will maximize benefits.

In general, benefit maximization in any normal planning problem means minimizing cost while maintaining the performance of the system within acceptable limits. Costs include the following:

- *Capital cost:* In this case, the capital cost of the renewable DG units is the sole responsibility of the customer.

- *Running cost (operation and maintenance cost):* As with the capital cost, operation and maintenance are the sole responsibilities of the customer.
- *Cost of unserved energy due to interruption (maximizing the system reliability):* Based on the current practice of deploying DG units in distribution systems, this cost represents the impact of renewable DG on the reliability of such distribution systems. In this regard, the following should be noted:
    1. A distribution network is fed from a transmission network, and when the connection to the transmission system is lost, i.e., the distribution network is islanded, all DG units are required to shut down for loss-of-main protection. This practice is normal, and DG therefore does not play a role in increasing the reliability of the supply [8].
    2. If islanding is allowed, the system can not rely solely on renewable DG units to supply the island's load. Renewable DG units are characterized by high levels of random power fluctuation that result in power mismatch issues, causing stability problems with respect to voltage and frequency [91].
    3. Conversely, renewable DG has the potential to improve the distribution system supply adequacy by increasing the amount of generated power in the system. Furthermore, renewable DG can also improve the reliability of the system from the perspective of relieving substation transformers and main feeders during peak load periods. This relief may result in extending the usable lifetime of the transformer and reducing the probability of premature failure due to overloading. However, these potential improvements in reliability and adequacy do not depend on the placement of the DG units on the feeders and is therefore outside the scope of this study. Thus, for the purposes of this study, it is assumed that the location of renewable DG units on a given feeder has no direct influence on the reliability of the distribution system.
- *Feeder power losses:* Network losses are a key consideration in the planning problem for the following reasons:
    1. While DG may unload lines and reduce losses, if they are improperly allocated, the reverse power flows from larger DG units can give rise to excessive losses and can overheat feeders.
    2. Minimizing system power losses has a positive impact on relieving the feeders, reducing the voltage drop, and improving the voltage profile and has other environmental and economical benefits.

Therefore, based on these considerations, the objective of the proposed planning problem is, for all possible operating conditions, to minimize the annual energy losses of the system without violating system constraints.

4.3 Modeling of the Renewable Resources and Load Data

In this work, for the site under study, the hourly solar irradiance and wind speed data are modeled by Beta and Rayleigh probability density functions (pdf), respectively (solar model 1 and wind model 4). The biomass DG is considered as a firm generation DG. In other words, the output power of such DG is considered constant at its rated value with no associated uncertainties. The load profile is assumed to follow the IEEE-RTS system (load model 2).

For solar irradiance and wind speed, based on solar model 1 and wind model 4, each season in the year is represented by a typical day. Thus, there are 96 time segments for the year (24 for each season) and Beta pdf and Rayleigh pdf are utilized to model the hourly solar irradiance and wind speed. Here, the Beta and Rayleigh probability distribution functions that are required for estimating the hourly solar irradiance and wind speed, are based on three years of historical data that have been collected from the site under study. Considering a month to be 30 days, each time segment then has 270 irradiance and wind speed level data points (3 years x 30 days per month x 3 months per season). From this data, the mean and standard deviation for each time segment are calculated, and from them, the Beta and Rayleigh probability density functions are generated for each hour.

To incorporate the output power of the solar DG and wind-based DG units as multi-state variables in the planning formulation, the continuous pdf of each has been divided into states (periods), in each of which the solar irradiance and wind speed are within specific limits. In other words, for each time segment, there are a number of states for the solar irradiance and wind speed. The number of states is carefully selected for the Beta and Rayleigh distributions because a small number of states affects accuracy, while a large number increases the complexity of the problem. In this work, the step is adjusted to be 0.1 Kw/m^2 for the solar irradiance and 1m/s for wind speed.

The probability of the solar irradiance and wind speed DG for each state during any specific hour is calculated using equations (4.1) and (4.2), respectively.

$$P_s\{G_y\} = \int_{s_{y1}}^{s_{y2}} f_b(v).dv \qquad (4.1)$$

$$P_v\{G_w\} = \int_{v_{w1}}^{v_{w2}} f_r(v).dv \quad (4.2)$$

After generating the hourly solar irradiance and wind speed states, the different levels of power output from the solar DG and the wind-based DG can be calculated along with their probabilities, using equations (3.24) and (3.65)-(3.69). For simplicity, the average value of each state is utilized to calculate the output power for that state (e.g., for wind speed, if the second state has limits of 1 m/s and 2 m/s, the average value for this state is (v_{a2}) =1.5 m/s).

4.4 Site matching

This section details the steps for selecting the optimum PV module and wind turbine for a specific site. The selection is based on the capacity factor (CF) of the available PV modules and wind turbines. A capacity factor can be defined as the ratio between the average output power and the rated power. The hourly average output power of a PV module or a wind turbine is the summation of the power produced at all possible states for this hour multiplied by the corresponding probability of each state. Once the average output power is calculated for each time segment, the average output power is calculated for the typical day in each season, and hence, the annual average output power.

For this study, the optimal PV module or wind turbine is selected based on the highest CF criteria. However, it must be mentioned that selecting the candidate wind turbine based on the highest CF may not lead to optimal loss minimization from a planning perspective because implementing the highest CF restricts the search area to a multiple of the selected wind turbine rating (e.g., if the turbine with the highest CF has a rating of 1 MW, then the wind-based DG penetration at the candidate buses must be a multiple of that rating).

This problem does not appear with PV modules because their ratings are very small compared to the required amount of solar DG (e.g., if the PV module with the highest CF has a rating of 60 W and the required solar DG penetration is 1.236 MW at a specific bus, this level can be achieved by using a PV panel consisting of 20,600 modules).

4.5 Combined Generation Load Model

The modeling of different types of renewable DG and the load are utilized to generate a combined annual generation-load model. Assuming that wind speed states and solar irradiance states are independent, the probability of any combination of them ($P\{C_g\}$) is obtained by convolving the two probabilities, as given in equation (4.3):

$$P\ \{C_g\} = P_v\{G_w\} * P_s\{G_y\} \quad (4.3)$$

Since the load and the output power of the biomass DG units are constant during each hour, the probability of each is 1. Hence, they are not incorporated into equation (4.3).

Based on this concept, a generation-load model for different types of renewable DG units is obtained by listing all possible combinations of renewable DG output power and the load for the whole year. The complete generation-load model is given as equation (4.4):

$$R = [\{C_g, P\{C_g\}\ \} : g = 1 : N] \quad (4.4)$$

where

C A matrix of 4 columns that include all possible combinations of the wind output power states and solar output power states as well as the load states and the firm generation of the biomass DG (i.e., column 1 represents the output power of wind-based DG as a percentage of the rated power, column 2 represents the output power of the solar DG as a percentage of the rated power, column 3 represents the constant output power of the biomass DG, and column 4 represents the different load levels).

Here, a small-scale example of the generation-load model is presented.

Consider that for the t^{th} time segment (hour), the probability distribution for wind speed and solar irradiance are W^t and S^t, respectively, and are given by W^t= [{0, 0.3}, {0.5, 0.6}, {1, 0.1}]; S^t= [{0, 0.4}, {0.5, 0.5}, {1, 0.1}];

The first element of each set is the output of the DG as a percentage of the rated power; the second element is the probability of occurrence during the t^{th} time segment. The load during this hour is assumed to be 0.65 of the peak load, while the biomass DG output is constant at the rated power.

The number of wind speed states *w*=3.

The number of solar irradiance states *y*=3.

The total number of states *N* = 3*3 =9. Matrix C_g is as shown in Table 4-1, while *P* (C_g) is as shown in Table 4-2.

Table 4-1 Different Combinations of Load and Wind Power (Matrix *Cg*)

State	Wind-based DG output as a percentage of rated power	Solar DG output as a percentage of rated power	Biomass DG output as a percentage of rated power	Load as a percentage of peak load
1	0	0	1	0.65
2	0	0.5	1	0.65
3	0	1	1	0.65
4	0.5	0	1	0.65
5	0.5	0.5	1	0.65
6	0.5	1	1	0.65
7	1	0	1	0.65
8	1	0.5	1	0.65
9	1	1	1	0.65

Table 4-2 Probability of Different Combinations of Load and Renewable Output Power (*P*(*Cg*))

State	Probability	State	Probability	State	Probability
1	0.3*0.4=0.12	**4**	0.6*0.4=0.24	**7**	0.1*0.4=0.04
2	0.3*0.5=0.15	**5**	0.6*0.5=0.30	**8**	0.1*0.5=0.05
3	0.3*0.1=0.03	**6**	0.6*0.1=0.06	**9**	0.1*0.1=0.01

4.6 Planning problem formulation

This section presents the proposed probabilistic formulation for a local distribution company's (LDC) planning problem with respect to the system under study. The rationale behind the proposed technique is to accommodate the probabilistic generation-load model into the deterministic optimal power flow (OPF) equations. In other words, the number of active/reactive power flow equations, (4.6) and (4.7), is equal to the total number of states. For each state, the penetration of the renewable DG units is changed based on the generation-load model, while the power loss is calculated and then weighted according to the probability of occurrence of this state during the entire year, in order to calculate the energy losses. The optimum allocations of the DG units are then determined so that, for all operating conditions, the total energy losses are minimized without violating the system constraints.

To formulate an accurate planning strategy that determines the optimal fuel mix of renewable DG units, the following assumptions are made:

- More than one type of DG can be connected to the same bus.

- All the DG units are working at a unity power factor.
- The LDC will not make any upgrades in the system as a consequence of connecting the DG units, such as changing the feeders or adding regulating stations.
- In the radial system under study, there is an assumed maximum limit for investing in DG capacities for each bus [20].
- For the sake of simplicity, it is assumed that all buses in the system under study are subjected to the same wind profile and solar irradiance; if it is not true it only complicates the generation-load model.

For determining the optimal fuel mix of renewable resources, seven scenarios are proposed, along with an extra reference scenario for comparison:

1) *Scenario #1:* the reference scenario, in which no DG units are connected to the system (base case);
2) *Scenario #2:* only wind-based DG;
3) *Scenario #3:* only biomass DG units;
4) *Scenario #4:* only solar DG units;
5) *Scenario #5:* wind-based DG with solar DG;
6) *Scenario #6:* wind-based DG with biomass DG;
7) *Scenario #7:* solar DG with biomass DG.
8) *Scenario #8:* a mix of wind-based, solar and biomass DG.

The mathematical formulation is described in equations (4.5) - (4.16). This model is formulated as MINLP on a GAMS environment [92]. Since most of the distribution systems have a radial topology, in the formulation, bus 1 is the substation bus.

Objective function

The objective of the planning formulation is to minimize the annual energy losses in the distribution system for all possible combinations of load and DG output power. Since each time segment represents 90 hours (30 days per month x 3 months per season), the objective function can be described as follows:

$$Minimize \qquad Cost = \sum_{g=1}^{N} P_{loss_g} * P\{C_g\} * 90 \tag{4.5}$$

Constraints

1. *Power flow equations:*

$$P_{G_{g,1}} + C(g,1) * P_{DG\,W_i} + C(g,2) * P_{DG\,S_i} + C(g,3) * P_{DGb_i} - C(g,4) * P_{D_i} = \sum_{j=1}^{n} V_{g,i} * V_{g,i} * Y_{ij} * \cos(\theta_{ij} + \delta_{g,j} - \delta_{g,i}) \;\forall i, g \quad (4.6)$$

$$Q_{G_{g,1}} - C(g,4) * Q_{D_{g,i}} = -\sum_{j=1}^{n} V_{g,i} * V_{g,i} * Y_{ij} * \sin(\theta_{ij} + \delta_{g,j} - \delta_{g,i}) \quad \forall i, g \quad (4.7)$$

2. *Power loss equations:*

$$P_{loss_g} = 0.5 * \sum_{i=1}^{n} \sum_{j=1}^{n} G_{ij} * \left[(V_{g,i})^2 + (V_{g,j})^2 - 2 * V_{g,i} * V_{g,j} * \cos(\delta_{g,j} - \delta_{g,i})\right] \forall g \quad (4.8)$$

3. *Branch current equations:*

$$I_{g,ij} = \left|Y_{ij}\right| * \left[(V_{g,i})^2 + (V_{g,j})^2 - 2 * V_{g,i} * V_{g,j} * \cos(\delta_{g,j} - \delta_{g,i})\right]^{1/2} \quad \forall g, i, j \quad (4.9)$$

4. *Slack bus voltage and angle (assumed to be bus 1):*

$$V_{g,1} = 1.0$$
$$\delta_{g,1} = 0.0 \quad (4.10)$$

5. *Voltage limits at the other buses:*

$$V_{\min} \le V_{g,i} \le V_{\max} \quad \forall\, i \notin \textit{substation bus},\ g \quad (4.11)$$

6. *Feeder capacity limits:*

$$0 \le I_{g,ij} \le I_{ij_{\max}} \quad \forall i, j, g \quad (4.12)$$

7. *Discrete size of the DG units:*

a) *Wind-based DG units:*

$$P_{DGW_i} = a_{w1,i}.P_{rw1} + a_{w2,i}.P_{rw2} + ... \qquad \forall i \in B \tag{4.13}$$

where

$a_{w1,i}$, $a_{w2,i}$ … are integer variables. Prw_1, Prw_2 … are the available ratings of the wind-based DG units.

b) *Biomass DG units:*

$$P_{DGb_i} = a_{b1,i}.P_{rb1} + a_{b2,i}.P_{rb2} + ... \qquad \forall i \in B \tag{4.14}$$

where

$a_{b1,i}$, $a_{b2,i}$ … are integer variables. Prb_1, Prb_2 … are the available ratings of the biomass DG units.

c) *Solar DG units:*

Unlike the wind-based DG and the biomass DG, the solar DG rating has no limit because the PV array can be arranged to generate almost the power required.

8. *Maximum penetration on each bus:*

$$P_{DGW_i} + P_{DGS_i} + P_{DGb_i} \le P_{bus} \qquad \forall i \in B \tag{4.15}$$

9. *Maximum penetration of DG units in the system:*

The maximum penetration limit is calculated based on the average penetration of the renewable DG units:

$$\sum_{i=1}^{n} CF_w * P_{DGW_i} + \sum_{i=1}^{n} CF_s * P_{DGS_i} + \sum_{i=1}^{n} P_{DGb_i} \le x * \sum_{i=1}^{n} P_{D\,i} \tag{4.16}$$

4.7 Case Study

This section presents the general data, wind speed data, solar irradiance data, PV module characteristics, and wind turbine data for the system under study.

4.7.1 System under Study

The system under study, as shown in figure 4.2, is a typical rural distribution system with a peak load of 16.18 MVA. The main substation at bus 1 is used to feed a rural area, and the maximum feeder capacity is 300 A. The data of the system are given in appendix A.

For this study, the candidate buses for connecting the DG units are included in the set *B*:{19, 23, 24, 26, 28, 32, 33, 35, 37, 38, 39, 40}, based on Ontario's standard offer program, the maximum limit for investing in DG capacities on each bus is 10 MW (i.e. P_{bus}=10 MW), and the maximum penetration limit is 30% of the peak load (i.e., x=0.3).

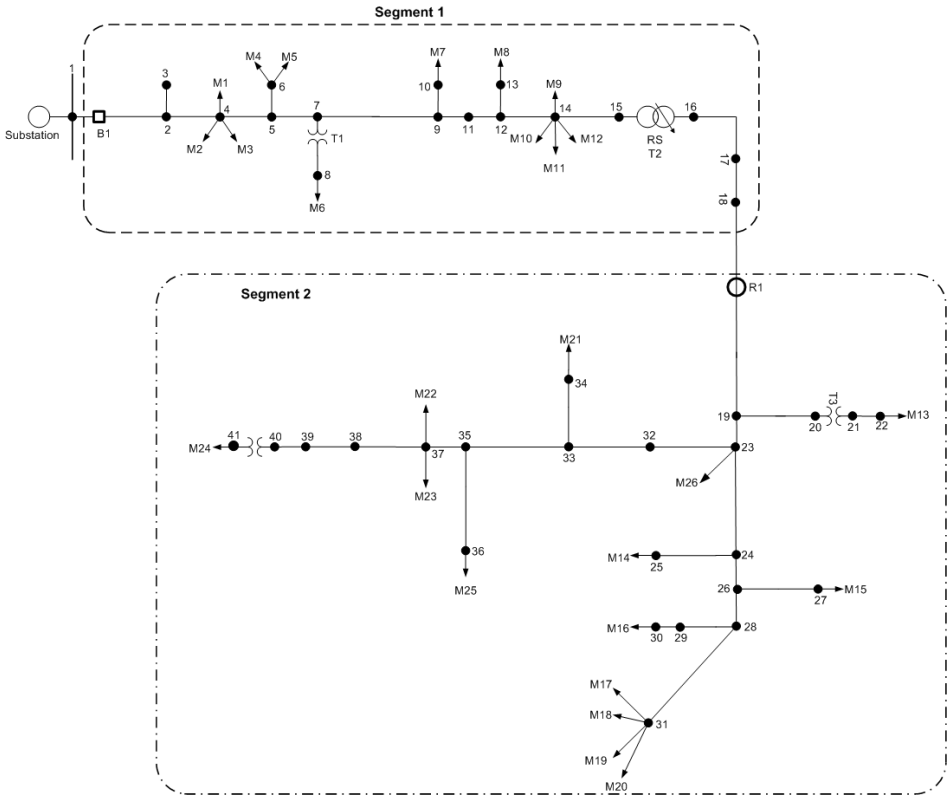

Figure 4-2 System under study

4.7.2 Wind Speed and Wind Turbine Data

The hourly wind speed data for the site under study have been utilized to generate a Rayleigh pdf (wind Model 4) for each time segment and thus to calculate the CF for each available wind turbine, as listed in Table 4-3. As shown in Figure 4-3, it is obvious that of all the turbines available, turbine 2 has the highest CF (0.2209); therefore, wind turbine type 2 is used for this study.

Table 4-3 Characteristics of the Wind Turbines Available

Features	Turbine 1	Turbine 2	Turbine 3	Turbine 4
Rated power	850 KW	1.1 MW	2 MW	3 MW
Cut-in speed (m/s)	4	4	4	4
Rated speed(m/s)	16	14	15	15
Cut-out speed (m/s)	25	24	25	25

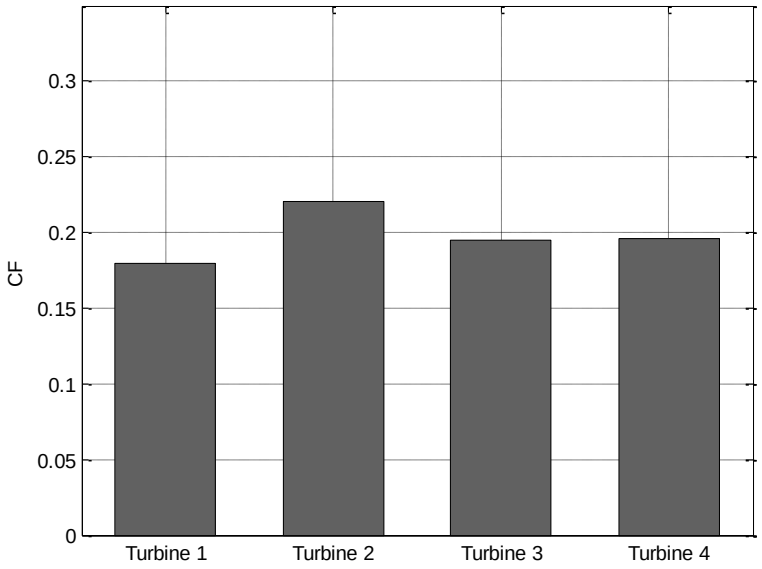

Figure 4-3 CF of the wind turbines available

4.7.3 Solar Irradiance and PV Module Data

The hourly solar irradiance data for the site under study have been utilized to generate a Beta pdf (solar model 1) for each time segment and thus to calculate the CF for each available PV module, as listed in Table 4-4. As shown in figure 4-4, it is obvious that of all the modules available, module D has the highest CF (0.174); therefore, module type D is used for this study.

Table 4-4 Characteristics of the PV Modules Available

Module characteristics	Module type			
	A	**B**	**C**	**D**
Watt peak (W)	50.00	53.00	60.00	75.00
Open circuit voltage (V)	55.50	21.70	21.10	21.98
Short circuit current (A)	1.80	3.40	3.80	5.32
Voltage at maximum power (V)	38.00	17.40	17.10	17.32
Current at maximum power (A)	1.32	3.05	3.50	4.76
Voltage temperature coefficient (mV/^{o}C)	194.00	88.00	75.00	14.40
Current temperature coefficient (mA/^{o}C)	1.40	1.50	3.10	1.22
Nominal cell operating temperature (^{o}C)	43.00	43.00	43.00	43.00

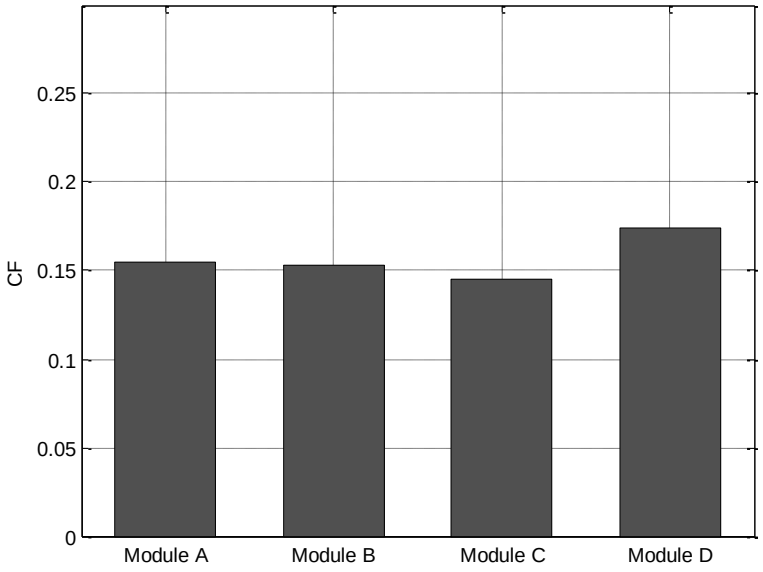

Figure 4-4 CF of the PV modules available

4.7.4 Biomass DG Unit Data

For this study, the ratings available for the biomass DG units have been selected to be 1MW and 0.5 MW.

4.7.5 Load Data

The load profile is assumed to follow the IEEE-RTS (load model 2). From this model and three years of historical data regarding the system under study hourly load, a typical daily load profile for each season has been generated as a percentage of the annual load as shown in Table 4-5.

Table 4-5 Load Profile

Hour	Winter	Spring	Summer	Fall
12-1 am	0.4757	0.3969	0.64	0.3717
1--2	0.4473	0.3906	0.60	0.3658
2--3	0.4260	0.3780	0.58	0.3540
3--4	0.4189	0.3654	0.56	0.3422
4--5	0.4189	0.3717	0.56	0.3481
5--6	0.4260	0.4095	0.58	0.3835
6--7	0.5254	0.4536	0.64	0.4248
7--8	0.6106	0.5355	0.76	0.5015
8--9	0.6745	0.5985	0.87	0.5605
9--10	0.6816	0.6237	0.95	0.5841
10--11	0.6816	0.6300	0.99	0.5900
11--12pm	0.6745	0.6237	1.00	0.5841
12--1	0.6745	0.5859	0.99	0.5487
1--2	0.6745	0.5796	1.00	0.5428
2--3	0.6603	0.5670	1.00	0.5310
3--4	0.6674	0.5544	0.97	0.5192
4--5	0.7029	0.5670	0.96	0.5310
5--6	0.7100	0.5796	0.96	0.5428
6--7	0.7100	0.6048	0.93	0.5664
7--8	0.6816	0.6174	0.92	0.5782
8--9	0.6461	0.6048	0.92	0.5664
9--10	0.5893	0.5670	0.93	0.5310
10--11	0.5183	0.5040	0.87	0.4720
11--12am	0.4473	0.4410	0.72	0.4130

4.8 Results

The data for the seven main scenarios discussed in section 5.6 are analyzed by the model to determine the optimal fuel mix of renewable DG units that will minimize system energy losses. The outcomes of

the planning problem for the seven scenarios proposed and for the reference scenario are shown in Table 4-6, Table 4-7 and figure 4-5 to figure 4-11. The results reveal that regardless of the combination of the renewable resources used to calculate the optimal fuel mix, there is a significant reduction in the annual energy losses for all proposed scenarios when compared to the reference scenario. In addition, the same scenarios were repeated after relaxing the discrete size constraints in order to measure how far the outcomes of the MINLP are from the global optimal.

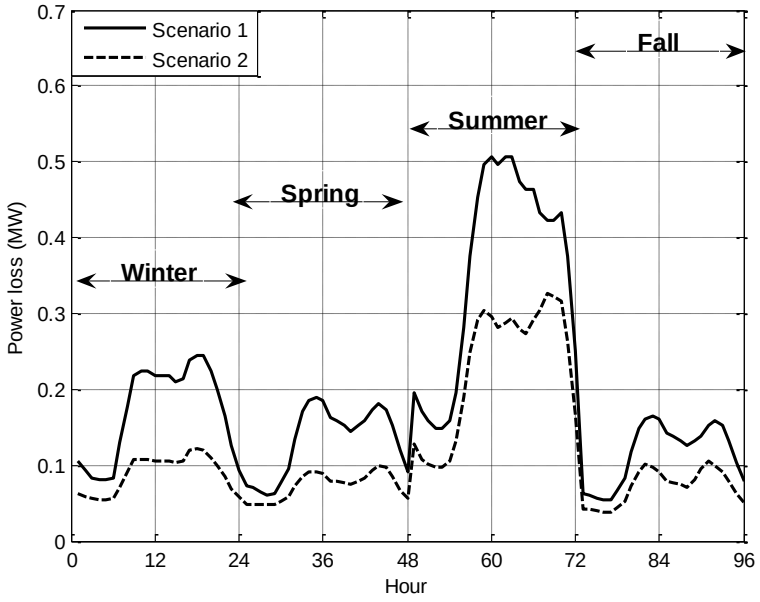

Figure 4-5 Power loss in a typical day of each season (scenario 1 vs. scenario 2)

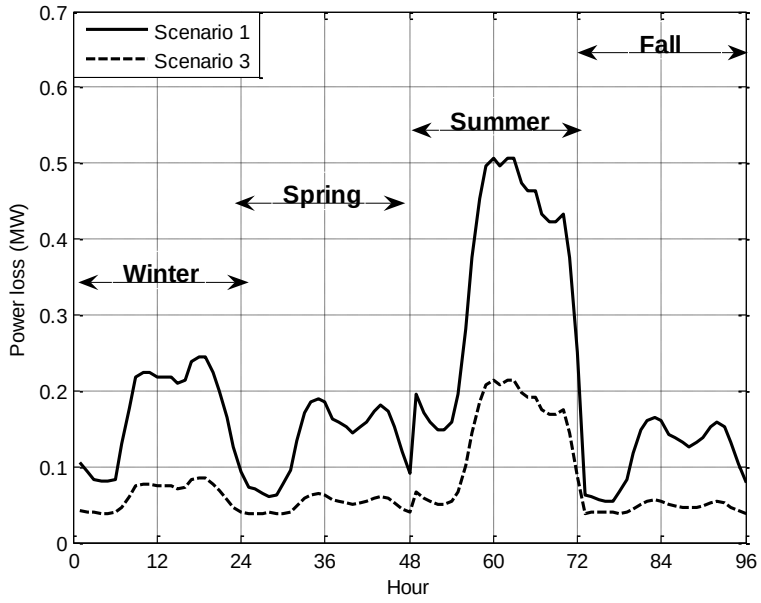

Figure 4-6 Power loss in a typical day of each season (scenario 1 vs. scenario 3)

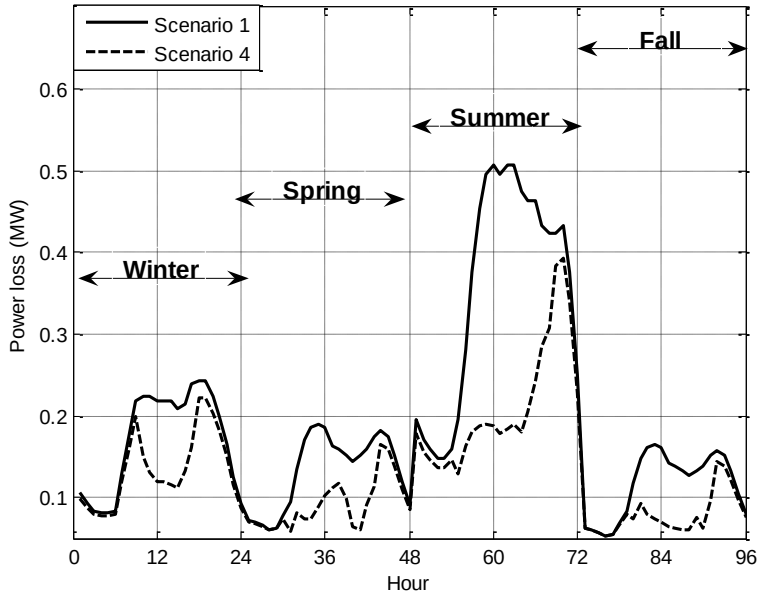

Figure 4-7 Power loss in a typical day of each season (scenario 1 vs. scenario 4)

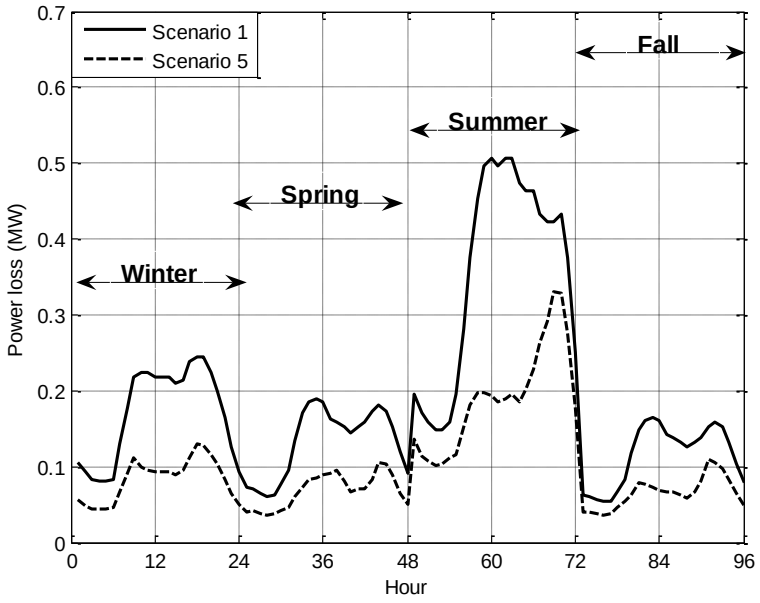

Figure 4-8 Power loss in a typical day of each season (scenario 1 vs. scenario 5)

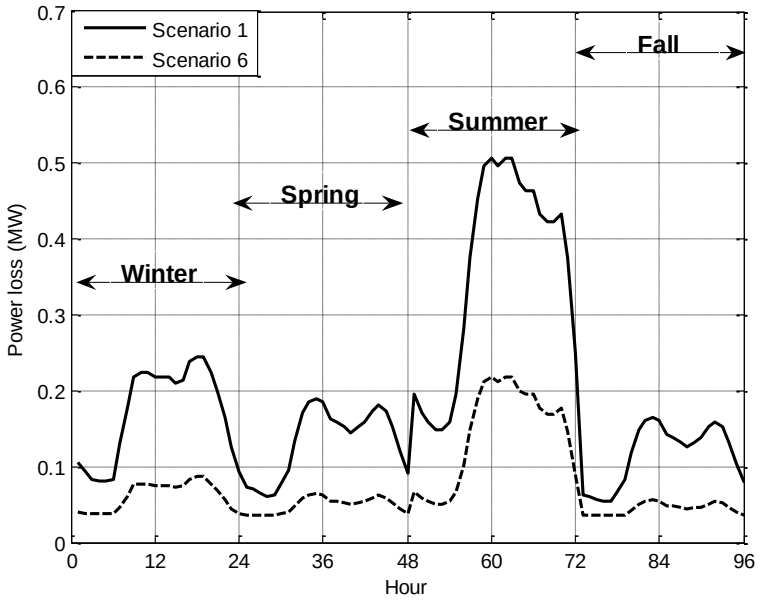

Figure 4-9 Power loss in a typical day of each season (scenario 1 vs. scenario 6)

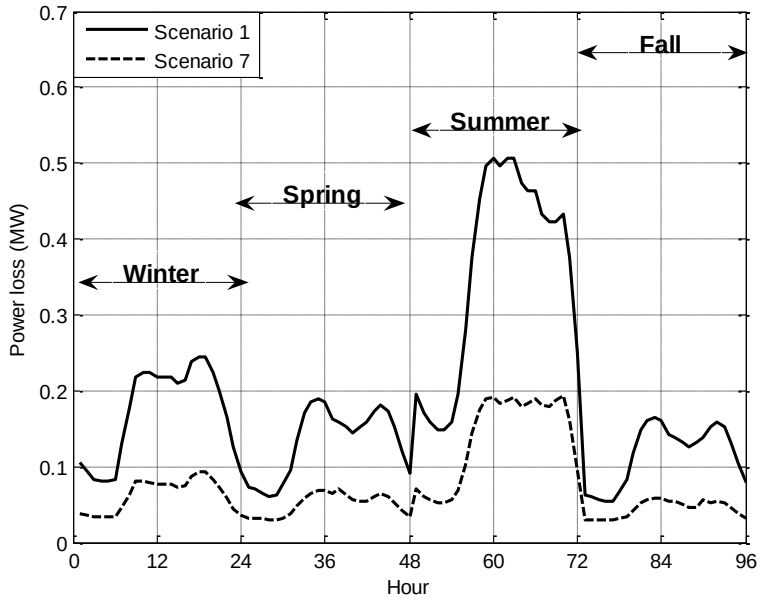

Figure 4-10 Power loss in a typical day of each season (scenario 1 vs. scenario 7)

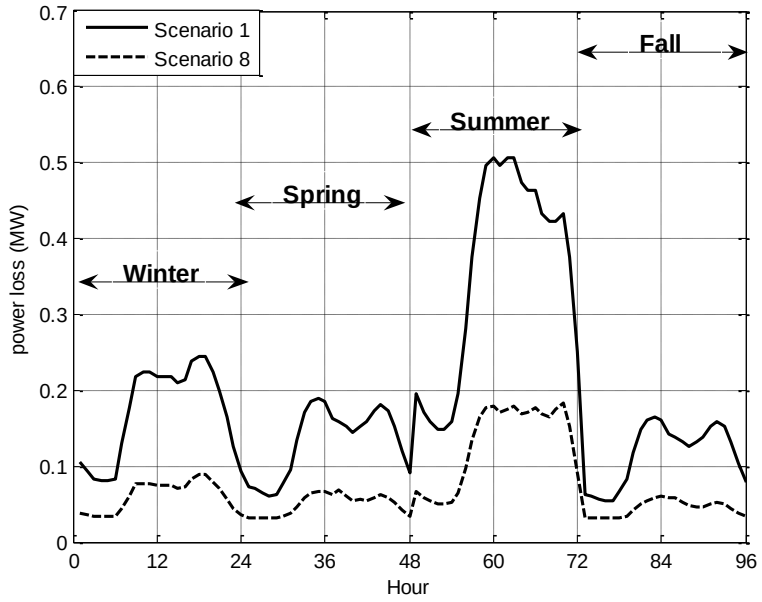

Figure 4-11 Power loss in a typical day of each season (scenario 1 vs. scenario 8)

Table 4-6 Results Using Discrete DG Sizes

Candidate Buses	No DG	Wind	Biomass	Solar
19	0	**4.4**	**2.5**	**6.88**
23	0	0	0	0
24	0	0	0	**1**
26	0	0	0	0
28	0	**1.1**	**1**	**1.23**
32	0	0	0	0
33	0	0	0	0
35	0	0	0	0
37	0	0	0	0
38	0	0	0	0
39	0	0	0	0
40	0	**2.2**	**1.5**	**3.17**
Annual Energy Loss (MWh)	**1676.23**	**1033.95**	**677.78**	**1105.25**
Contribution of each renewable DG (MW)	**0**	**7.7**	**5**	**12.28**
DG Type as a % of the Total DG Installation	**0**	**100**	**100**	**100**

Table 4-7 Results Using Discrete DG Size

Candidate Buses	Wind-Solar		Wind-Bio		Solar-Bio		Wind-Solar-Bio		
	Wind	Solar	Wind	Bio	Solar	Bio	Wind	Solar	Bio
19	**3.3**	**3.78**	**2.2**	**2.5**	**1.68**	**2.5**	**1.1**	**1.9**	**2.5**
23	0	0	0	0	0	0	0	0	0
24	0	**0.5**	0	0	0	0	0	0	0
26	0	0	0	0	0	0	0	0	0
28	**1.1**	**1.01**	0	**0. 5**	**1.12**	**0.5**	**0**	**0.7**	**0.5**
32	0	0	0	0	0	0	0	0	0
33	0	0	0	0	0	0	0	0	0
35	0	0	0	0	0	0	0	0	0
37	0	0	0	0	0	0	0	0	0
38	0	0	0	0	0	0	0	0	0
39	0	0	0	0	0	0	0	0	0
40	**1.1**	**2.16**	**1.1**	**1.5**	**1**	**1**	**1.1**	**0.99**	**1**
Annual Energy Loss (MWh)	**906.7445**		**701.984**		**653.0435**		**646.4955**		
Contribution of each renewable DG (MW)	**5.5**	**7.45**	**3.3**	**4.5**	**3.8**	**4**	**2.2**	**3.78**	**4**
DG Type as a % of the total DG Installation	**42.2**	**57.5**	**42.3**	**57.7**	**48.7**	**51.3**	**22.5**	**36.8**	**40.7**

4.8.1 Wind versus Solar

Although solar irradiance and wind speed involve large amounts of uncertainty, the loss reduction that results in scenario 2 (only wind-based DG) is higher than for scenario 4 (only solar DG). An explanation is that for at least one-third of the year (at night) the output power of the solar DG units is almost zero, as shown in figure 4-12. During these periods, the system acts similarly to the way it does in scenario 1 (no DG connected to the system), which has a negative effect on the loss reduction achieved in this scenario.

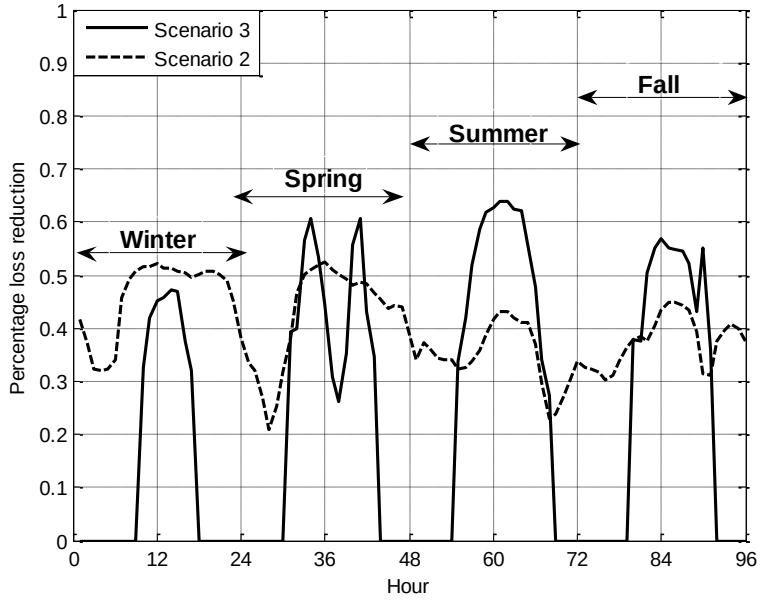

Figure 4-12 Hourly percentage power loss reduction (scenario 2 vs. scenario 3)

4.8.2 Biomass impact on system loss

The main advantage of the biomass DG is the firm output power generated, which is the basis for the following observations:

- The maximum reduction in loss occurs in scenario 8 (wind-solar-biomass).
- All scenarios that include biomass DG are superior to other scenarios from a loss-reduction perspective, and biomass is the dominant renewable resource in these scenarios.
- The difference between the maximum penetration and the actual penetration (CF x rating of the DG) of the renewable DG units is reduced for the scenarios that include biomass resources, as shown in figure 4.13.

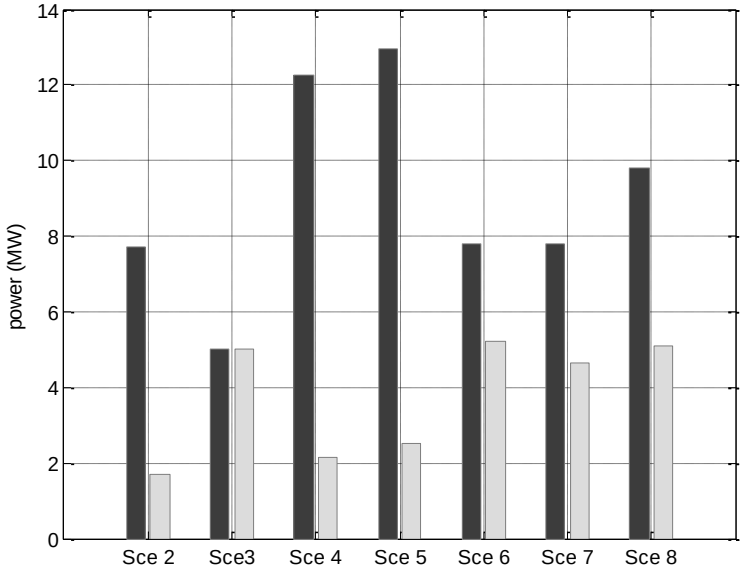

Figure 4-13 Comparison of the maximum penetration and actual penetration for all scenarios

4.8.3 The impact of the discrete size of the renewable DG units on the annual energy loss

As expected, relaxing the discrete size constraints has a positive impact on the annual energy loss reduction, as shown in Tables 4-6 to Table 4-9. However, the improvement in annual energy loss reduction is not more than 5% for any of the proposed scenarios, which means that the results obtained using the discrete size of the renewable DG units as one of the constraints are not far from the global optimality.

Table 4-8 Results with Discrete DG Size Constraint Relaxed

Candidate Buses	**No DG**	**Wind**	**Biomass**	**Solar**
19	0	**4.31**	**2.91**	**6.88**
23	0	0	0	0
24	0	0	0	**1**
26	0	0	0	0
28	0	**1.38**	**1**	**1.23**
32	0	0	0	0
33	0	0	0	0
35	0	0	0	0
37	0	0	0	0
38	0	0	0	0
39	0	0	0	0
40	0	**1.97**	**1.34**	**3.17**
Annual energy loss (MWh)	**1676.23**	**984.71**	**645.5**	**1105.25**
Contribution of each renewable DG (MW)	**0**	**7.66**	**5.25**	**12.28**
DG Type as a % of the total DG installation	**0**	**100**	**100**	**100**

Table 4-9 Results with Discrete DG Size Constraint Relaxed

Candidate Buses	**Wind-Solar**		**Wind-Bio**		**Solar-Bio**		**Wind-Solar-Bio**		
	Wind	**Solar**	**Wind**	**Bio**	**Solar**	**Bio**	**Wind**	**Solar**	**Bio**
19	**3.13**	**3.78**	**1.5**	**2.65**	**1.68**	**2.43**	**1.15**	**2.09**	**2.64**
23	0	0	0	0	0	0	0	0	0
24	0	**0.5**	0	0	0	0	0	0	0
26	0	0	0	0	0	0	0	0	0
28	**1**	**1.01**	**0**	**0.45**	**1.12**	**0.61**	**0**	**0.7**	**0.5**
32	0	0	0	0	0	0	0	0	0
33	0	0	0	0	0	0	0	0	0
35	0	0	0	0	0	0	0	0	0
37	0	0	0	0	0	0	0	0	0
38	0	0	0	0	0	0	0	0	0
39	0	0	0	0	0	0	0	0	0
40	**1.41**	**2.16**	**1.23**	**1.35**	**1**	**1.21**	**1**	**0.99**	**1.19**
Annual energy loss (MWh)	**873.09**		**638.08**		**631.47**		**615.71**		
Contribution of each renewable DG (MW)	**5.54**	**7.45**	**2.73**	**4.45**	**3.8**	**4.25**	**2.15**	**3.78**	**4.33**
DG Type as a % of the total DG installation	**42.6**	**57.4**	**38**	**62**	**47.2**	**52.8**	**21**	**37**	**42**

4.9 Discussion

In this chapter, a probabilistic planning technique is proposed for optimally allocating different types of DG (i.e., wind-based DG, solar DG, and biomass DG) into the distribution system so as to minimize the annual energy losses. Specifically, this technique is based on generating a probabilistic generation-load model that includes all possible operating conditions; hence, this model can be accommodated into a deterministic optimal power flow (OPF) formulation. The random behaviour of solar irradiance and wind speed are modeled by means of Beta and Rayleigh distributions, respectively. Biomass DG is considered as firm generation, and the load is modeled using the IEEE-RTS system. The optimization problem is formulated as mixed integer non-linear programming (MINLP), under a GAMS environment, taking into consideration the system's technical constraints, such as the voltage limits, the thermal limits of the feeder, the maximum investment capacity on each bus, the discrete size of the DG, and the maximum penetration limit of the DG units. The proposed planning technique has been applied to different scenarios for a typical rural distribution system provided by a local utility company. The results reveal that regardless of the combination of the renewable resources used to calculate the optimal fuel mix, there is a significant reduction in the annual energy loss for all scenarios proposed. Also for all scenarios, the proposed technique guarantees the optimal fuel mix for loss minimization during the entire planning period and ensures that, for all possible operating conditions, no system constraints will be violated.

Chapter 5

Supply Adequacy Assessment of Distribution Systems with Renewable DG

5.1 Introduction

The function of an electric power system, including generation, transmission and distribution, is to satisfy the system load requirement with a reasonable assurance of continuity and quality. The ability of the system to provide adequate supply of electrical energy is usually designated by the term of reliability.

The economical and social effects of loss of electrical service have great impacts on both the utility supplying electric energy and the end users of electric service. The cost of major power interruption confined to a certain area can be on the order of millions of dollars, depending on the duration and type of loads in this area. This cost can increase dramatically if the loads are commercial or industrial. Therefore, maintaining a reliable power supply is a very important issue for power system design and operation.

Moreover, the global trend toward increasing the sustainable power penetration in existing power systems dictates a very serious need to consider their effect on the system reliability. However, due to the high level of uncertainty associated with renewable resources, the adequacy assessment of power systems became more complicated.

Therefore, in this work, the problem of adequacy assessment for distribution systems with renewable distributed generation has been analyzed during different modes of operation (i.e., grid-connected mode and islanding mode). Two different approaches are proposed to assess the system reliability. The first approach is an analytical method in which the desired adequacy indices are evaluated from the mathematical model that represents the status of the system components, while the second one is an MCS, in which the random behaviour of the renewable resources, as well as the status of the system components, are modeled chronologically.

5.2 Modes of System Operation

The interconnection of distributed generation with electric power systems is regulated by the IEEE 1547 standards [8]. Thus, islanded operation of parts of the feeder is currently not permitted by the utilities. This means that following a fault, the DG has to disconnect and remain disconnected until

the fault is cleared. Therefore, with this philosophy of DG implementation, there will be no significant benefits of DG on reducing the period of interruption due to fault occurrence. To maximize the DG benefit, most of the recent work focuses on facilitating the islanding operation of the system. Islanding operation means that the DG units will remain connected during the fault, if it has enough capacity to feed the loads located on the island. However, after clearing the fault, synchronization between the DG and the utility is required in order to restore normal operation without causing momentary interruption.

For distribution systems, the grid-connected mode and islanding mode can be defined as follows:

- ***Grid-connected mode***

The distribution system is operating in grid-connected mode if:

Case 1: At least one transformer is still in service;

Case 2: A failure in any of the distribution system component out of the main breaker protection zone (i.e., any failure downstream recloser R can be isolated while the rest of the system is still connected to the grid as shown in figure 4-1).

- ***Islanding mode***

Part of the distribution system is operating in islanding mode if:

Case 1: All the transformers are out of service;

Case 2: A failure in any component of the distribution system in the main breaker (CB) protection zone (i.e., any failure upstream recloser R involves disconnecting the system from the grid as shown in figure 4-1), and the rest of the system downstream recloser R can work in the islanding mode.

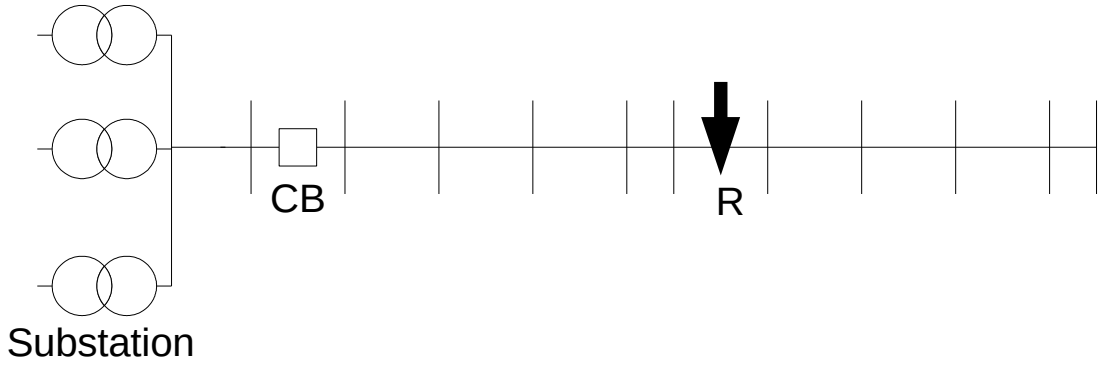

Figure 5-1 Schematic diagram of a radial distribution system

5.3 Definition of the Reliability Events

Prior to examining the proposed approaches and techniques for the distribution system reliability assessment, this section provides definitions for the important reliability events.

Outage: The state of a component when it is not available to perform its function.

Outage rate: Number of outages per year for a certain component.

Forced outage rate: The percentage of time that a given point in the supply chain is non-functional due to forced outages.

Repair time: Time taken to repair the damaged component including time to reach the component, time to isolate the component from the system, time to repair or replace parts, and time to restore the component to active service again.

Interruption: The loss of service to one or more customer, due to one or more component outage.

Duration of interruption: The period from the initiation of an interruption to a customer until the restoration of power again to that customer.

Momentary interruption: An interruption restored by automatic, supervisory, or manual switching at a site where an operator is immediately available. Usually less than 5 minutes.

Sustained interruption: Any interruption not classified as a momentary event, or any interruption that is longer than 5 min.

5.4 Reliability Evaluation Criteria

This section presents the existing criteria for supply adequacy assessment for power systems.

5.4.1 Deterministic Criterion

The deterministic criteria were the earliest techniques used by many utilities to determine required generating capacity [93]. They are based on the comparison of the available reserve capacity with the capacity of the largest generating unit, or a fixed percentage of the total installed capacity, or a fixed percentage of the peak load, or a mix of these. While deterministic criteria are easy to implement, they do not take into consideration the stochastic nature of the system components.

5.4.2 Probabilistic Criterion

The probabilistic criteria [94] are based on considering a large number of operational situations which enable the evaluation of the system risk state. These operational situations are generated

probabilistically using either analytical or simulation method. Finally, average indices weighting the various events according to the probability of their occurrence are obtained.

The advantage of the probabilistic criteria vs. the deterministic criteria is the ability of capturing the random nature of system components and load behaviour in a consistent manner.

The reliability indices used to quantify the system risk state are:

LOLE (***loss of load expectation***): The expected number of days or hours in the study period, during which the generating capacity will be inadequate to satisfy the load

LOEE (***loss of energy expectation***): The expected energy that cannot be supplied during the study period. Also LOEE can be termed as EUE (*expected unserved energy*) or EENS (*expected energy not served*)

LOLP (***loss of load probability***): The probability of loss of load during the study period. This can be calculated by dividing LOLE by the number of days or hours in the study period.

Utilization of probabilistic techniques will permit the capture of the random nature of system components and load behaviour in a consistent manner, which should be considered an advantage over the deterministic criteria.

5.4.3 Well-being Criteria

System well-being criteria incorporate deterministic criteria in the probabilistic framework. The different well-being states associated with a generation system are healthy, marginal, and at risk as shown in figure 5-2. A system is said to be operating in the healthy state when it has a sufficient amount of reserve capacity to meet a deterministic criterion, as well as enough available generation capacity to serve the load. Whenever the system has enough available generation capacity, but does not have sufficient margin to meet the specified deterministic criterion, it is in the marginal state. The system is in the risk state when the load exceeds the available capacity. The probabilities associated with healthy, marginal, and at risk states of the system are collectively recognized as well-being indices. Deterministic criteria are based on the comparison of available reserve capacity with either a fixed percentage of the total installed capacity, the capacity of the largest unit, or the capacity of the largest unit plus a percentage of the peak load.

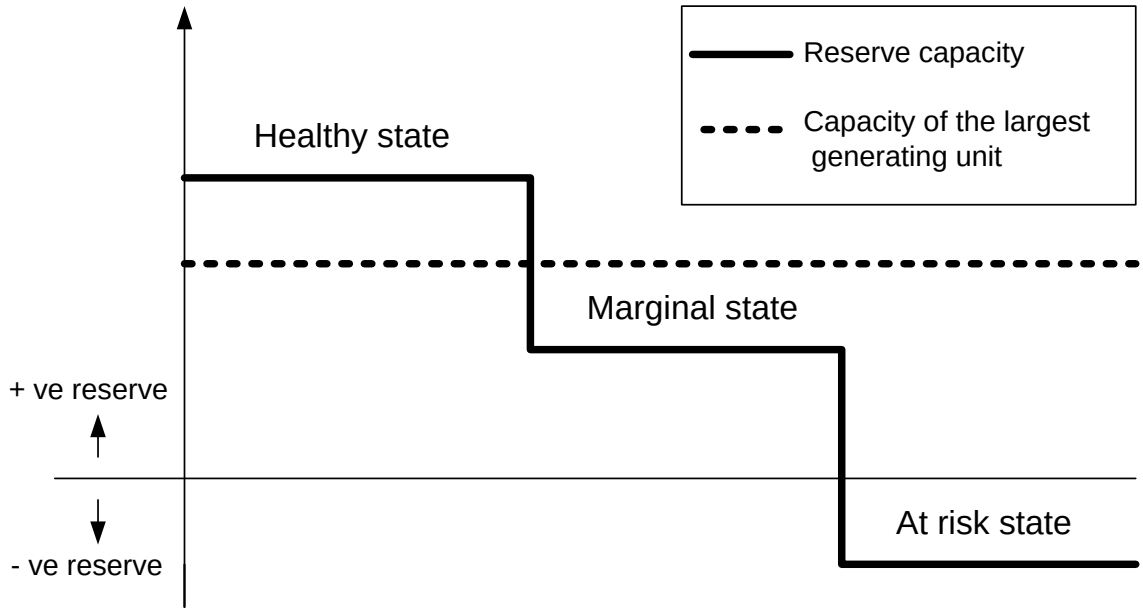

Figure 5-2 Well-being criteria

5.5 Methods of Reliability Evaluation

The different methods for evaluating the system reliability, via calculating reliability indices, can be classified into two main categories:

1. Analytical methods;
2. Simulation methods.

5.5.1 Analytical Method for Reliability Evaluation

The analytical methods evaluate the expected values of desired reliability indices utilizing numerical solution from a mathematical model that represents the status of the system components. The steps required to accomplish this work are as follows:

- *Classification of the system components*

This is the first step in the analytical method, whereby the system components are classified into different categories. The system components can be classified based on different criteria, such as the function of the components, the resources, the power characteristics, the size, and the cost characteristics. In this work, the function and the resource of the components are the two main criteria utilized to classify the system components as follows:

1. Passive components

The function of these components is to transmit power from the generation to loads (e.g., cables, transmission lines, circuit breakers, and bus bars).

2. Active components

The function of these components is to generate adequate amount of power to satisfy the load (e.g., generating units).

The second step is to classify the active components, based on the energy resource, into the following two categories:

– *Conventional generating units*

These generating units guarantee firm output power during all periods of healthy operation (e.g., diesel generators). In this work, transformers will be considered as conventional generating units.

– *Renewable generating units*

These generating units cannot guarantee firm output power because of the intermittent nature of their resources (e.g., wind, and solar).

3. Loads

Unlike generation, there are no up and down states for the load; however, the load changes from its peak value to its minimum value with time.

- *Availability modeling of the system components*

Having divided the system components into categories, the availability model of each category is then created based on the forced outage rate (*FOR*) of each component.

1. Passive components

There are two states for each of these components: 1) a *down state* in which the component is out of service - the probability of this state is *FOR*.; 2) an *up state* in which the component is in service - the probability of this state is (1-*FOR*)

2. Active components

Modeling of the active components means creating a multi-state availability model (MSAM) that shows the states of the generator's output power with their probabilities.

– *Conventional generating units*

There are two states for each conventional generating unit to create MSAM: 1) *down state*, in which the generator is out of service with zero power generated - the probability of this state is *FOR*.; 2) *up*

state, in which the generator can generate power up to its rating - the probability of this state is (1-*FOR*).

– *Renewable generating units*

The power output characteristics of renewable generating units are quite different from those of conventional generating units. The output of renewable generating units depends strongly on the behaviour of the renewable resource, as well as the performance characteristics of the generator. In other words, the available capacity of such generators has different states and during each state there is a probability of a hardware failure which depends on the *FOR* of the generator. For example, if the probability of capacity level state (k) is $P\{RenewableGen_k\}$, then the probability of the generator to be down during this state is $P\{RenewableGen_k\}$ times its *FOR*. The procedure to create a MSAM for each renewable generating unit is briefly described as follows:

- Select a proper pdf to describe the random behaviour of the renewable resource;
- Generate the discrete form of the continuous pdf with a reasonable step (tradeoff between accuracy and computation complexity);
- Calculate the probability of each discrete state [20];
- From the power performance curve of the generating unit, calculate the output power states with their probabilities;
- Use the *FOR* of the generating unit with the output power states to create the MSAM of this unit.

3. Load

In order to proceed with an accurate adequacy assessment, the load duration curve LDC will be created based on the IEEE-RTS, as mentioned in chapter 3.

- *Combining the generation and load models*

After creating the generation model for each category of the generating units, all these models are combined together to create the total MSAM of the whole system. Hence, the generating system represented by the MSAM, and the load represented by the LDC, are convolved to calculate the desired reliability indices.

5.5.2 Simulation Method for Reliability Evaluation

Simulation methods estimate the reliability indices via simulating the actual behaviour of the system either deterministically or randomly. Therefore simulation methods can be further divided into the following:

1. Deterministic simulation method: in this method the simulation does not include the uncertainty associated with the system behaviour;
2. Monte Carlo Simulation (MCS) method: in this method the simulation actually describes the random behaviour of the system.

Here, MCS method is the better choice among the simulation methods to assess reliability of the distribution system. The steps of the MCS method are in the following subsection.

5.5.2.1 Monte Carlo Simulation for reliability assessment

In MCS the study period is divided into segments (usually hourly), and then the system state is examined. This process is repeated chronologically from one segment to another until the entire simulation period has been scanned. Finally, the results are averaged to calculate the desired adequacy indices. The steps required to accomplish this work are as follows:

- *Renewable resources and load modeling*

The MCS method requires a sequential form of wind speed data which can be generated either by using actual historical data or synthetically. In this work the wind speed data are generated synthetically using proper pdf. The procedure to simulate the renewable DG output power using MCS is as follows:

1. Divide the entire year into time segments, each referring to a particular hourly interval;
2. Model the renewable resource behaviour during each hour by a proper pdf;
3. Use the historical data to calculate the hourly average and standard deviation of the renewable resource. From these data calculate the parameters of the pdf for each hour;
4. Find the cumulative distribution function (cdf) for each hour, then the inverse transformation of each cdf;
5. Use these cdfs to simulate the hourly renewable resource using MCS.
6. Calculate the output power of the renewable DG units from the input/output relation of each DG.

7. Combine the chronological output power of the renewable DG with the chronological pattern of the up and down states of the renewable DG unit, explained in the next section, to get a more accurate behaviour of the renewable DG units.

The MCS also requires chronological load data, which can be generated by the same method as the renewable resources. However, because load variation is much slower than wind speed, the load will be assumed to be constant during a given time segment and changes discretely for every time segment. The load value during each time segment is determined from the historical hourly load data regarding the system under study.

- *Generating unit modeling*

For modeling the hardware availability of different generating units as well as the system components (e.g., feeders, busbars, and circuit breakers), the up and down states of the generating units should be simulated using proper distribution

After simulating the operating states for the generating units, the power output from the different units is determined for each time segment depending on whether each generating unit is in the up or down state.

- *Combining the generation and load models*

The last stage in MCS is to combine the developed generation and load models to obtain the required adequacy indices. For each time segment, the system state is checked and stores with its duration. For at risk state, the amount of energy curtailment is also stored. This procedure is repeated chronologically for the entire study period, and the simulation is repeated for several study periods in order to reach the desired accuracy. The MCS stops, after N simulated study periods, when the ratio of standard deviation of the sample mean of the reliability index of interest to the sample mean of the same index becomes less than a given predetermined tolerance.

5.6 Segmentation Concept for Island Reliability Assessment

Using MCS, the adequacy assessment during the islanding mode of operation is straightforward, from the recorded date regarding the status of the system components and the output of the generating units during each time interval. Analytically, however, the system reliability during islanding mode of operation is evaluated using the segmentation concept as follows:

5.6.1 Calculating the Probability of the Island to be created

Distribution system components can be divided into two main groups:

1. Components which are responsible for transmitting power from distribution substation to customers (lines, transformers…).
2. Components which are responsible for protecting the system from abnormal operation, and restoring power to non-faulted areas (switches, fuses, reclosers, circuit breakers….)

Depending on the configuration of the distribution system, a segmentation concept is used for reliability evaluation [95, 96]. In other words, the distribution system is modeled in terms of segments rather than components. A segment is a group of components whose entry component is a switch or a protective device, and each segment has only one switch or protective device. The concept of segmentation as shown in figure 5-3 is based on the fact that any fault in a component downstream of a protection device and within its zone of protection will cause an interruption of power to those customers in that zone. This means that all the customers in any zone have the same reliability level and can be treated as one customer. Moreover, any segment can operate in the islanded-mode if and only if there is a DG, connected to the segment, with an output power matching the segment's load during the island period.

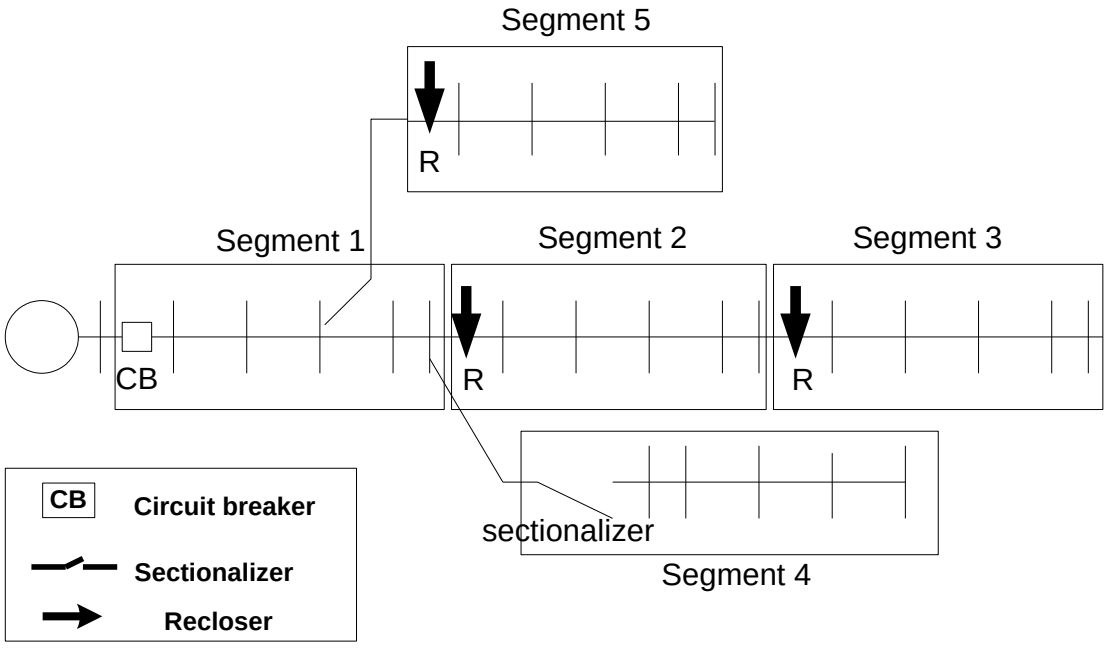

Figure 5-3 Segmentation concept

Based on the segmentation concept, the down time of each segment, as well as the probability of island creation, can be determined as follows:

Reliability evaluation of each segment is based on two different sets; where each set includes certain number of segments.

1. The first set includes all the segments in the series path between the main utility source and the segment under study. A failure of any component in any of these segments requires waiting out the repair time of this component to restore power. As shown in figure 4-3, if the reliability of seg #3 is calculated; hence, $set\#1:\{seg\#1, seg\#2, seg\#3\}$. In other words, a failure of any segment in set #1 will cause a *sustained interruption* to the segment under study.
2. The second set consists of all segments which are not in the series path between the segment under study and the main utility source, but in which a fault in any of their components will cause interruption to the segment under study. This requires waiting out the switch operation time to isolate the faulted segment and restore power again from the main source, e.g., for seg #3 $set\#2:\{seg\#4\}$. In other words, a failure of any segment in set #2 will cause a *momentary interruption* to the segment under study.

In this work, only sustained interruption is considered; therefore, all reliability calculations are based only on set #1 as follows:

The down time of any segment can be calculated as follows;

$$DT_g = \left(\sum_{j \in set\,G} \sum_{i=1}^{m} sfr_i \times rt_i \right) \tag{5.1}$$

The island is created when a fault has occurred in any segment of set 1 except the segment under study. For example segment 3 will operate in the islanding mode if the fault occurred in the substation, segment 1, or segment 2. Hence, the probability of segment *g* to be working in the islanded mode ($P_g\{island\}$) in each instant of the year can be calculated as follows:

$$P_g\{island\} = \frac{\left(\sum_{\substack{j \in set\,G \\ j \neq g}} DT_j \right)}{8760} \tag{5.2}$$

5.6.2 Calculating the Probability of the Island to be a Success

Once the probability of creating an island is calculated, the next step is to calculate the probability of an island being a success. The necessary condition for an island to be successful is;

$$P_G \geq P_L + P_{loss} \tag{5.3}$$

Here, the power loss in the island is considered to be 5% [25] of the current load.

So the probability of an island to be a success (P_g {*success*}) depends on the probability of the DG units in the island to match the total island load and the island losses (P_g{*enoughDG*}) during the period of islanding. Given that the probability that the DG units match the load and the probability of creating an island are independent, the probability of success for the islanding mode can be obtained by convolving the two probabilities as shown in the following equation:

$$P_g\{success\} = P_g\{island\} \times P_g\{enoughDG\}. \tag{5.4}$$

5.7 Proposed Approach for Adequacy Assessment

In this approach analytical and MCS techniques are utilized to assess the distribution system adequacy when integrated with renewable DG units during different modes of operation; whereas the criteria utilized to assess the distribution system adequacy is well-being criteria. During the grid-connected mode, from the load perspective, the substation transformers act as generating units. Therefore, the adequacy of the distribution system will be assessed based on the assumption that generating units of the distribution system are the substation transformers and the DG units. During the islanding mode of operation, the island adequacy is assessed based on the assumption that the island is acting as SAPS during an islanding period which is typically short. The most important issue during the islanding mode of operation is to determine the probability of the island to be a success (the DG power output within the island matches the load) or a failure (there is a deficit in power generation). Therefore, unlike SAPS, there will be only two states to assess the island adequacy: 1) *success state* which corresponds to the *healthy* and *marginal* states in SAPS; 2) *failure state* which corresponds to the *at-risk* state in SAPS. The island creation probability is calculated based on the status of the system components, such as feeders, bus bars, and protection devices.

Regarding well-being criteria, the deterministic criterion applied in this work is presented mathematically as:

$$C_R \geq C_{LU} \tag{5.5}$$

Here, LOLE is the reliability index of interest; nevertheless, more indices will be calculated. The block diagram in figure 5-4 summarizes the proposed adequacy assessment technique.

Furthermore, after calculating the Adequacy indices, the segmentation concept is utilized to calculate SAIDI.

In this work the following control strategies are applied:

1. The renewable DG units are controlled to operate at unity power factor.
2. The renewable resources data used are the average hourly values and the variations within the hour are not considered.
3. Only dispatchable DG units are allowed to supply reactive power in the island.
4. There is no storage option, so renewable DG output power is regulated based on load requirement; no surplus is allowed. This strategy is applied only during the islanding mode of operation. However, during the grid-connected mode, the Standard Offer Program (SOP) gives the DG owner the privilege to inject all the generated power in the system.
5. Load curtailment strategy is applied only during grid-connected mode; however, any deficit in generation during islanding mode results in islanding failure.
6. All generating unit ratings are given in MW; however, the reactive power is considered as constant percentage of the load, based on the assumption that all loads are working on constant power factor.

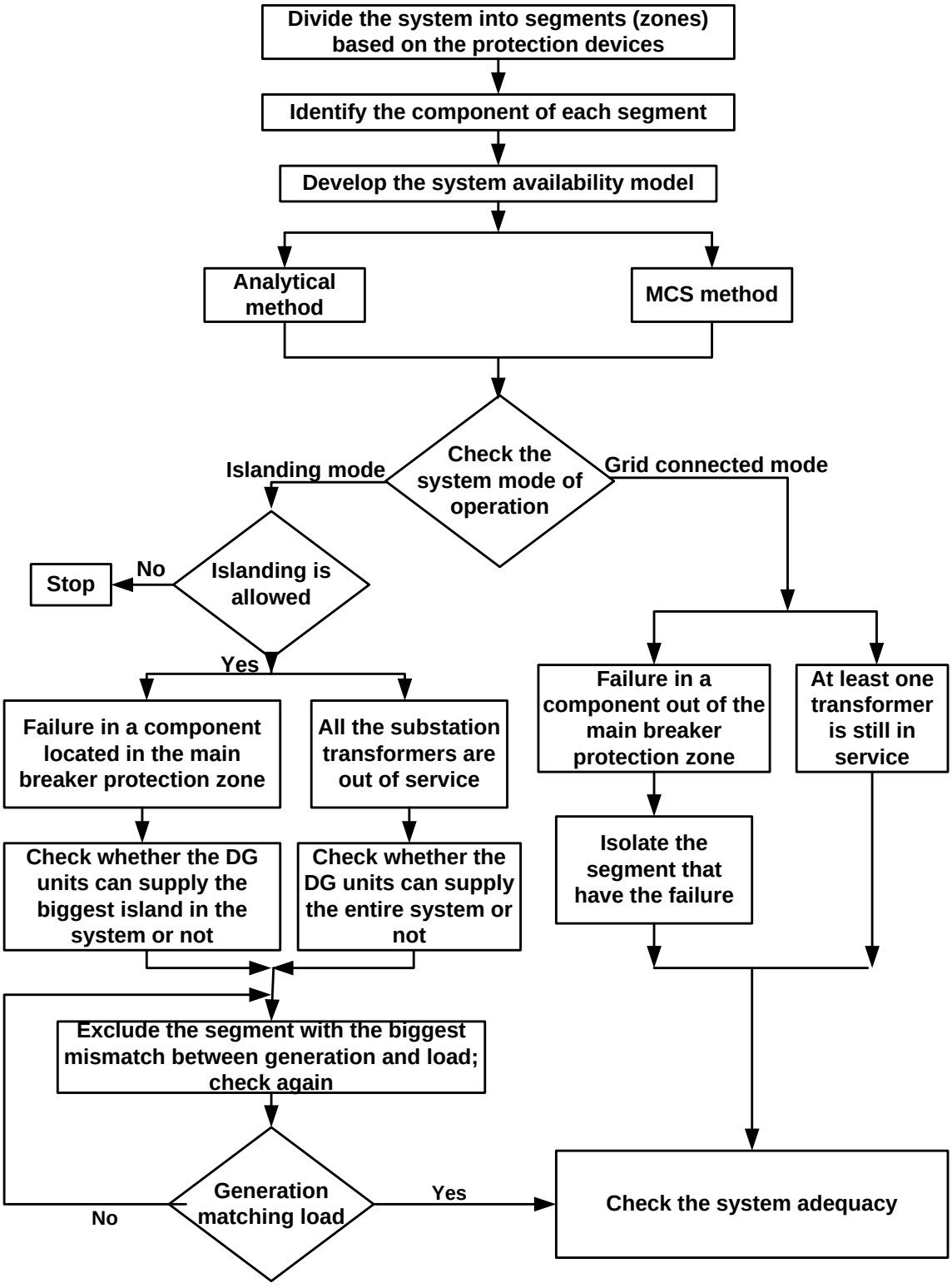

Figure 5-4 Proposed adequacy assessment technique

5.8 Case Study

This section presents the results of applying the proposed approaches of reliability evaluation on a practical rural distribution system using different scenarios. For each scenario, the amount and type of the renewable resources integrated into the system might change.

The system under study, as shown in figure 5-5, is a practical rural distribution system. The main substation at bus 1 consists of 4 transformers each of 5 MW with *FOR* of 0.02. The regulating station between buses 15 and 16 is used to boost the voltage in order to maintain the voltage drop at the end users within accepted limits. The data of the system are given in appendix A. Based on the segmentation concept this system is divided into two segments, where segment 1 has an aggregated peak load of 8.096 MW and is protected by the circuit breaker B1. Segment 2 has an aggregated peak load of 8.165 MW and is protected with the recloser R1.

If the distribution system is to rely only on the renewable DG units to supply the load during the islanding operation, stability problems might arise. This is due to the fact that wind-based DG units are characterized by a high level of random power fluctuations that are relatively higher than load fluctuations, leading to power mismatch. Conventional DG units, such as diesel generators, respond to these stability problems by changing the supplied power to match the demand through either excitation or governor controls, which consequently control the island frequency and voltage. This calls for sharing the load between renewable and conventional DG units. In this way, the useful capacity of the renewable DG units is calculated and added to the available capacity of the conventional DG units in order to create the generation model. Therefore, in order to allow islanding operation, a certain level of penetration of conventional DG should exist in the island. In this work, the penetration level is 60 % of the island peak load; it is coming from two diesel DG units each of 2.5 MW (60% of the peak load in segment 2) [91] connected to bus 28 with *FOR* of 0.05. From the location of the DG units it can be concluded that only segment 2 can work in the islanding mode if the generated power of the DG units matches the load during the islanding period.

Based on the system configuration figure 5-5, the modes of the system operation are as follows:

- *Grid-connected mode*

    1. *Case 1*: At least 1 transformer is in service; In this case the total power from the transformers and the DG units are aggregated and compared to the total load to check the system status.

2. *Case 2*: A failure at segment 2. In this case only the power from the transformers is compared to the load of segment 1 to check the status of this segment.

- *Islanding mode*

1. *Case 1*: The 4 transformers are out of service; In this case only the power of the DG units is compared to the total load to check the system status; however during at-risk states, the power of the DG units will be compared to the loads of segment 2.
2. *Case 2*: A failure occurred in segment 1. In this case only the power of the DG units is compared to the load of segment 2 to check the status of this segment.

Based on the amount and type of the renewable resource connected into the distribution system, two different scenarios are proposed as follows:

- Only wind-based DG units are connected to the distribution system;
- Wind-based DG units, as well as solar DG units, are connected to the distribution system.

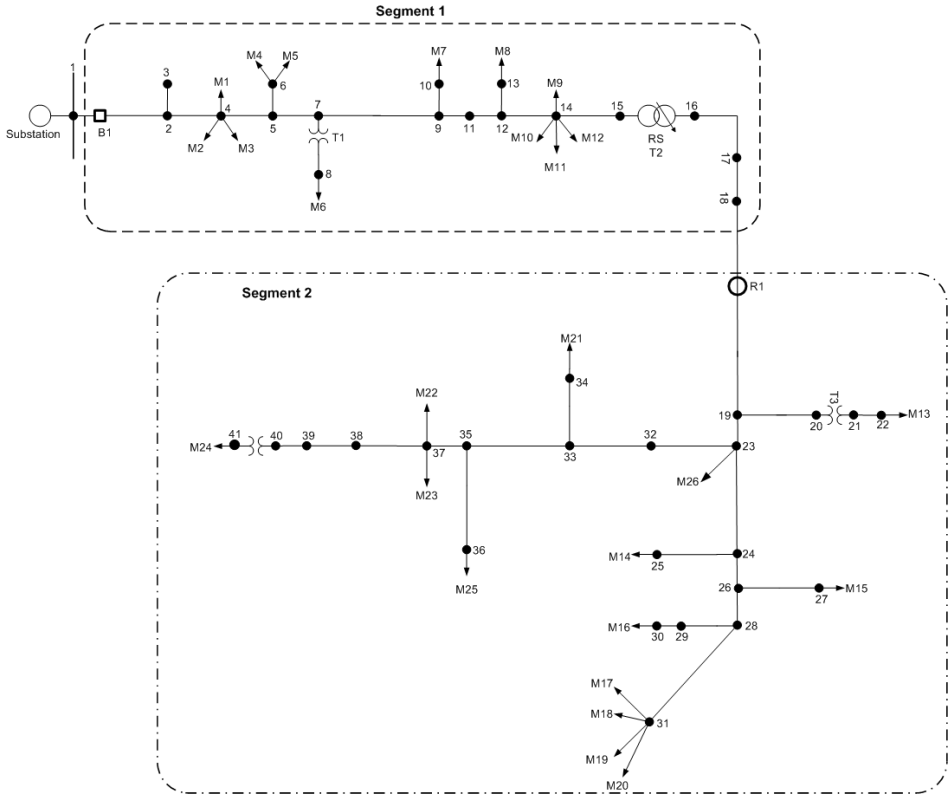

Figure 5-5 System under study

5.8.1 First Scenario

In this scenario besides the fixed number of Diesel DG units, there are two identical wind-based DG units, each of 2 MW rating, connected at bus 39. Both wind-based DG units have the following characteristics:

- Cut-in speed=4 m/s.
- Nominal speed=14 m/s.
- Cut-off speed= 25 m/s.
- A 4% Forced Outage Rate (FOR) (MTTF=1920h, MTTR=80h) [30] is assumed for all wind turbines.

5.8.1.1 Results

In this section the MCS and analytical techniques are applied to the system under study to assess its adequacy during different modes of operation.

- **Monte Carlo Technique**
  - *Wind speed simulation*

Weibull pdf (3.1) has been utilized to simulate the hourly wind speed, while Weibull cdf with its inverse transformation are as shown in (5.6) and (5.7):

$$F(v) = 1 - e^{[-(\frac{v}{c})^k]} \tag{5.6}$$

$$V = -c\ln(1-u)^{1/k} = -c\ln(u)^{1/k} \tag{5.7}$$

u: random numbers uniformly distributed on [0,1]

  - *Hardware simulation*

Hardware simulation includes the simulation of the up and down state of all the system components (e.g., generating units, feeders, etc). The up and down states of all the system components have been simulated using exponential distributions [52] as:

$$\text{Up time} = -\text{MTTF} \times \ln(X_1) \tag{5.8}$$

$$\text{Down time} = -\text{MTTR} \times \ln(X_2) \tag{5.9}$$

X_1 and X_2: random numbers uniformly distributed on [0,1].

- *Load modeling*

The hourly load values are based on historical data from the years 2005, 2006, and 2007. Since the reliability assessment needs to be studied over a large number of years, the hourly loads are assumed to be the same every year.

- *Stopping criterion*

Let X be the reliability index of interest; $E(X)$ and $\sigma(X)$ are the mean and the standard deviation. Hence, the stopping criterion is as follows

$$\frac{\sigma[E(X)]}{E(X)} \leq \varepsilon \tag{5.11}$$

where ε is the specified tolerance.

In this work, *LOLE* has been considered as the reliability index of interest.

- **Analytical Technique**

- *Modeling of the passive components*

Based on equations (5.1) to (5.3), the probability of a failure in segment 2 is calculated to be **0.000898**. However, the probability of island creation in segment 2 is calculated to be **0.00084**.

- *Modeling of the conventional generating units*

The availability models of the 2 diesel DG units and the 4 transformers are as shown in Table 5-1 and Table 5-2, respectively.

- *Modeling of renewable generating units*

In this work, Weibull pdf has been utilized to describe the annual wind speed profile (wind model 1); hence the discrete form is created with a step of 1m/s for wind speed states (i.e., the wind speed states are: 1m/s, 2 m/s, 3 m/s,…until the maximum observed wind speed in the area under study). Based on the wind turbine's performance curve and the wind speed characteristics in the area under study, the output power of each wind turbine is shown in Table 5-3, while the complete availability model of the two wind turbines is shown in Table 5-4.

- *Modeling of the load*

As mentioned in chapter 3, the IEEE-RTS system, which divides the load into ten levels, has been utilized to describe the load profile (load model 1). Based on the total peak load and the peak load of each segment, the load levels are as shown in figure 4-6.

- *Combining the generation and load models*

During the grid-connected mode the total generation model should include the power from transformers, diesel DG units, and the wind-based DG units; however, during the islanding mode, the total generation model should only include the power from diesel DG units and wind-based DG units. The MSAMs of the two cases are shown in figure 4-7 and figure 4-8 respectively.

Table 5-1 MSAM of the Diesel DG Units

State no	Description	Output power MW	Probability
1	2 up& zero	5	0.9025
2	1up & 1	2.5	0.095
3	zero up& 2	0	0.0025

Table 5-2 MSAM of the Transformers

State no	Description	Output power MW	Probability
1	4 up& zero	20	0.92236816
2	3 up& 1	15	0.07529536
3	2 up& 2	10	0.00230496
4	1 up& 3	5	0.00003136
5	zero up& 4	0	0.00000016

Table 5-3 Single Wind Turbine MSAM

State no	wind speed (m/s)	Power output of the wind turbine (MW)	Probability With *FOR*=0	Probability With *FOR*=0.04
1	4 and	0	0.347	0.37312
2	5	0.2	0.125	0.12
3	6	0.4	0.119	0.11424
4	7	0.6	0.105	0.1008
5	8	0.8	0.087	0.08352
6	9	1	0.069	0.06624
7	10	1.2	0.051	0.04896
8	11	1.4	0.036	0.03456
9	12	1.6	0.024	0.02304
10	13	1.8	0.015	0.0144
11	14 to	2	0.022	0.02112

Table 5-4 MSAM for the Two Wind Turbines

state no	Power output of the 2 wind turbines (MW)	Probability with *FOR*=0.04
1	0	0.3480448
2	0.2	0.0096
3	0.4	0.1243392
4	0.6	0.008064
5	0.8	0.116352
6	1	0.0052992
7	1.2	0.1006848
8	1.4	0.0027648
9	1.6	0.0820224
10	1.8	0.001152
11	2	0.06528
12	2.4	0.0470016
13	2.8	0.0331776
14	3.2	0.0221184
15	3.6	0.013824
16	4	0.0202752

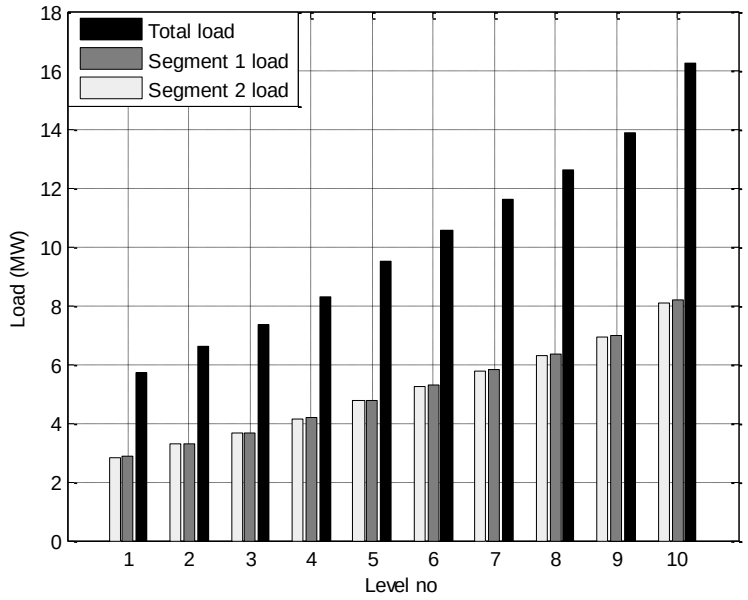

Figure 5-6 Load profile

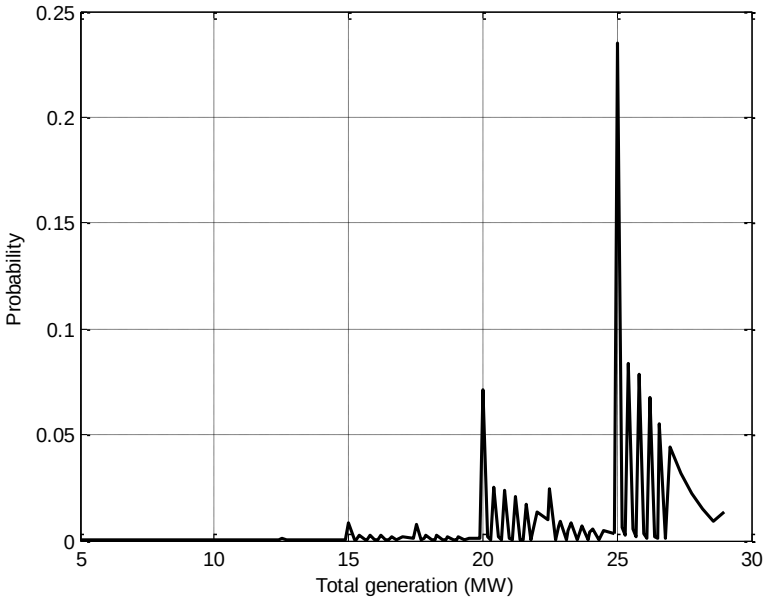

Figure 5-7 MSAM for the total generation

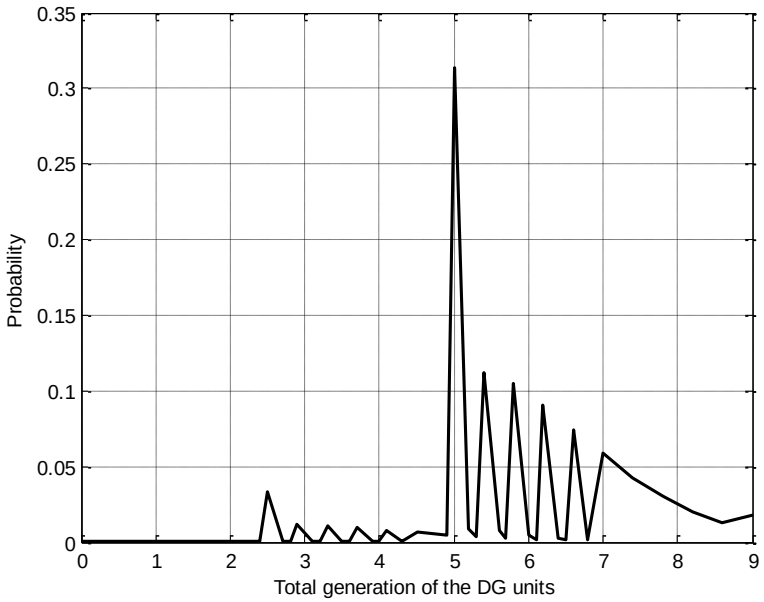

Figure 5-8 MSAM for the DG units only

The outcomes of the two techniques during different modes of operation are listed in Table 5-5 and Table 5-6 which reveal that the results of the two techniques are very close to each other.

From Table 5-2 it is evident that the probability of all 4 transformers being out of service is almost zero; therefore, case 1 of the islanding mode of operation (4 transformers are out of service) is neglected in the study.

From Table 5-6 it can be figured out that allowing the islanding brings a notable improvement in system adequacy

Further, a comparative study was conducted between the results of case 1 of the grid-connected mode and the results of this case with no DG connected to the system. The rationale behind this is to study the effect of DG implementation on the adequacy of the distribution system during grid-connected mode. Figure 5-9 and figure 5-10 show that there is remarkable improvement in LOLE and LOEE in case of DG connected, when compared to the no-DG case.

Table 5-5 Adequacy Indices in Grid-connected Mode (Scenario 1)

Grid-connected mode				
Adequacy indices	**Case 1**		**Case 2**	
	MCS	Analytical	MCS	Analytical
LOLE (hr/year)	7.22	8.022	0.0046	0.0051
LOLP	0.0824	0.092	5.25E-05	5.76E-05
LOEE (MWh/year)	10.521	11.533	0.0041	0.0044
Period of healthy state(hr/year)	8523.1	8529.622	7.7700	7.7594
Probability of Healthy state	97.304	97.370	0.0886	0.0885
Period of Marginal state (hr/year)	229.68	222.356	0.0920	0.1060
Probability of Marginal state	2.622	2.538	0.0011	0.0012

Table 5-6 Adequacy Indices in Islanding Mode (Scenario 1)

Islanding mode (case 2)				
Adequacy indices	**Islanding not allowed**		**Islanding allowed**	
	MCS	Analytical	MCS	Analytical
LOLE (hr/year)	7.1892	7.3584	2.2300	2.401
LOLP	0.00081	0.00084	0.0262	0.027
LOEE (MWh/year)	35.824	36.71	13.910	14.017

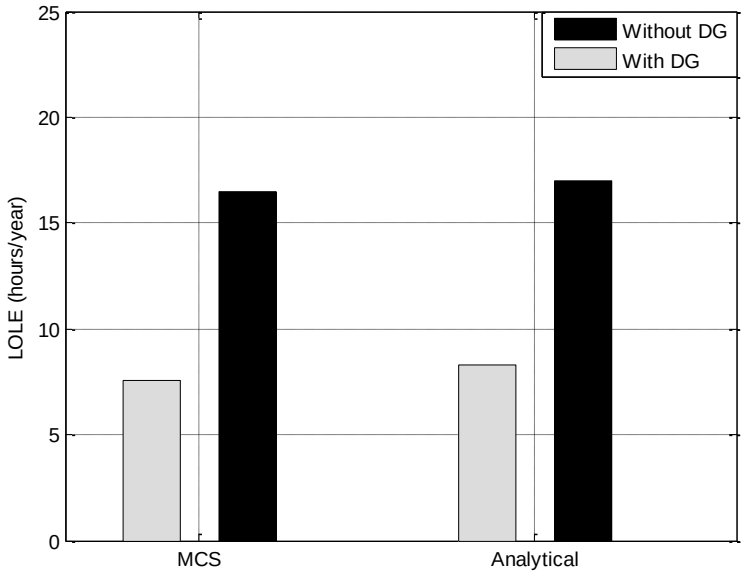

Figure 5-9 Comparison between LOLE with and without DG units

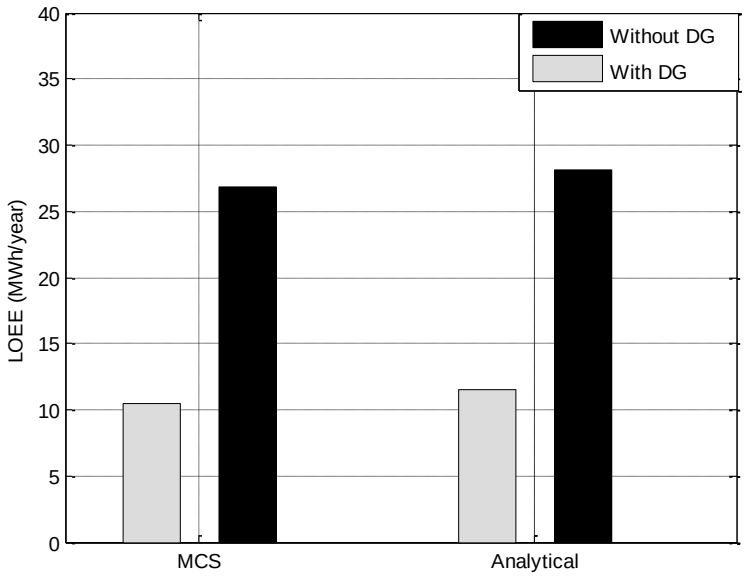

Figure 5-10 Comparison between LOEE with and without DG units

5.8.2 Second Scenario

In this scenario besides the fixed number of diesel DG units, there are two different types of renewable resources:

- Wind-based DG unit of 2 MW rating, connected at bus 39 which has the following characteristics:
  - Cut-in speed=4 m/s.
  - Nominal speed=14 m/s.
  - Cut-off speed= 25 m/s.
  - A 4% Forced Outage Rate (*FOR*) (MTTF=1920h, MTTR=80h) [30] is assumed for the wind turbine.
- Solar DG unit of rating 2 MW, consisting of 40000 modules, each has the following characteristics:
  - Watt peak (W) = 50.00
  - Open circuit voltage (V) = 55.50
  - Short circuit current (A) =1.80
  - Voltage at maximum power (V) = 38.00
  - Current at maximum power (A) = 1.32
  - Voltage temperature coefficient (mV/oC) = 194.00
  - Current temperature coefficient (mA/oC) =1.40
  - Nominal cell operating temperature (oC) = 43.00
  - A 4% Forced Outage Rate (*FOR*) (MTTF=1920h, MTTR=80h) [30] is assumed for the Solar DG.

5.8.2.1 Results

In this section the MCS and analytical technique are applied to the system under study to assess its adequacy during different modes of operation. It has to be mentioned here that the main difference between this scenario and the previous one is the modeling of the renewable resources and the load, either using MCS or analytical technique. However, modeling of all other components, such as the transformers, the diesel DG units, and all passive components are the same for both scenarios. Therefore, to avoid any duplication, this section presents only the modeling of the renewable resources and the load using MCS and analytical technique.

- **Monte Carlo Technique**

  - *Wind speed simulation*

As in the first scenario, Weibull pdf (3.1) has been utilized to simulate the hourly wind speed.

  - *Solar irradiance simulation*

Here the clearness index is modeled using MCS; hence, solar irradiance is calculated from (3.32). Finally the hourly output power of the solar DG unit is calculated using equations (3.65) to (3.69).

  - *Load modeling*

The hourly load values are based on historical data from the years 2005, 2006, and 2007. Since the reliability assessment needs to be studied over a large number of years, the hourly load are assumed to be the same every year.

- **Analytical Technique**

  - *Modeling of the renewable resources*

As mentioned in chapter 3, there is no pdf that can describe the annual solar irradiance. Since in this scenario, wind speed is combined with solar irradiance; therefore, wind speed is modeled using wind model 3; whereas, solar irradiance is modeled using solar model 2. In both models, the year is divided into four seasons, and a typical day is generated for each season. The day representing each season is further subdivided into 24-hour segments (time segments), each referring to a particular hourly interval for the entire season. Thus, there are 96 time segments for the year (24 for each season). Considering three years of historical data, each time segment then has (270) wind speed and solar irradiance level data points (3 years x 30 days per month x 3 months per season). Then for each hour, the discrete form is created, for each continuous pdf, with a step of 1m/s for wind speed states and 0.1 for clearness index states. From the wind turbine performance curve and the PV module characteristics, the output power of the wind-based DG and the solar DG can be calculated. Hence, a complete availability model of the wind-based DG and the solar DG, for each hour, can be created.

  - *Load modeling*

The load profile is assumed to follow the IEEE-RTS (load model 2). From this model and three years of historical data regarding the system under study hourly load, a typical daily load profile for each season has been generated as a percentage of the annual load as shown in Table 5-7.

Table 5-7 Load Profile

Hour	Winter	Spring	Summer	Fall
12-1 am	0.4757	0.3969	0.64	0.3717
1--2	0.4473	0.3906	0.60	0.3658
2--3	0.4260	0.3780	0.58	0.3540
3--4	0.4189	0.3654	0.56	0.3422
4--5	0.4189	0.3717	0.56	0.3481
5--6	0.4260	0.4095	0.58	0.3835
6--7	0.5254	0.4536	0.64	0.4248
7--8	0.6106	0.5355	0.76	0.5015
8--9	0.6745	0.5985	0.87	0.5605
9--10	0.6816	0.6237	0.95	0.5841
10--11	0.6816	0.6300	0.99	0.5900
11--12pm	0.6745	0.6237	1.00	0.5841
12--1	0.6745	0.5859	0.99	0.5487
1--2	0.6745	0.5796	1.00	0.5428
2--3	0.6603	0.5670	1.00	0.5310
3--4	0.6674	0.5544	0.97	0.5192
4--5	0.7029	0.5670	0.96	0.5310
5--6	0.7100	0.5796	0.96	0.5428
6--7	0.7100	0.6048	0.93	0.5664
7--8	0.6816	0.6174	0.92	0.5782
8--9	0.6461	0.6048	0.92	0.5664
9--10	0.5893	0.5670	0.93	0.5310
10--11	0.5183	0.5040	0.87	0.4720
11--12am	0.4473	0.4410	0.72	0.4130

The results of this scenario for grid-connected mode and islanding mode are summarized in Table 5-8 and Table 5-9, respectively. From the results listed in both tables, it can found that the same observations found in the first scenario are valid in this scenario.

Table 5-8 Adequacy Indices in Grid-connected Mode (Scenario 2)

Grid-connected mode				
Adequacy indices	**Case 1**		**Case 2**	
	MCS	Analytical	MCS	Analytical
LOLE (hr/year)	4.166	3.7516	0.0043	0.0047
LOLP	0.0476	0.04282	4.905E-05	5.36E-05
LOEE (MWh/year)	3.08	2.9	0.0040	0.0042
Period of healthy state(hr/year)	8571.6	8592.8	7.7700	7.7594
Probability of Healthy state	97.85	98.09	0.0886	0.0885
Period of Marginal state (hr/year)	184.23	163.404	0.0920	0.1060
Probability of Marginal state	2.10	1.87	0.0011	0.0012

Table 5-9 Adequacy Indices in Islanding Mode (Scenario 2)

Islanding mode (case 2)				
Adequacy indices	**Islanding not allowed**		**Islanding allowed**	
	MCS	Analytical	MCS	Analytical
LOLE (hr/year)	7.1892	7.3584	2.1876	2.8891
LOLP	0.00081	0.00084	0.0249	0.0329
LOEE (MWh/year)	35.824	36.71	11.781	13.076

5.9 Extra Reliability Indices Calculation

The outcomes of the proposed adequacy assessment can be used, with the aid of segmentation concept, to calculate other reliability indices; this can be done as follows:

Based on the segmentation concept, since all the customers in any given segment are treated as one customer, then the down time of any segment, equation 5.1, will be equal to the *System Average Interruption Duration Index* ($SAIDI_g$) of this segment. To calculate *SAIDI* of the whole system ($SAIDI_s$), $SAIDI_g$ must be weighted based on the number of customers in each segment as follows:

$$SAIDI_s = \sum_g SAIDI_g \times W_g \tag{5.12}$$

$$W_g = \frac{C_g}{C_s} \tag{5.13}$$

Based on the load points provided in Appendix A, the total number of customers in the system is 26: 12 of them lay in segment 1 and 14 are in segment 2. Hence, *SAIDI* for each segment as well as *SAIDI* for the whole system are calculated as in Table 5-10, whereas the improvement in *SAIDI* is shown in Table 5-11.

Table 5-10 SAIDI for Different Segments and the Whole System

	Islanding not allowed		**Islanding allowed**			
			Scenario 1		**Scenario 2**	
	MCS	**Analytical**	**MCS**	**Analytical**	**MCS**	**Analytical**
***SAIDI*$_1$**	7.1892	7.3692	7.1892	7.3692	7.1892	7.3692
***SAIDI*$_2$**	14.9992	15.2394	10.04	10.2712	9.9976	10.7593
SAIDIs	11.3946	11.607	8.7242	8.9318	8.7014	9.1946

Table 5-11 Improvement in SAIDI

	Scenario 1		**Scenario 2**	
	MCS	**Analytical**	**MCS**	**Analytical**
% Improvement in *SAIDI*$_1$	0	0	0	0
% Improvement in *SAIDI*$_2$	33.06	32.60	33.35	29.40
% Improvement in *SAIDIs*	23.44	23.05	23.64	20.78

5.10 Discussion

In this chapter the adequacy of a radial distribution system including different types of DG units has been assessed during different modes of operation, namely grid-connected and islanded modes. Analytical technique has been utilized to assess the system adequacy by modeling the load behaviour using IEEE_RTS system and creating the multi-state availability model of all the generating units. Moreover, a new implementation of the islanding mode of operation has been conducted so as to measure its impact on system adequacy from the LOLE and LOEE perspective. The Monte Carlo simulation technique, which is the most common technique for this kind of analysis, has also been used for the same problem in order to check the validity of the analytical technique. The results show that there is no significant difference between the outcomes of the two proposed techniques. Moreover, it was found that integrating DG units with the system has a notable impact on the improvement of system adequacy, and that allowing an islanding mode of operation adds even more improvement to this adequacy.

Chapter 6
Optimal Allocation of ESS in Distribution Systems

6.1 Introduction

Environmental concerns and fuel cost uncertainties associated with the use of conventional energy sources have resulted in rapid growth in the amount of wind energy connected to distribution grids. However, based on Ontario's standard offer program (SOP), the utility has the right to curtail (spill) wind energy in order to avoid any violation of the system constraints. This means that any increase in wind energy production over a specific limit might be met with an increase in the wind energy curtailed.

In spite of their cost, energy storage systems (ESSs) are considered to be a viable solution to this problem. Therefore, in this chapter a methodology for allocating an ESS in a distribution system with a high penetration of wind energy is proposed. The ultimate goal is to maximize the benefits for both the DG owner and the utility by sizing the ESS to accommodate all amounts of spilled wind energy and by then allocating it within the system in order to minimize the annual cost of the electricity. In addition, a cost/benefit analysis has been conducted in order to verify the feasibility of installing an ESS from the perspective of both the utility and the DG owner.

6.2 Methodology

Successfully integrating energy storage with distributed generation in grid-connected applications involves much more than selecting an adequately sized system based on one of the many commercially available technologies. The optimal integration of storage with grid-tied DG systems requires a thorough understanding of the following:

- The application for which the storage is being used and the benefits integrated storage would provide for that application;
- The available storage technologies and their suitability for the application;
- The requirements and constraints of integrating an ESS with both the load (residential, commercial, or microgrid) and the utility grid.

This section therefore presents the rationale behind the integration of an ESS with the distribution system in Ontario, Canada. The rationale is based on the nature of the relationship between the DG owner on one side and the Ontario Power Authority (OPA), the independent electricity system

operator (IESO), and the utility on the other side. This relationship can be summarized and analyzed as follows:

- The IESO, and not the utilities, is the market maker and dispatcher for all Metered Market Participants (transmission-connected and large distribution- connected generators and loads).
- Based on Ontario's standard offer program (SOP), distributed generation (DG) units are exclusively distribution-connected generators up to 10 MW. These are "non-firm energy" (that is, when it provides energy, the generator is paid based on the output) and are NOT dispatched by the IESO.
- At this time, there is no penalty for the mismatch caused by the SOP-connected DG unit as it does NOT bid into the generation market. This situation could change in the future as the penetration of DG units increases.
- The SOP DG owner does not sell to the utility, but to the OPA at standard fixed rates (13 cents/KWh for wind and 40 cents/kWh for solar) based on output. The utility is just a meter/bill settlement agency.
- The utility is responsible for ensuring that the system runs well and produces good power quality. Therefore, it has specific overriding rights to curtail the output of the DGs in order to maintain the following:
  1. Maximum of 60 % reverse power flow through the substation transformer;
  2. Nodal voltage between +/- 6 % of the nominal voltage;
  3. Equipment limits (transformers, lines, regulator, etc.) that must not be exceeded.
- At this time, the OPA does not pay the DG owner for spilled/dumped energy. However, with storage, the DG owner could be paid since they did supply the grid.

These regulations provide deep insight regarding the suitable application of an ESS. For example, installing an ESS in order to mitigate the problem of the uncertainty associated with wind-based DG output will not add value for either the utility or the DG owner because, so far, there is no penalty for the mismatch. However, installing an ESS to accommodate the spilled energy will add value for both the utility and the DG owner, as is explained later.

The proposed methodology has thus been inspired by the last two points, for the following reasons:

- Any intention to increase the penetration of wind energy will produce an increase in the amount of spilled wind energy in order to avoid any violation of the system constraints. This difficulty will eventually lead to a limitation imposed on the use of renewable energy.

- Due to the nature of wind speed and load, in Ontario, the amount of spilled wind energy is at its maximum value during the night when wind speed is high and loads are light. Therefore, if the utility can store this energy at night in the off-peak period and release it during the day in the on-peak period, it can take advantage of the difference between off-peak and on-peak electricity prices.
- With energy storage, the DG owner would be paid for the amount of energy that would otherwise be spilled, because it would no longer be spilled.

Based on the above discussion, the proposed application of an ESS is to store wind energy at night rather than spilling it and to release it during the day. The details of this application can be summarized as follows:

- The ESS will be allowed to charge and discharge for several hours (high energy application).
- The ESS will be charged during the off-peak night and discharged during the on-peak day, resulting in one charge/discharge cycle every day.
- The ESS will be charged mainly by the spilled wind energy.
- If the ESS can accommodate more energy, that is, if it is not fully charged, it will be charged from the utility.

The last point guarantees that the ESS will be fully utilized year round because spilled wind energy cannot fully charge the ESS every day, especially during the summer when the amount of spilled wind energy is very low.

The added value for the utility and the DG owner is as follows:

- Added value to the utility:
    1. Ability to take advantage of the price deferential between off-peak and on-peak periods
    2. Some reduction in losses because of the ability to optimally allocate the ESS in the system
    3. Peak shaving
    4. Improved system reliability through the use of a dispatchable source of energy
- Added value to the DG owners:
    1. Payment for the amount of spilled energy

Regarding the added value to the utility, the main focus of this study will be on the first two points; quantifying the last two points is beyond the scope of this work.

6.3 Procedures

This section presents the procedures that must be conducted in order to accomplish the proposed work as shown in figure 6-1.

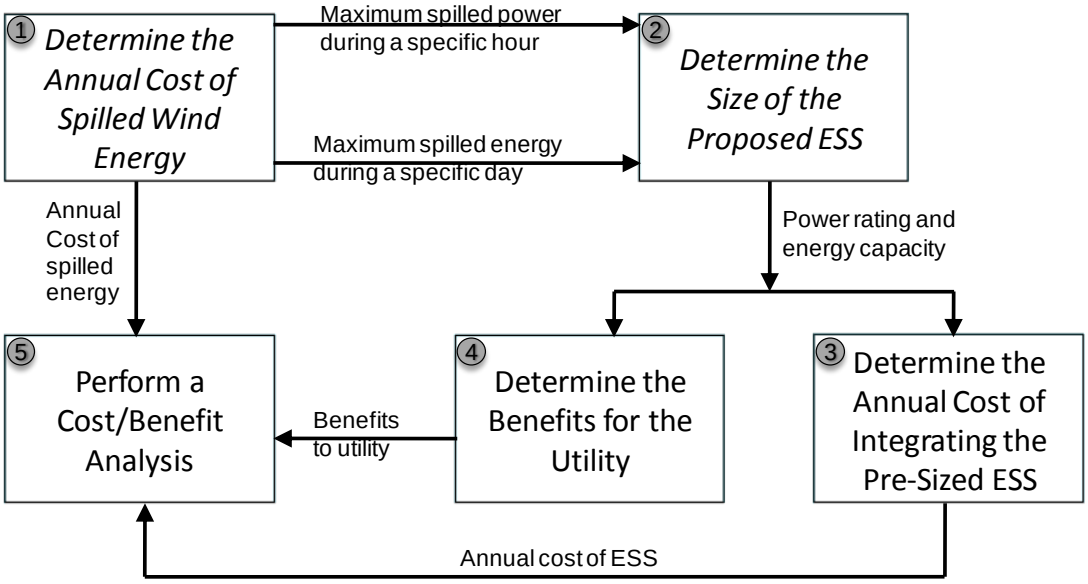

Figure 6-1 Proposed steps for optimal allocation of ESS in distribution systems

6.3.1 Determine the Annual Cost of Spilled Wind Energy

Computing the annual cost of spilled wind energy requires first a calculation of the expected amount of spilled wind energy, the cost of which is based on the time at which it is spilled.
Calculating the expected amount of spilled wind energy requires the following steps:

6.3.1.1 Wind speed modeling

In this work ARMA technique is utilized to estimate the hourly wind speed for the entire year (wind model 6). The generated wind speed is then combined with the wind turbine parameters, as in equation (3.24), in order to evaluate the electrical power generated as a function of time.

6.3.1.2 Load modeling

The load profile is assumed to follow the IEEE-RTS system (load model 2). This system provides weekly peak load in percent of the annual peak load, daily peak load cycle in percent of the weekly peak, and hourly peak load in percentage of the daily peak load

6.3.1.3 Hourly electricity price modeling

In Ontario, the on-peak hours are described as hours 8-23 and off-peak are the rest. Therefore, the electricity price is modeled as the daily average prices of on/off peak periods, which are calculated from the hourly electricity prices provided by the IESO [97].

The annual predicted wind energy and the load model are then incorporated into an OPF to determine the amount of spilled energy. The objective of the OPF is to maximize the wind energy; the constraints include all the technical constraints of the distribution system. A curtailment index is used to determine the amount of spilled wind energy that avoids violation of the system constraints. The OPF formulation is as follows:

Objective function

$$Maximize \qquad Cost = \sum_{t=1}^{8760} \sum_{i=1}^{n} PDG_{t,i} * CI_{t,i} \tag{6.1}$$

This objective function guarantees that, during each time segment (t), all the generated wind energy will be injected into the system as long as none of the system constraints is violated.

The curtailment index ($CI_{t,i}$), which has a value between zero and one, determines the amount of spilled wind energy.

Constraints

1. *Power flow equations:*

$$PG_{t,1} + PDG_{t,i} * CI_{t,i} - PD_{t,i} = \sum_{j=1}^{n} V_{t,i} * V_{t,i} * Y_{ij} * \cos(\theta_{ij} + \delta_{t,j} - \delta_{t,i}) \quad \forall i,t \tag{6.2}$$

$$QG_{t,1} - QD_{t,i} = -\sum_{j=1}^{n} V_{t,i} * V_{t,i} * Y_{ij} * \sin(\theta_{ij} + \delta_{t,j} - \delta_{t,i}) \quad \forall i,t \tag{6.3}$$

2. *Branch current equations:*

$$I_{t,ij} = \left|Y_{ij}\right| * \left[(V_{t,i})^2 + (V_{t,j})^2 - 2 * V_{t,i} * V_{t,j} * \cos(\delta_{t,j} - \delta_{t,i})\right]^{1/2} \quad \forall t, i, j \tag{6.4}$$

3. *Slack bus voltage and angle (assumed to be bus 1):*

$$V_{t,1} = 1.0$$
$$\delta_{t,1} = 0.0 \quad (6.5)$$

4. *Voltage limits at the other buses:*

$$V_{\min} \le V_{t,i} \le V_{\max} \qquad \forall\, i \notin substation\, bus,\ t \quad (6.6)$$

5. *Feeder capacity limits:*

$$0 \le I_{t,ij} \le I_{ij_{\max}} \qquad \forall i, j, t \quad (6.7)$$

6. *Reverse power flow:*

$$-0.6 * S_R \le PG_{t,1} \le S_R \qquad \forall t \quad (6.8)$$

These constraints guarantee that the reverse power flow will not exceed 0.6 of the substation rating.

6.3.2 Determine the Size of the Proposed ESS

In this step, the size of the ESS is calculated with respect to power rating and energy capacity so that it will accommodate all the expected spilled energy calculated from the previous step.

The maximum spilled power during a specific hour is used to determine the power rating of the ESS, and the maximum spilled energy during a specific day is utilized to determine the energy capacity of the ESS.

6.3.3 Determine the Annual Cost of Integrating the Pre-Sized ESS

This step involves the calculation of the annual cost of integrating each type of ESS technology available in the market and suitable for the proposed application, as follows [69]:

The total annual cost (*TAC*) of the ESS is the sum of three terms: the total annual capital cost, the maintenance cost, and the replacement cost. The total capital cost is itself the sum of the following three terms:

- The total cost for the power electronics:

$$PCS = PCSU * P_{ESS} \quad (6.9)$$

– The total cost for the storage units:

$$SUC = SUCU * \frac{E_{ESS}}{\eta} \tag{6.10}$$

– The total cost for the balance of plant:

$$BOP = BOPU * \frac{E_{ESS}}{\eta} \tag{6.11}$$

$$TCC = PCS + SUC + BOP \tag{6.12}$$

– The annualized capital cost is then

$$ACC = TCC * CRF \tag{6.13}$$

– The CRF [69] is given as

$$CRF = \frac{i_r (1+i_r)^z}{(1+i_r)^z - 1} \tag{6.14}$$

When batteries are used as the storage element, they may have to be replaced one or more times during the life of the plant. This cost is annualized (per kilowatt hour) as

$$A = F * [(1+i_r)^{-r} + (1+i_r)^{-2r} + ...] * CRF \tag{6.15}$$

Battery life is the fixed number of charge/discharge cycles. The replacement period in years can then be calculated as

$$r = \frac{C}{N * 365} \tag{6.16}$$

– The annual battery replacement cost is then

$$ARC = A * \frac{E_{ESS}}{\eta} \tag{6.17}$$

– The annual fixed operation and maintenance cost is

$$OMC = OM * P_{ESS} \tag{6.18}$$

– The total annual cost (*TAC*) is then

$$TAC = ACC + OMC + ARC \tag{6.19}$$

6.3.4 Determine the Benefits for the Utility

In this step, the benefits returned to the utility due to the integration of the ESS are quantified. As mentioned in Section 6.2, the benefits to be considered in this work are the price differential between on-peak and off-peak periods and the reduction in power loss. To quantify the benefits, the OPF from step one is used with some modifications to accommodate the ESS equations. The objective function of the OPF is to minimize the total annual cost of electricity; this objective function implicitly includes the cost of losses. The decision variables of the OPF are the optimum size and location of the ESS. The OPF is formulated to have a dynamic nature: in other words, the OPF is run hour by hour for an entire day, repeating the same process for the next day, and so on. The link between consecutive days is through the stored energy in the ESS at the end of the day, which is transferred to the next day.

In the OPF formulation, the ESS is considered to be a load during charging periods (off-peak) and a generator during discharge periods (on-peak). Matrices *A*1 and *A*2 are used to define the charging and discharging periods. Matrix *A*1 has one column with 24 binary elements, with all elements corresponding to off-peak hours being ones and all elements corresponding to on-peak hours being zeros. Matrix *A*2 is the complementary version of matrix *A*1. The objective function is comprised of two parts: 1) the off-peak period, during which the ESS is considered to be a load, and the utility is paying the cost of stored energy; 2) the on-peak period, during which the energy released from the ESS is considered to be free energy, which is the reason it is subtracted from the total demand.

Objective function

$$\begin{aligned}&\sum_{D=1}^{365}\Big(\sum_{t=1}^{24}\Big[\sum_{i=}^{N}(P_{D,t,i}^{CH} + PD_{D,t,i}) + Ploss_{D,t}\Big] * A1 * Coff_D + \\ &\Big[\sum_{i=}^{N}(-P_{D,t,i}^{DISCH} + PD_{D,t,i}) + Ploss_{D,t}\Big] * A2 * Con_D\Big)\end{aligned} \tag{6.20}$$

Constraints

The following power flow equations apply:

$$PG_{D,t,1} + PDG_{D,t,i} + P_{D,t,i}^{DISCH} * A2 - (PD_{D,t,i} + P_{D,t,i}^{CH} * A1) = \sum_{j=1}^{N} V_{D,t,i} * V_{D,t,j} * Y_{ij} * \cos(\theta_{ij} + \delta_{D,t,j} - \delta_{D,t,i}) \ \forall D,t,i \quad (6.21)$$

$$QG_{D,t,1} - QD_{D,t,i} = \sum_{j=1}^{N} V_{D,t,i} * V_{D,t,j} * Y_{ij} * \sin(\theta_{ij} + \delta_{D,t,j} - \delta_{D,t,i}) \ \forall D,t,i \quad (6.22)$$

Since charging and discharging power at each bus are day dependent, in order to obtain a fixed value for the optimum power rating on each bus for the entire year, charging and discharging are considered to be less than or equal to a specific value that is not day dependent.

$$P_{D,t,i}^{CH} \le Pi \quad \forall D,t,i \quad (6.23)$$

$$P_{D,t,i}^{DISCH} \le Pi \quad \forall D,t,i \quad (6.24)$$

Since the utility has no authority to bid in the electricity market, any reverse power flow should come from the wind-based DG units, not from the ESS. To guarantee that all the reverse power flow is coming from the wind-based DG units during any hour, the output power of the ESS must be less than the total demand during that hour:

$$\sum_{i} P_{D,t,i}^{DISCH} \le \sum_{i} PD_{D,t,i} \quad \forall D,t \quad (6.25)$$

The charging and discharging energies are calculated from the hourly input and output power of the ESS, as follows:

$$E_{D,i}^{CH} = \sum_{t} P_{D,t,i}^{CH} * A1 \quad \forall D,i \quad (6.26)$$

$$E_{D,i}^{DISCH} = \sum_{t} P_{D,t,i}^{DISCH} * A2 \quad \forall D,i \quad (6.27)$$

The following constraints guarantee that the energy released from the ESS during the on-peak period is less than or equal to the stored energy during the off-peak period. The difference is the final energy stored in the ESS at the end of the day, which is considered to be the initial energy stored for the next day:

$$E_{D,i}^{CH} \geq E_{D,i}^{DISCH} \quad \forall D, i \tag{6.28}$$

$$E_{D,i}^{FINAL} = E_{D,i}^{CH} - E_{D,i}^{DISCH} \quad \forall D, i \tag{6.29}$$

Equation (33) is the same as (26) but is related to the energy.

$$E_{D,i}^{CH} + E_{D-1,i}^{FINAL} \leq E_i \quad \forall D, i \tag{6.30}$$

In order to accommodate all the spilled energy, the aggregated energy capacity and power rating of all ESSs on all buses must be equal to the values calculated in the first procedure.

$$\sum_i E_i = \frac{E_{ESS}}{\eta_{ESS}} \tag{6.31}$$

$$\sum_i P_i = P_{ESS} \tag{6.32}$$

The hourly power loss is calculated as follows:

$$Ploss_{D,t} = 0.5 * \sum_{i=1}^{N} \sum_{j=1}^{N} G_{ij} * \left[(V_{D,t,i})^2 + (V_{D,t,j})^2 - 2 * V_{D,t,i} * V_{D,t,j} * \cos(\delta_{D,t,j} - \delta_{D,g,i}) \right] \forall D, t \tag{6.33}$$

The rest of the OPF constraints are as calculated in equations (6.4) – (6.8).

6.3.5 Perform a Cost/Benefit Analysis

In this step, the total benefits for the utility and the DG owner are compared to the annual cost of integrating the ESS.

6.4 Case Study

The system under study, as shown in figure 4.5, is a typical rural distribution system with a peak load of 16.18 MVA. The main substation at bus 1 is used to feed a rural area, and the maximum feeder capacity is 300 A. There are three wind-based DG units, with ratings of 8.5 MW, 4 MW, and 10.3 MW, connected at buses 19, 28, and 40, respectively. The power curve parameters of the wind turbines are given in Table 6-1.

Table 6-1Wind Turbine Power Curve

Features	Wind
Cut-in speed	4
Rated	14
Cut-out speed	24

6.4.1 Wind Speed and Wind Turbine Data

The ARMA model for the wind speed profile in the area under study was developed using the system identification toolbox in the MATLAB program. Hourly wind speed time data from 2004 to 2008 were used to develop the ARMA model and to calculate the hourly mean and standard deviation of the wind speed. The complete ARMA (4, 3) model for the system under study is as follows:

$$y_t = -0.8248y_{t-1} + 0.02911y_{t-2} + 0.8248y_{t-3} + 0.943y_{t-4} + e_t \\ -1.835e_{t-1} - 1.785e_{t-2} - 0.9612e_{t-3} \quad (6.34)$$

6.4.2 Load Data

The load profile was calculated based on the hourly load data for the system under study and the IEEE-RTS system, and is shown in Table 4-7 as a percentage of the annual peak load.

6.5 Results

This section presents the outcome of each of the steps proposed, the goal of which is the optimal integration of the ESS with the distribution system.

Figure 6.1 presents the amount of wind energy that wind-based DG units can generate versus the amount of wind energy that the distribution system can accommodate without violating any system constraints. Figure 6-2 reveals that the energy is spilled during the night and that the maximum amount of energy is spilled during winter nights. The sum of the hourly differences between these two curves determines the amount of spilled energy; however, the maximum difference during a specific hour gives the maximum power of the spilled energy. The maximum amount of energy spilled during one day, the maximum spilled power, and the total annual spilled energy is shown in Table 6-2. The annual cost of the spilled energy, based on the electricity price, is also presented in the same table.

The maximum spilled power and maximum spilled energy, calculated from the first procedure, are utilized to determine the capacity of the ESS. The power rating for different ESS technologies is the same; however, the energy capacity is calculated based on the efficiency of each technology. The

characteristics of different ESS technologies are provided in [69]. Table 6-3 shows the capacity and the annual cost of some of the ESS technologies that are suitable for the proposed application.

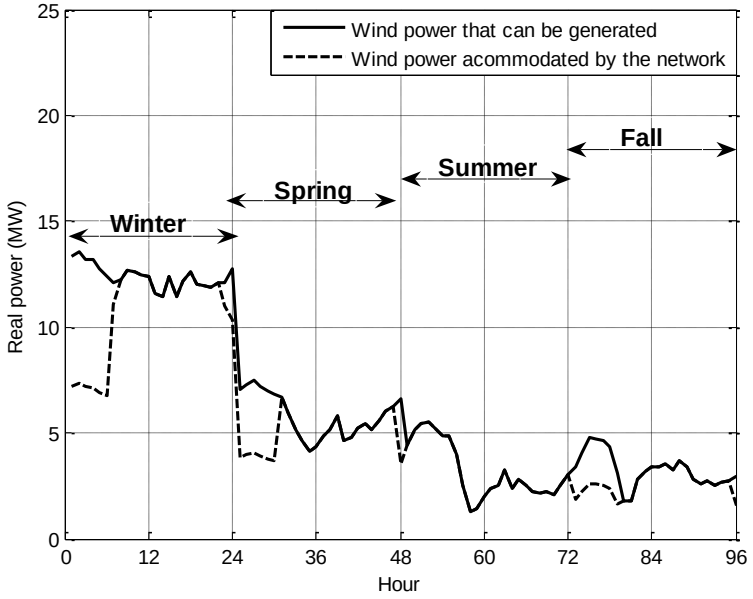

Figure 6-2 Typical day of each season showing the difference between the wind energy expected to be generated and the wing energy accommodated by the network

Table 6-2 Cost of Spilled Energy

Max amount of spilled power during the entire year P_{ESS}	6 MW
Max amount of spilled energy during a specific day E_{ESS}	40 MWh
Total annual spilled energy	7063.9 MWh
Total annual cost of spilled energy (million dollars)	0.92

Table 6-3 Annual Cost of Different ESS Technologies

Technology	**Efficiency**	**Power rating (MW)**	**Energy capacity (MWh)**	**Annual cost of installing ESS (million $)**
LA	0.75	6	53.33	2.42
VRLA	0.75	6	53.33	5.56
Na/S	0.77	6	51.94	2.49
Zn/Br	0.77	6	51.94	1.17
VRB	0.70	6	57.14	2.55

The least costly ESS technology was selected to be integrated with the distribution system and was optimally allocated using the OPF presented in Section III. The optimum allocation of the ESS in the distribution system is shown in Table 6-4, and Table 6-5 shows the benefits for the utility from the perspective of both electricity cost and power losses.

Table 6-4 Optimum Allocation of ESS in the Distribution System

bus	**MWh**	**MW**
4	19.48	2
9	12.99	1.5
28	8.44	0.5
39	4.55	1
40	6.49	1

Table 6-5 Utility Profit

		Total	Load	Losses
Annual electricity cost (million $)	without storage	5.11	4.97	0.142
	with storage	4.68	4.56	0.121
Profit (million $)		0.43	0.41	0.021

The total annual profits for both the DG owner and the utility compared to the annual cost of different ESS technologies are shown in figure 6-3. It can be seen that the net profit is not huge for either the utility or the DG owner, which was expected due to the high cost of the ESS. In addition, the results show that the only economically feasible ESS technology is Zn/Br.

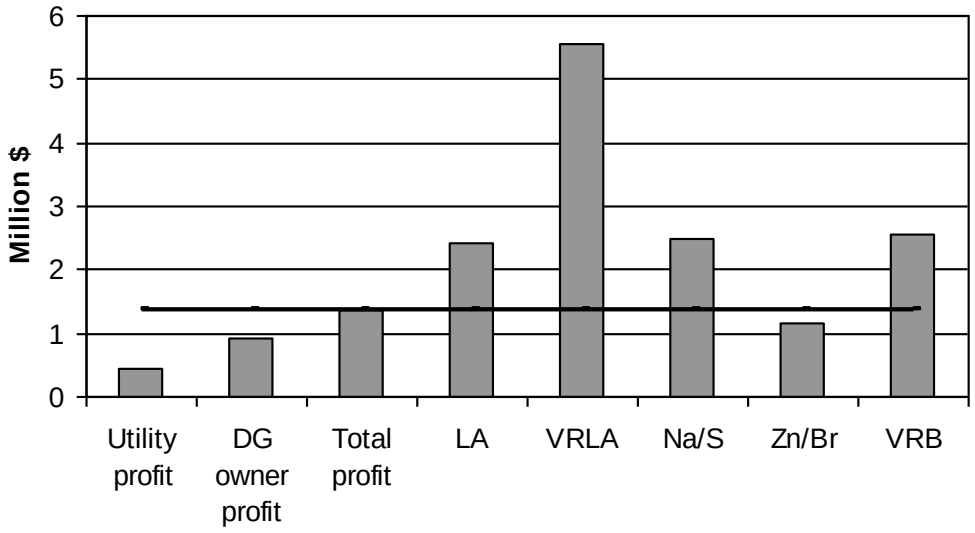

Figure 6-3 Total profit compared to the annual cost of different ESS technologies

6.6 Discussion

In this work, a methodology is proposed for optimally allocating ESS in distribution systems with a high penetration of wind energy. The aggregated capacity of an ESS is determined so as to accommodate all amounts of spilled wind energy, and the ESS is optimally allocated in the system in order to minimize the annual electricity cost. The annual hourly wind speed and load profile are generated using the ARMA technique and the IEEE-RTS system, respectively, and the daily on/off peak electricity prices are collected from the IESO website. Further, these data are incorporated into two separate OPF formulations in order to determine the annual cost of spilled energy and the optimum allocation of the ESS in the distribution system. A cost/benefit analysis was also conducted by comparing the annual cost of different ESS techniques with the total profit for both the utility and the DG owner. The results show that integrating an ESS with the distribution system for the proposed application is economically feasible only when the least expensive ESS is used. These findings are not conclusive, however, because the study did not take into account all possible benefits for the utility. If other benefits of an ESS are quantified, such as peak shaving and the enhancement of reliability, the results should be more promising.

Chapter 7
Conclusions and Contributions

7.1 Conclusions

The research in this thesis tackled the problem of distribution system planning and reliability assessment with renewable DG. The following points summarize the work presented in this thesis:

1. This work started with an overview regarding the different approaches used to model wind speed and solar irradiance, accompanied by the advantages, the disadvantages, and the applications of each approach. In the same context, a novel technique to estimate annual wind speed was proposed. The proposed technique is based on two steps utilizing three years of historical data. The first step is to divide the data into clusters, while in the second step a constrained Grey predictor is utilized to estimate the wind speed profile. Furthermore, in order to model solar irradiance chronologically, the cdf of the clearness index pdf was determined, and then inverted using a Lambert W function; hence, MCS is used to model the hourly clearness index.

2. In order to optimally allocate renewable DG units in distribution systems, a probabilistic planning technique was proposed for optimally allocating different types of DG (i.e., wind-based DG, solar DG, and biomass DG) into the distribution system so as to minimize annual energy losses. The key idea in this work is to generate a probabilistic generation-load model that includes all possible operating conditions; hence, this model can be accommodated into a deterministic optimal power flow (OPF) formulation. The objective of the proposed technique was to minimize annual energy losses, while the constraints included the voltage limits, the thermal limits of the feeder, the maximum investment capacity on each bus, the discrete size of the DG units, and the maximum penetration limit of the DG units. The main contributions of this technique can be summarized in the following points:

   - The proposed technique guarantees no violation of any of the system constraints under any operating conditions
   - The technique guarantees the optimum allocation of the renewable DG units for all possible operating conditions

- A by-product of the proposed technique is a power flow solution for all possible operating conditions, which will provide a useful database for the system operator
- Because the mathematical formulation is generic, the objective function can be expanded to accommodate additional terms, such as capital and running costs of the DG units; therefore this technique has applications beyond the minimization of energy loss.

3. Regarding the impact of renewable DG on distribution system reliability, a methodology was proposed to assess the distribution system supply adequacy during different modes of operation, using analytical and MCS techniques. In the analytical technique, a MSAM is generated for each supply in the system, and these are then combined to create the total generation availability model. The segmentation concept is used in this technique to determine the probability of the island being successful or failing. In the MCS technique, the hourly wind speed and solar irradiance are modeled using Weibull and the clearness index pdf, while an exponential pdf is used to model the random behaviour of the hardware of the renewable DG units, transformers, Diesel DG units, and the system components. Further, segmentation concept is exploited to determine more reliability indices such as SAIDI.
4. Finally in this work, a methodology was proposed to optimally allocate ESS in distribution systems so as to mitigate the problems created due to the high penetration of renewable DG units into the system. The ultimate goal of this methodology was to maximize the profit to both the utility and the DG owner. This was done by sizing the ESS to accommodate all the expected curtailed wind energy, allocating them in the system to minimize the annual energy losses, and scheduling them to store energy during off-peak periods and release it during on-peak periods to take the advantage of the difference between off-peak and on-peak electricity prices.

7.2 Contributions

The main contributions of this thesis can be highlighted as follows:

1. A novel technique for annual wind speed estimation using constrained Grey predictor was proposed.
2. A new utilization of the clearness index to model solar irradiance using MCS technique was introduced.
3. A new utilization of segmentation concept to assess the supply adequacy of distribution systems, using analytical technique, was presented.

4. A novel framework was introduced for optimally allocate different types of DG into distribution systems. The proposed framework combines the random behaviour of renewable DG units, the discrete size of the available DG, and the load profile into a deterministic optimal power flow formulation. The model has the privilege of maintaining no violation of any of the system constraints under any operating condition.

Appendix A: Distribution System Data

Table A- 1 System data

From	To	Length	R(ohm/Km)	X(ohm/Km)	Charge(μs/Km)
1	2	5.7000	0.169111	0.418206	3.9540
2	3	1.0100	0.169111	0.418206	3.9540
2	4	0.4000	0.169111	0.418206	3.9540
4	5	0.3800	0.169111	0.418206	3.9540
5	6	0.1300	0.169111	0.418206	3.9540
5	7	0.1700	0.169111	0.418206	3.9540
7	9	0.2600	0.169111	0.418206	3.9540
9	10	0.1400	0.169111	0.418206	3.9540
9	11	0.3800	0.169111	0.418206	3.9540
11	12	0.5600	0.169111	0.418206	3.9540
12	13	0.3000	0.169111	0.418206	3.9540
12	14	3.3300	0.169111	0.418206	3.9540
14	15	1.0300	0.169111	0.418206	3.9540
16	17	1.0800	0.169111	0.418206	3.9540
17	18	1.6400	0.169111	0.418206	3.9540
18	19	0.4700	0.169111	0.418206	3.9540
19	20	0.4700	0.348124	0.468482	3.7571
21	22	0.9600	1.391924	0.478811	3.5971
19	23	0.1900	0.348124	0.468482	3.7571
23	24	1.9400	0.348124	0.468482	3.7571
24	25	2.4500	0.348124	0.468482	3.7571
24	26	1.6300	0.348124	0.468482	3.7571
26	27	1.2000	0.552276	0.485241	3.6035
26	28	2.1200	0.348124	0.468482	3.7571
28	29	0.7300	0.552276	0.485241	3.6035
29	30	0.7500	0.552276	0.485241	3.6035
28	31	2.5400	0.348124	0.468482	3.7571
23	32	0.3600	0.276519	0.458580	3.8280
32	33	0.2600	0.276519	0.458580	3.8280
33	34	3.5800	0.552276	0.485241	3.6035
33	35	0.7700	0.276519	0.458580	3.8280
35	36	2.0800	0.348124	0.468482	3.7571
35	37	4.5100	0.276519	0.458580	3.8280
37	38	3.2400	0.169111	0.418206	3.9540
38	39	0.3000	0.169111	0.418206	3.9540
39	40	0.5000	0.169111	0.418206	3.9540

Table A- 2 Load data

Name	Bus no	P(Kw)	Q(kvar)
M1	4	6251.96	2054.92
M2	4	152.00	49.96
M3	4	9.50	3.12
M4	6	187.92	106.50
M5	6	715.14	405.29
M6	8	3187.25	1047.60
M7	10	576.00	507.98
M8	13	19.00	0.00
M9	14	19.00	6.24
M10	14	142.50	46.84
M11	14	161.50	53.08
M12	14	23.75	7.81
M13	22	47.50	15.61
M14	25	289.75	95.24
M15	27	152.00	49.96
M16	30	194.75	64.01
M17	31	142.50	46.84
M18	31	123.50	40.59
M19	31	104.50	34.35
M20	31	147.25	48.40
M21	34	204.25	67.13
M22	37	47.50	15.61
M23	37	57.00	18.73
M24	41	2166.00	711.93
M25	36	80.75	26.54
M26	23	9.50	3.12

Bibliography

[1] A. Champers, "Distributed Generation: A Nontechnical Guide," *PennWell, Tulsa, Oklahoma*, p. 283, 2001.

[2] P. Dondi, D. Bayoumi, C. Haederli, D. Julian, and M. Suter, "Network integration of distributed power generation," London, United kingdom, 2002, pp. 1-9.

[3] T. Ackermann, G. Andersson, and L. Soder, "Distributed generation: A definition," *Electric Power Systems Research*, vol. 57, pp. 195-204, 2001.

[4] P. A. Daly and J. Morrison, "Understanding the potential benefits of distributed generation on power delivery systems," Little Rock, AR, United states, 2001, pp. A21-A213.

[5] A. Schweer and J. Tzschoppe, "Impact of increasing contribution of dispersed generation on the power system," *Elektrizitaetswirtschaft*, vol. 98, pp. 46-48, 1999.

[6] H. L. Willis and W. G. Scott, *Distributed Power Generation*. New York: Marcel Dekker, 2000.

[7] R. Lasseter, A. Akhil, C. Marnay, J. Stephens, J. Dagle, R. Guttromson, A. S. Meliopoulous, R.Yinger, and J. Eto, "Integration of Distributed Energy Resources-The CERTS MicroGrid Concept," *Rep. LBNL-50829*, April 2002.

[8] "IEEE Application Guide for IEEE Std 1547, IEEE Standard for Interconnecting Distributed Resources with Electric Power Systems," *IEEE Std 1547.2-2008*, pp. 1-207, 2009.

[9] K. Nara, Y. Hayashi, K. Ikeda, and T. Ashizawa, "Application of tabu search to optimal placement of distributed generators," in *Power Engineering Society Winter Meeting, 2001. IEEE*, 2001, pp. 918-923 vol.2.

[10] K. Kyu-Ho, L. Yu-Jeong, R. Sang-Bong, L. Sang-Kuen, and Y. Seok-Ku, "Dispersed generator placement using fuzzy-GA in distribution systems," in *Power Engineering Society Summer Meeting, 2002 IEEE*, 2002, pp. 1148-1153 vol.3.

[11] W. Caisheng and M. H. Nehrir, "Analytical approaches for optimal placement of distributed generation sources in power systems," *IEEE Transactions on Power Systems*, vol. 19, pp. 2068-2076, 2004.

[12] I. E. Davidson and N. M. Ijumba, "Optimization model for loss minimization in a deregulated power distribution network," in *Africon Conference in Africa, 2002. IEEE AFRICON. 6th*, 2002, pp. 887-894 vol.2.

[13] N. Acharya, P. Mahat, and N. Mithulananthan, "An analytical approach for DG allocation in primary distribution network," *International Journal of Electrical Power & Energy Systems*, vol. 28, pp. 669-678, 2006.

[14] H. Hedayati, S. A. Nabaviniaki, and A. Akbarimajd, "A Method for Placement of DG Units in Distribution Networks," *IEEE Transactions on Power Delivery*, vol. 23, pp. 1620-1628, 2008.

[15] V. H. M. Quezada, J. R. Abbad, and T. G. S. Roman, "Assessment of energy distribution losses for increasing penetration of distributed generation," *IEEE Transactions on Power Systems*, vol. 21, pp. 533-540, 2006.

[16] A. P. Agalgaonkar, S. V. Kulkarni, and S. A. Khaparde, "Multi-attribute decision making approach for strategic planning of DGs," in *Power Engineering Society General Meeting, 2005. IEEE*, 2005, pp. 2985-2990 Vol. 3.

[17] G. Celli, E. Ghiani, S. Mocci, and F. Pilo, "A multiobjective evolutionary algorithm for the sizing and siting of distributed generation," *IEEE Transactions on Power Systems*, vol. 20, pp. 750-757, 2005.

[18] G. Celli and F. Pilo, "Penetration level assessment of distributed generation by means of genetic algorithms," in *IEEE Proc. Of Power System Conference* Clemson, SC, 2002.

[19] R. E. Brown, P. Jiuping, F. Xiaorning, and K. Koutlev, "Siting distributed generation to defer T&D expansion," in *Transmission and Distribution Conference and Exposition, 2001 IEEE/PES*, 2001, pp. 622-627 vol.2.

[20] W. El-Khattam, Y. Hegazy, and M. Salama, "An integrated distributed generation optimization model for distribution system planning," in *Power Engineering Society General Meeting, 2005. IEEE*, 2005, p. 2392 Vol. 3.

[21] W. El-Khattam, K. Bhattacharya, Y. Hegazy, and M. M. A. Salama, "Optimal investment planning for distributed generation in a competitive electricity market," *IEEE Transactions on Power Systems*, vol. 19, pp. 1674-1684, 2004.

[22] G. Celli and F. Pilo, "MV network planning under uncertainties on distributed generation penetration," Piscataway, NJ, USA, 2001, pp. 485-90.

[23] G. Carpinelli, G. Celli, F. Pilo, and A. Russo, "Distributed generation siting and sizing under uncertainty," in *Power Tech Proceedings, 2001 IEEE Porto*, 2001, p. 7 pp. vol.4.

[24] A. Keane and M. O'Malley, "Optimal Allocation of Embedded Generation on Distribution Networks," *IEEE Transactions on Power Systems*, vol. 20, pp. 1640-1646, 2005.

[25] J. A. Greatbanks, D. H. Popovic, M. Begovic, A. Pregelj, and T. C. Green, "On optimization for security and reliability of power systems with distributed generation," in *Power Tech Conference Proceedings, 2003 IEEE Bologna*, 2003, p. 8 pp. Vol.1.

[26] D. H. Popovic, J. A. Greatbanks, M. Begovic, and A. Pregelj, "Placement of distributed generators and reclosers for distribution network security and reliability," *International Journal of Electrical Power and Energy Systems*, vol. 27, pp. 398-408, 2005.

[27] A. Keane and M. O'Malley, "Impact of distributed generation capacity on losses," in *Power Engineering Society General Meeting, 2006. IEEE*, 2006, p. 7 pp.

[28] V. Calderaro, A. Piccolo, and P. Siano, "Maximizing DG penetration in distribution networks by means of GA based reconfiguration," in *Future Power Systems, 2005 International Conference on*, 2005, pp. 6 pp.-6.

[29] P. N. Vovos, G. P. Harrison, A. R. Wallace, and J. W. Bialek, "Optimal power flow as a tool for fault level-constrained network capacity analysis," *IEEE Transactions on Power Systems*, vol. 20, pp. 734-741, 2005.

[30] G. P. Harrison. and A. R. Wallace, "Maximizing distributed generation capacity in deregulated markets," in *IEEE Transmission and Distribution Conference and Exposition*. vol. 2, 2003.

[31] L. F. Ochoa, C. J. Dent, and G. P. Harrison, "Maximisation of intermittent distributed generation in active networks," in *SmartGrids for Distribution, 2008. IET-CIRED. CIRED Seminar*, 2008, pp. 1-4.

[32] A. Keane and M. O'Malley, "Optimal distributed generation plant mix with novel loss adjustment factors," in *Power Engineering Society General Meeting, 2006. IEEE*, 2006, p. 6 pp.

[33] A. Keane and M. O'Malley, "Optimal Utilization of Distribution Networks for Energy Harvesting," *IEEE Transactions on Power Systems*, vol. 22, pp. 467-475, 2007.

[34] R. G. Deshmukh. and R. Ramakumar., "Reliability analysis of combined wind-electric and conventional generation systems," *Sol. Energy*, vol. 28, 1982.

[35] M. A. Khallat and S. Rahman, "A Probabilistic Approach to Photovoltaic Generator Performance Prediction," *IEEE Transactions on Energy Conversion*, vol. EC-1, pp. 34-40, 1986.

[36] W. Xifan, D. Hui-Zhu, and R. J. Thomas, "Reliability Modeling of Large Wind Farms and Associateed Electric Utility Interface Systems," *IEEE Transactions on Power Apparatus and Systems,* vol. PAS-103, pp. 569-575, 1984.

[37] C. Singh and Y. Kim, "An efficient technique for reliability analysis of power systems including time dependent sources," *IEEE Transactions on Power Systems,* vol. 3, pp. 1090-1096, 1988.

[38] C. Singh and A. Lago-Gonzalez, "Reliability Modeling of Generation Systems Including Unconventional Energy Sources," *IEEE Transactions on Power Apparatus and Systems,* vol. PAS-104, pp. 1049-1056, 1985.

[39] L. L. Bucciarelli, "Estimating loss-of-power probabilities of stand-alone photovoltaic solar energy systems," *Sol. Energy,* vol. 32, 1984.

[40] L. L. Bucciarelli., "The effect of day-to-day correlation in solar radiation on the probability of loss-of-power in a stand-alone photovoltaic solar energy systems," *Sol. Energy,* vol. 36, 1986.

[41] E. Ofry and A. Braunstein, "The Loss of Power Supply Probability as a Technique for Designing Stand-Alone Solar Electrical (Photovoltaic) Systems," *IEEE Transactions on Power Apparatus and Systems,* vol. PAS-102, pp. 1171-1175, 1983.

[42] S. A. klein. and W. A. Beckman., "Loss-of-load probability for a stand-alone photovoltaic systems," *Sol. Energy,* vol. 39, 1987.

[43] G. Desrochers, M. Blanchard, and S. Sud, "A Monte-Carlo Simulation Method for the Economic Assessment of the Contribution of Wind Energy to Power Systems," *IEEE Transactions on Energy Conversion,* vol. EC-1, pp. 50-56, 1986.

[44] R. Billinton and L. Gan, "Wind power modeling and application in generating adequacy assessment," in *WESCANEX 93. 'Communications, Computers and Power in the Modern Environment.' Conference Proceedings., IEEE,* 1993, pp. 100-106.

[45] R. Billinton, C. Hua, and R. Ghajar, "A sequential simulation technique for adequacy evaluation of generating systems including wind energy," *IEEE Transactions on Energy Conversion,* vol. 11, pp. 728-734, 1996.

[46] S. H. Karaki, R. B. Chedid, and R. Ramadan, "Probabilistic performance assessment of wind energy conversion systems," *IEEE Transactions on Energy Conversion,* vol. 14, pp. 217-224, 1999.

[47] S. H. Karaki, R. B. Chedid, and R. Ramadan, "Probabilistic performance assessment of autonomous solar-wind energy conversion systems," *IEEE Transactions on Energy Conversion,* vol. 14, pp. 766-772, 1999.

[48] S. H. Karaki, R. B. Chedid, and R. Ramadan, "Probabilistic production costing of diesel-wind energy conversion systems," *IEEE Transactions on Energy Conversion,* vol. 15, pp. 284-289, 2000.

[49] R. Billinton and R. Karki, "Capacity expansion of small isolated power systems using PV and wind energy," New York, NY, United states, 2002, p. 27.

[50] R. Billinton and R. Karki, "Maintaining supply reliability of small isolated power systems using renewable energy," *IEE Proceedings: Generation, Transmission and Distribution,* vol. 148, pp. 530-534, 2001.

[51] R. Billinton and R. Karki, "Reliability/cost implications of utilizing photovoltaics in small isolated power systems," *Reliability Engineering and System Safety,* vol. 79, pp. 11-16, 2003.

[52] R. Karki and R. Billinton, "Reliability/cost implications of PV and wind energy utilization in small isolated power systems," *IEEE Transactions on Energy Conversion,* vol. 16, pp. 368-373, 2001.

[53] R. Billinton and Bagen, "A sequential simulation method for the generating capacity adequacy evaluation of small stand-alone wind energy conversion systems," Winipeg, Manitoba, Canada, 2002, pp. 72-77.

[54] R. Billinton and Bagen, "Generating capacity adequacy evaluation of small stand-alone power systems containing solar energy," *Reliability Engineering and System Safety,* vol. 91, pp. 438-443, 2006.

[55] R. Billinton, Bagen, and Y. Cui, "Reliability evaluation of small stand-alone wind energy conversion systems using a time series simulation model," *IEE Proceedings: Generation, Transmission and Distribution,* vol. 150, pp. 96-100, 2003.

[56] J. P. Barton and D. G. Infield, "Energy storage and its use with intermittent renewable energy," *IEEE Transactions on Energy Conversion,* vol. 19, pp. 441-448, 2004.

[57] R. B. Schainker, "Executive overview: Energy storage options for a sustainable energy future," Denver, CO, United states, 2004, pp. 2309-2314.

[58] W. Leonhard and M. Grobe, "Sustainable electrical energy supply with wind and pumped storage - A realistic long-term strategy or Utopia?," Denver, CO, United states, 2004, pp. 1221-1225.

[59] C. H. Lo and M. D. Anderson, "Economic dispatch and optimal sizing of battery energy storage systems in utility load-leveling operations," *IEEE Transactions on Energy Conversion,* vol. 14, pp. 824-829, 1999.

[60] D. K. Maly and K. S. Kwan, "Optimal battery energy storage system (BESS) charge scheduling with dynamic programming," *IEE Proceedings: Science, Measurement and Technology,* vol. 142, pp. 453-458, 1995.

[61] F. A. Chacra, P. Bastard, G. Fleury, and R. Clavreul, "Impact of energy storage costs on economical performance in a distribution substation," *IEEE Transactions on Power Systems,* vol. 20, pp. 684-691, 2005.

[62] F. D. Galiana, F. Bouffard, J. M. Arroyo, and J. F. Restrepo, "Scheduling and pricing of coupled energy and primary, secondary, and tertiary reserves," *Proceedings of the IEEE,* vol. 93, pp. 1970-1982, 2005.

[63] R. S. Garcia and D. Weisser, "A wind-diesel system with hydrogen storage: Joint optimisation of design and dispatch," *Renewable Energy,* vol. 31, pp. 2296-2320, 2006.

[64] C. Abbey and G. Joos, "A stochastic optimization approach to rating of energy storage systems in wind-diesel isolated grids," *IEEE Transactions on Power Systems,* vol. 24, pp. 418-426, 2009.

[65] E. Koutroulis, D. Kolokotsa, A. Potirakis, and K. Kalaitzakis, "Methodology for optimal sizing of stand-alone photovoltaic/wind-generator systems using genetic algorithms," *Solar Energy,* vol. 80, pp. 1072-1088, 2006.

[66] A. R. Prasad and E. Natarajan, "Optimization of integrated photovoltaic-wind power generation systems with battery storage," *Energy,* vol. 31, pp. 1607-1618, 2006.

[67] P. D. Brown, J. A. Pecas Lopes, and M. A. Matos, "Optimization of pumped storage capacity in an isolated power system with large renewable penetration," *IEEE Transactions on Power Systems,* vol. 23, pp. 523-531, 2008.

[68] J. K. Kaldellis and D. Zafirakis, "Optimum energy storage techniques for the improvement of renewable energy sources-based electricity generation economic efficiency," *Energy,* vol. 32, pp. 2295-2305, 2007.

[69] P. Poonpun and W. T. Jewell, "Analysis of the cost per kilowatt hour to store electricity," *IEEE Transactions on Energy Conversion,* vol. 23, pp. 529-534, 2008.

[70] G. Boyle, *Renewable Energy*: Oxford University Press, 2004.

[71] Justus C G, *Winds and System Performance*. Philadelphia: Franklin Institute Press, 1978.

[72] S. H. Jangamshetti and V. G. Rau, "Site matching of wind turbine generators: a case study," *Energy Conversion, IEEE Transactions on*, vol. 14, pp. 1537-1543, 1999.

[73] A. W. L. Yao, S. C. Chi, and J. H. Chen, "An improved Grey-based approach for electricity demand forecasting," *Electric Power Systems Research*, vol. 67, pp. 217-224, 2003.

[74] R. Billinton, C. Hua, and R. Ghajar, "Time-series models for reliability evaluation of power systems including wind energy," *Microelectronics Reliability*, vol. 36, pp. 1253-1261, 1996.

[75] J. Hetzer, D. C. Yu, and K. Bhattarai, "An economic dispatch model incorporating wind power," *IEEE Transactions on Energy Conversion*, vol. 23, pp. 603-611, 2008.

[76] S. Roy, "Market constrained optimal planning for wind energy conversion systems over multiple installation sites," *IEEE Transactions on Energy Conversion*, vol. 17, pp. 124-129, 2002.

[77] B. S. Borowy and Z. M. Salameh, "Optimum photovoltaic array size for a hybrid wind/PV system," *IEEE Transactions on Energy Conversion*, vol. 9, pp. 482-488, 1994.

[78] Z. M. Salameh, B. S. Borowy, and A. R. A. Amin, "Photovoltaic module-site matching based on the capacity factors," *IEEE Transactions on Energy Conversion*, vol. 10, pp. 326-331, 1995.

[79] F. N. Fritsch, R. E. Shafer, and W. P. Crowley, "Algorithm 443: Solution of the transcendental equation $we^{w}=x$," Comm. ACM, 1973.

[80] K. G. T. Hollands and R. G. Huget, "Probability Density Function for the Clearness Index with Applications," *Solar Energy*, vol. 30, pp. 195-209, 1982.

[81] G. Tina, S. Gagliano, and S. Raiti, "Hybrid solar/wind power system probabilistic modelling for long-term performance assessment," *Solar Energy*, vol. 80, pp. 578-588, 2006.

[82] S. Conti and S. Raiti, "Probabilistic load flow using Monte Carlo techniques for distribution networks with photovoltaic generators," *Solar Energy*, vol. 81, pp. 1473-1481, 2007.

[83] J. F. Orgill, Hollands, K.T.G., "Correlation equation for hourly diffuse radiation on horizontal surface," *Solar Energy*, vol. 19, 1977.

[84] G. N. Tiwari and M. K. Ghosal, *Renewable energy resources: basic principles and applications.* : Alpha Science International Ltd, 2005.

[85] G. M. masters, *Renewable and efficient electric power systems*. New Jersey: Jone Wiley & Sons, 2004.

[86] J. M. S. Pinheiro, C. R. R. Dornellas, M. T. Schilling, A. C. G. Melo, and J. C. O. Mello, "Probing the new IEEE Reliability Test System (RTS-96): HL-II assessment," *IEEE Transactions on Power Systems,* vol. 13, pp. 171-176, 1998.

[87] C. Singh and Y. Kim, "Efficient technique for reliability analysis of power systems including time dependent sources," *IEEE Transactions on Power Systems,* vol. 3, pp. 1090-1096, 1988.

[88] C. Singh and A. Lago-Gonzalez, "Improved algorithms for multi-area reliability evaluation using the decomposition-simulation approach," *IEEE Transactions on Power Systems,* vol. 4, pp. 321-328, 1989.

[89] "IEEE reliability test system - a report prepared by the reliability test system task force of the application of probability methods subcommittee," *IEEE Transactions on Power Apparatus and Systems,* vol. PAS-98, pp. 2047-2054, Nov. 1979.

[90] R. N. Allan and R. Billinton, "CONCEPTS OF POWER SYSTEM RELIABILITY EVALUATION," *International Journal of Electrical Power and Energy System,* vol. 10, pp. 139-141, 1988.

[91] R. N. Allan, R. Billinton, A. M. Breipohl, and C. H. Grigg, "Bibliography on the application of probability methods in power system reliability evaluation," *IEEE Transactions on Power Systems,* vol. 14, pp. 51-57, 1999.

[92] D. Zhu, R. P. Broadwater, K.-S. Tam, R. Seguin, and H. Asgeirsson, "Impact of DG placement on reliability and efficiency with time-varying loads," *IEEE Transactions on Power Systems,* vol. 21, pp. 419-427, 2006.

[93] A. Pregelj, M. Begovic, and A. Rohatgi, "Recloser allocation for improved reliability of DG-enhanced distribution networks," Tampa, FL, United States, 2007.

[94] R. Karki and R. Billinton, "Cost-effective wind energy utilization for reliable power supply," *IEEE Transactions on Energy Conversion,* vol. 19, pp. 435-440, 2004.

[95] "http://www.powerauthority.on.ca/sop/."

[96] *GAMS—A User's Guide.* . New York, 2008.

[97] "http://www.ieso.ca."